toxins

MDPI

Review

Molecular Biology of *Escherichia coli* Shiga Toxins' Effects on Mammalian Cells

Christian Menge

Friedrich-Loeffler-Institut/Federal Research Institute for Animal Health, Institute of Molecular Pathogenesis, Naumburger Str. 96a, D-07743 Jena, Germany; christian.menge@fli.de; Tel.: +49-3641-804-2430

Received: 17 April 2020; Accepted: 20 May 2020; Published: 23 May 2020

Abstract: Shiga toxins (Stxs), syn. Vero(cyto)toxins, are potent bacterial exotoxins and the principal virulence factor of enterohemorrhagic *Escherichia coli* (EHEC), a subset of Shiga toxin-producing *E. coli* (STEC). EHEC strains, e.g., strains of serovars O157:H7 and O104:H4, may cause individual cases as well as large outbreaks of life-threatening diseases in humans. Stxs primarily exert a ribotoxic activity in the eukaryotic target cells of the mammalian host resulting in rapid protein synthesis inhibition and cell death. Damage of endothelial cells in the kidneys and the central nervous system by Stxs is central in the pathogenesis of hemolytic uremic syndrome (HUS) in humans and edema disease in pigs. Probably even more important, the toxins also are capable of modulating a plethora of essential cellular functions, which eventually disturb intercellular communication. The review aims at providing a comprehensive overview of the current knowledge of the time course and the consecutive steps of Stx/cell interactions at the molecular level. Intervention measures deduced from an in-depth understanding of this molecular interplay may foster our basic understanding of cellular biology and microbial pathogenesis and pave the way to the creation of host-directed active compounds to mitigate the pathological conditions of STEC infections in the mammalian body.

Keywords: Shiga toxin; verotoxin; STEC; EHEC; O157; receptor; cytotoxicity; apoptosis; modulation

Key Contribution: Shiga toxins, syn. Vero(cyto)toxins, are potent bacterial exotoxins of enterohemorrhagic *Escherichia coli* (EHEC). The toxins are principally known to exert ribotoxic activity in eukaryotic target cells followed by rapid protein synthesis inhibition and cell death. The review aims at comprehensively describing the different facets of the Shiga toxins' cellular modes of action that additionally comprise modulation of intercellular communication as this is an integral part of the pathogenesis of EHEC-associated diseases.

1. Introduction

Enterohemorrhagic *Escherichia coli* (EHEC), a subset of Shiga toxin-producing *E. coli* (STEC), are food-borne pathogens that can evoke life-threatening diseases, such as hemorrhagic colitis (HC) and hemolytic-uremic syndrome (HUS), in humans [1]. STEC strains producing the Shiga toxin 2e variant cause edema disease (ED) in piglets [2]. The pathogenesis of STEC-associated diseases originates from colonization and multiplication of the pathogens at intestinal mucosal surfaces. STEC strains, including the highly virulent O104:H4 strain which caused the large outbreak of HUS and HC in Germany in 2011, are not invasive [3–5]. Despite the fact that viable bacteria were occasionally found at necropsy in mesenteric lymph nodes in natural hosts [6], STEC cannot be detected in extra-intestinal tissues in the course of systemic disease manifestations [7,8]. Shiga toxins (Stxs), potent bacterial exotoxins produced and released by STEC, represent the principal virulence factors implicated in pathogenesis [9].

For EHEC-associated human diseases, the following model is generally considered [9–12]: Many EHEC strains inherit the ability to settle on the enteric mucosa by inducing attaching and effacing

(AE) lesions, leading to tight association of single bacteria or small size colonies to the intestinal epithelial cells. These alterations are primarily independent of the Stxs' effects [13] and encoded by the locus of enterocyte effacement (LEE) in the STEC chromosome [14,15]. While the LEE is a key and prominent molecular determinant in pathogenesis, neither all EHEC nor STEC contain the LEE, indicating that some strains deploy additional virulence and colonization factors [16]. Stxs are produced by the pathogens during colonization and replication [5,17] and become released as free proteins liberated from the periplasmic space of the Gram-negative cell wall [18] or enclosed in outer membrane vesicles released by the bacteria [19]. Even in the absence of canonical Stx receptors on intestinal epithelial cells, luminal Stx facilitates the damage of the intestinal barrier indirectly, i.e., via effects on the underlying lamina propria [20], or by direct means because Stx2, but not Stx1, damages crypt epithelial cells [21]. The histological appearance of the tissue damage, manifesting mainly in the cecum and colon, is dominated by focal, intimate adhesion of the bacteria to the epithelial cells at the villus tips. The microvilli of the brush border are thickened or fused to each other or effaced from the apical cell poles of enterocytes. Attachment sites are underlaid by massive intracellular aggregates of cytoskeletal components. The regular arrangement of cells is disturbed, and ulceration occurs [13]. The loss of mature, fully differentiated epithelial cells is partially compensated for by immature epithelial cells. Fibrin exudation and hemorrhage is present in the submucosa. Neutrophilic infiltration is frequently found in the altered intestinal wall [22–25]. Because of the damaged epithelial layer [26], the transmigration of granulocytes [27] and by active Gb_3/CD77-receptor-independent transport processes [28–30], Stxs reach the subepithelial layers of the intestinal wall [28], inducing a thrombotic microangiopathy in capillaries and arterioles. Augmented adherence of the highly virulent O104:H4 strain to intestinal epithelium, lacking the LEE locus but possessing the pAA virulence plasmid and expressing the corresponding phenotype of aggregative adherence to intestinal epithelial cells, might also facilitate systemic absorption of Stxs [3]. Swelling of the endothelial cells, in synergy with a widening of the subendothelial space, results in constriction of the vessel lumen, frequently clogged by thrombi. Smooth muscle cells in the tunica media may also be affected by necrotic processes. The proximity of the vessels is characterized by edema or hemorrhage [25]. These alterations are believed to be causative to the hemorrhagic character of HC. Bound to erythrocytes [31], neutrophils [32], platelets [33], or within host blood cell-derived microvesicles [34] in the blood stream, Stxs circulate through the entire body presumably accompanied by endotoxemia [35]. Subsequently, organ damage outside the gastrointestinal tract develops. Endothelial cells of the kidneys and the central nervous system are directly targeted by the Stxs [25]. Induction of a microangiopathy in the capillaries of the respective organs [25] is followed by edema and hemorrhage of the affected organ and ischemic damage to the functional organ tissue, e.g., necrosis of the renal glomeruli and tubuli in case of HUS [25,36,37]. Besides direct effects of the Stxs on endothelial cells, comprehensively reviewed by Bauwens et al. [38], evidence exists that the toxins also directly act on neuronal cells [39] as well as innate [40,41] and adaptive immune cells [42]. While the clinical meaning of the former remains elusive [43], the presumptive importance of the latter effects recently became appreciated [9].

The epidemiological link between STEC infections and development of HUS was established in 1985 [44]. Nevertheless, therapeutic options to treat human patients suffering from STEC-associated diseases are still limited at present and, if available [45], not directly counteracting the detrimental effects of the Stxs. Options to protect exposed human individuals against the development of Stx-induced diseases are not available [46] despite the fact that vaccination of piglets against Stx2e proved to be an effective strategy against ED in affected farms [47]. Preventive measures in place to mitigate the human health threat are implemented for the food chain (following the farm-to-fork concept) but are mainly limited to later stages of the chain (post-harvest food safety). Currently, no measures are effectively targeting wildlife and livestock ruminants which are the most important STEC reservoir [48]. Interestingly, Stxs are increasingly utilized as biotechnological tools to study cellular processes [49] and to develop novel therapeutic strategies for cancer treatment [50,51], adding Stxs and derivatives thereof to the toolbox for host directed therapy.

The recent unprecedented HUS outbreak in Europe 2011, caused by an unusual hybrid strain of the serotype O104:H4, which lacked the LEE locus [3], stresses the fact that Stxs are the principal virulence factors and the only common denominator of STEC strains posing a threat to human health. Consequently, novel efforts to counteract STEC must be directed against the Stxs [52,53] and all bacterial strains harboring the respective genetic information as the primary target [14,54]. Such targeted attempts apparently cannot be circumvented by tackling other STEC factors, i.e., vaccinating ruminants with antigens implicated in STEC adhesion [55] and iron metabolism [56]. Irrespective of significant species and tissue differences in cell susceptibility and tissue distribution of receptors, a comprehensive knowledge of the molecular mechanisms of Stx–host interactions needs to be considered to mitigate human health risk.

2. Variants and Molecular Structure of Shiga Toxins

The family of Stxs was named after the cytotoxin of *Shigella dysenteriae* type 1, a cytotoxin known since the early nineteen-hundreds. Like some other bacterial toxins (Cholera toxin (CT) of *Vibrio cholerae*, heat-labile enterotoxin (LT) of *Escherichia coli*), Stxs belong to the heteromeric protein toxins, consisting of one active (StxA-; 32 kDa) and five receptor-binding (StxB-; 7.7 kDa) subunits [1]. In 1977, Konowalchuk et al. [57] described a cytotoxin of an *Escherichia coli* (*E. coli*) isolate, for which, according to its toxicity for Vero cells, the term Vero(cyto)toxin was coined. O'Brien and LaVeck confirmed its close relationship to the Shigella cytotoxin [58]. Since then, several cytotoxins produced by *E. coli* and resembling the Shigella toxin have been discovered and can be assigned to one of two groups. The first comprises the *Shigella dysenteriae* toxin and the prototypic Stx1 of *E. coli* (also referred to as Stx1a; see Scheutz et al. [59]), at protein sequence level differing by only one amino acid [60]. In this review, reference is made to a number of studies having been conducted before introduction of the novel nomenclature. It is almost impossible to assign the current nomenclature to the toxins used in the cited studies in retrospect. For this reason, the author refrained from using the novel designation rather refers to the prototypic toxins as "Stx1" and "Stx2" throughout. Further variants, Stx1c [61] and Stx1d [62], possess a 91%–95% homology to Stx1 at the nucleotide sequence level. The second group, being only approximately 56% homologous to Stx1 at nucleotide sequence level, comprises the prototypic Stx2 (also referred to as Stx2a) and its variants Stx2c [63], Stx2d [64], Stx2e [65], Stx2f [66], and Stx2g [67]. Antisera against variants are partially cross-protective within but not between toxin groups [68]. Stx2e, the causative agent of ED in piglets is most distantly related to the other Stx2 variants in terms of protein sequence, biological activity, and receptor usage [69,70]. Genes for Stx1, Stx2, and Stx2 variants are encoded within the STEC genome as part of the genome of lambdoid bacteriophages [71]. STEC strains are often capable of producing more than one toxin type because possession of several *stx*-converting phages is common. Phages foster horizontal transmission of *stx* genes between different *E. coli* strains as well as to *Citrobacter freundii* and *Enterobacter cloacae* strains [72].

The *stx* genes encode for two polypeptide chains forming the toxin subunits. Translation products each consist of a peptide chain for the mature subunit, preceded by an N-terminal signaling sequence of 22 (StxA) and 19-20 (StxB) amino acids, respectively [63,73,74]. Upon transfer into the periplasmic space of the *E. coli* cell, the signal sequences are cleaved off by the membrane bound signal peptidase I [74].

Five B subunits of Stx1 form a pentameric ring without establishing covalent bonds [75]. Each B subunit consists of 69 amino acids with an internal disulfide bond between cysteine residues at position 4 and 57 (Table 1) [76]. The Stx1 B subunit appears as a secondary structure with two three-stranded anti-parallel β-sheets, positioned to the outside of the pentamer [77]. Two three-stranded sheets of neighboring monomers build up a six-stranded β-sheet with the β2-sheet of one monomer interacting with the β6-sheet of the consecutive monomer via hydrogen bonds. Adjacent monomers form a pocket in which up to three potential receptor binding sites are located [78]. Each monomer also possesses an α-helix, directed to the center of the pentameric ring, which, together with the α-helices of the other four monomers, forms an 11 Å-wide pore (Figure 1) [77]. While the central α-helices undergo

conformational changes at low pH, as it occurs upon endocytosis when the toxin reaches the endosomal compartment, the β-sheets forming the receptor binding sites on the B subunits' outer surfaces are comparably stable [79].

Table 1. Function of amino acid residues in the Shiga toxin B subunits.

Amino Acid in Toxin:			Allocated Function:	Reference:
Stx1	**Stx2** [1]	**Stx2e**		
(-20)-(-1)	(-19)-(-1)	(-19)-(-1)	signal sequence	[63,73,74]
	Ala1		hydrogen bond to Ser53; part of receptor binding site II	[80]
3–8			β1-sheet	[77]
Cys4	Cys3		disulfide bond to Cys57 (essential for receptor binding); part of receptor binding site II	[76,80,81]
9–14			β2-sheet, interaction with β6-sheet of the adjacent monomer (receptor binding site I [2])	[77]
Lys13			part of receptor binding site I [2]	[82]
10–20			hydrophilic domain: receptor binding, binding of neutralizing antibodies, highly conserved in all Stxs (antigenic domain?)	[76]
Asp16			receptor binding	[83]
Asp17			part of receptor binding site I [2]	[82,83]
		Asn17	receptor specificity for Gb_4	[83]
Asp18	Asp17		receptor specificity for Gb_3/CD77	[81]
20–24			β3-sheet	[77]
Thr21			part of receptor binding site I [2]	[82,84]
27–31			β4-sheet	[77]
Glu28			part of receptor binding site I [2]	[82,84]
Phe30			located between receptor binding site I and II; essential for both binding sites	[85]
Asn32			part of receptor binding site II	[84]
Arg33		Arg32	part of receptor binding sites II and III	[80,84,86]
Trp34	Trp33		part of receptor binding site III	[78,80,87]
Asn35	Asn34		part of receptor binding site III?	[80]
36–46			α-helix, forming the central pore of the pentamer together with the α-helices of the other four B subunits; in contact with the anti-parallel α-helix of the A_2 fragment; conformational changes occur here at low pH (impacting on the translocation of the A_2 fragment)	[77,79,88]
Ala43		Ala42	receptor binding	[86]
49–53			β5-sheet	[77]
Lys53		Lys52	receptor binding (involved in determination of receptor specificity?)	[81]
	Ser53		hydrogen bond to Ala1; part of receptor binding site II	[80]
Cys57	Cys56		Disulfide bond to Cys4 (essential for receptor binding); part of receptor binding site II	[76,80,81]
Gly60		Gly59	part of receptor binding site I [2]	[82,86]
65–68			β-sheet, interaction with the β2-sheet of the adjacent monomer (receptor binding site I [2])	[77]
Glu65			receptor specificity for Gb3; part of receptor binding site I 2	[82,84]
		Gln64	localization of the toxin in the E. coli cell	[81]
			receptor specificity for Gb4	[83]
		Lys66	receptor specificity for Gb4	[81,83]
Phe68	Phe67	Phe67	receptor binding	[89]
Arg69	Asn68	Asn68	receptor binding	[89]
	C-terminal 4 (-5)		receptor binding	[83]

[1] referring to Stx2 B subunit with 68 amino acids; [2] forming hydrogen bonds between polar and acidic side-chains of the B subunits and polar groups of the carbohydrates [77,82].

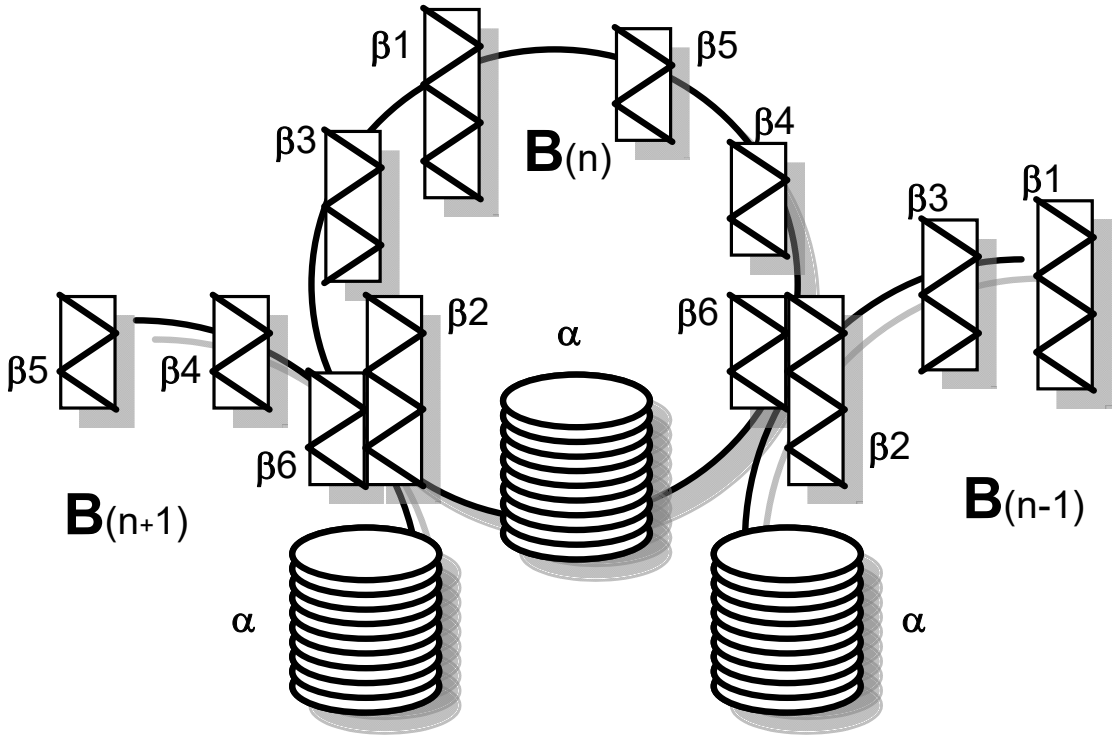

Figure 1. Simplified structural model of the Shiga toxin 1 B subunit as part of a pentamer (for details see text).

The A subunit of Stx1 consists of 293 amino acids. Two cysteine residues in position 242 and 261 are connected by a disulfide bond [73]. In between, arginine residues at position 248 and 251 are part of a trypsin-sensitive cleavage site. Proteolytic cleavage separates the enzymatically active 27 kDa A_1 fragment from the 6 kDa A_2 fragment which is indispensable for the holotoxin structure [73,90]. Nine amino acids (residues 279–287) of the C-terminus of A_2 form an α-helix, which is situated in an anti-parallel manner relative to the five α-helices of the B subunits surrounding it in the holotoxin [80,88,91]. The α-helix of A_2 extends by 11 Å into the 20 Å-deep central pore of the B pentamer [80,88]. The other parts of the A subunit rest on the pentameric ring (Figure 2). Two β-sheets each of the A_1 and the A_2 fragment are non-covalently attached to the ring, building an asymmetric structure irrespective of the symmetric structure of the pentamer [80,88]. Establishment of this formation particularly relies on amino acids in position 277–278 and 288–289, which are located in vicinity to the α-helix of the A_2 fragment. They are interlinked with charged and aromatic amino acids outside the pore on the planar surface of the B pentamer [91] such that the A subunit is interacting with three of the five B subunits in the holotoxin [80,88].

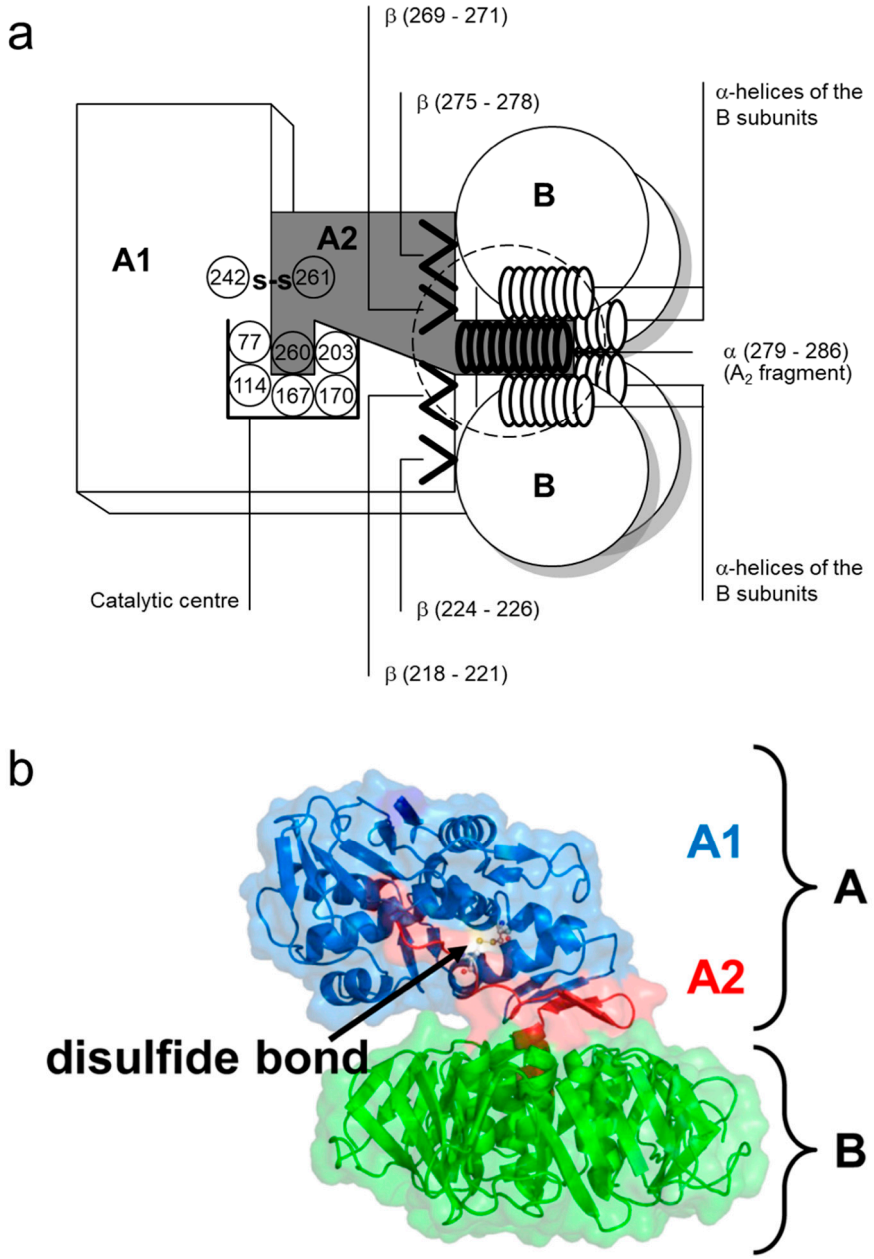

Figure 2. Structural model of Shiga toxin holotoxin. (**a**) Simplified scheme depicting the instrumental structural and functional elements of Stx1 and their approximate localization in the holotoxin (numbers in brackets refer to amino acid residues participating in formation of the structure), (**b**) Ribbon diagram of Stx2. The A_1 fragment of the A subunit is colored in blue and the A_2 fragment in red; the B5 pentamer is portrayed in green. The cysteine residues Cys242 and Cys261 form the disulfide bridge between the A_1 and the A_2 fragment. For a planar view on the surface of the B subunit pentamer the reader is referred to Figure 4a. Part b of Figure 2 reproduced from reference [92]. Elsevier, 2018.

Toxins of the Stx2 group are comprised of an A subunit with 296–297 amino acids and B subunits with 68–70 amino acids [63,93,94]. Intramolecular disulfide bonds in the A subunit of Stx2 are formed between cysteine residues at position 241 and 260. The carboxy-terminus of the A subunit forms a short α-helix within the central pore of the B pentamer [80]. Amino acids essential for the holotoxin formation are highly conserved within the amino acid sequence of the Stx2 A subunit which is only 55% homologous to the A subunit of Stx1 [95], but the toxins exhibit further structural differences. As opposed to Stx1, in which the enzymatic cleft of the holotoxin is blocked by a methionine in position 260

of the A_2 fragment [88], the cleft in Stx2 remains to be accessible for water molecules [80]. The tyrosine residue in position 77 further distinguishes the catalytic center of Stx2 from that of Stx1 [80]. The molecular mechanism of the enzymatic activity of all Stxs is nearly identical, even though the Stx2 A_1 fragment has a higher affinity for and a faster association and dissociation with mammalian ribosomes than the Stx1 A_1 fragment [96]. Irrespectively, differences in receptor binding sites of the particular B subunits, resulting in differences in the affinity of the toxins for the Stx receptor Gb_3/CD77, are mainly held responsible for the differences in the relative in vitro and in vivo potency of Stx subtypes [97] and the type and degree of tissue alterations which are caused by Stx1- and Stx2-producing *E. coli* in humans, respectively [80].

Like other members of the AB_5 family of bacterial exotoxins, Stxs are transiently localized in the periplasm before being secreted into the extracellular milieu, e.g., incorporated in bacterial outer membrane vesicles. If experimentally expressed in the absence of their cognate B subunits, the A subunits of Stxs and of heat-labile enterotoxin (LT) of enterotoxic *E. coli* (ETEC) were found to be degraded rapidly by periplasmic proteases, suggesting that the B subunit contributes to stability of the A subunit in the periplasm [98]. By contrast, a recent study suggests that the A and B subunits are not released as a holotoxin and that, unlike other AB_5 toxin family members, Stxs are produced by STEC as unassembled A and B subunits. A preformed AB_5 complex is not required for cellular toxicity or in vivo toxicity to mice, and toxin assembly is assumed to occur at the cell membrane [99]. Differences to other AB_5 toxins in maintaining an intact AB_5 conformation seems to be due to a small hydrophobic patch in the central pore of the B pentamer, which in other AB_5 toxins is larger and plays a critical role in the engagement of the A subunit and the B pentamer [100].

3. Receptor Globotriaosylceramide (Gb_3/CD77)

Globotriaosylceramide (Gb_3) acts as the functional receptor for most Stxs. Because Gb_3 is also present on immune cells, it became listed as the CD77 leukocyte antigen. Globotetraosylceramide (Gb_4) was identified as the functional receptor for Stx2e. Of note, evidence exists that several binding sites varying in the affinity for Stxs do exist on host cells [83,101]. It was considered plausible that Gb_3/CD77 and Gb_4 are accompanied by non-functional receptors [102]. However, Gb_3/CD77 does not exist as a chemically defined single molecular structure. It rather represents a group of glycosphingolipids, sharing a common carbohydrate group but significantly differing in the components constituting their lipid moiety. These lipid components impact the affinity of toxin receptor-binding as well as on the subsequent route the toxins are transported along into intracellular compartments. Consequently, toxin binding sites with varying affinity on cellular surfaces may reflect the presence of different Gb_3/CD77 species, several of which, independent of their affinity, may all act as functional receptors [101].

3.1. Structure, Synthesis, and Regulation of Cell Surface Expression

Gb_3/CD77 and Gb_4 are neutral glycosphingolipids of the globo-series. The lipid parts of these molecules are composed of a ceramide, an amide-linkage between a sphingosine molecule, and a fatty acid. Neutral glycosphingolipids contain oligosaccharides that are attached to the terminal hydroxy group of the sphingosines in a β1-glycosidic manner [103]. By coupling glucose and galactose to ceramide, lactosylceramide (Gal β1-4Glcβ1-1Cer) is synthetized, the Stx receptor precursor [104]. Another galactose residue is added by the UDP-galactose:lactosylceramide α1-4-galactosyl transferase (Gb_3-synthetase) to create Gb_3/CD77 (Galα1-4Galβ1-4Glcβ1-1Cer) (Figure 3) [103,105,106]. Further addition of N-acetyl-galactosamine by the N-acetyl-galactosyl transferase results in formation of Gb_4 (GalNAcβ1-3Galα1-4Galβ1-4Glcβ1-1Cer) [107].

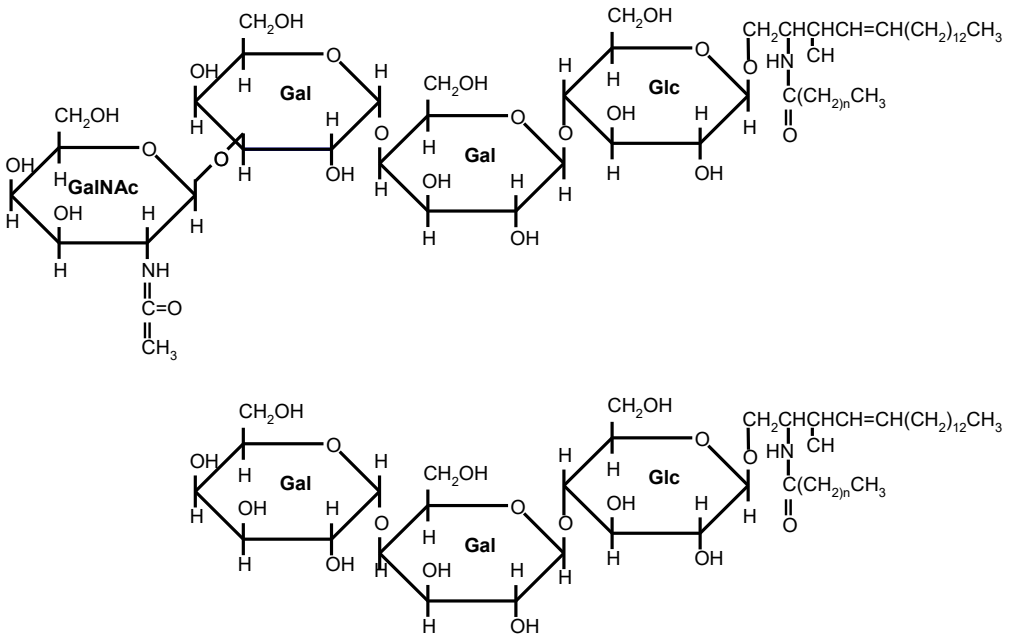

Figure 3. Molecular structure of globotetraosylceramide Gb_4 (**top**) and globotriaosylceramide Gb_3 (**bottom**).

For most toxin-sensitive cells, the presence of approximately 1×10^6 to 1×10^7 receptor molecules per cell has been estimated [102,108,109], however, expression on cells and in tissues depends on a number of factors. Active cellular division processes appear to be the principal prerequisite for maximum sensitivity of the target cells [110], as sensitivity varies with the phase of the cell cycle of the individual cell. Pudymaitis et al. [111] reported that Vero cell cultures exhibit highest sensitivity when in the transition from the G1 to the S phase, before sensitivity drops by one order of magnitude. In the G1 phase, maximum levels of Gb_3/CD77 receptor synthesis and subsequent cell surface expression is accompanied by maximum binding of toxin molecules by the cells. Because the Gb_3/CD77 content of the cultures remained rather constant during the cell cycle, an elevated surface exposition and receptor turnover was believed to facilitate toxin uptake [111]. By contrast, Majoul et al. [112] described that synthesis and surface expression of Gb_3/CD77 reached highest levels between G2 and M phase. In turn, Stx1 irreversibly arrests HCT116 cells in the S phase within 24 h, presumably by activation of the S phase checkpoint prior to inducing apoptosis [113].

Glycosphingolipids are known to be detectable in cells yet not available for ligand binding at the cell surface. Their exposition not only depends on cellular functions, but their small head residues located close to the cell membrane can easily be masked by long-chained carbohydrates or proteins [111,114].

Surface expression of Gb_3/CD77 also is a function of the degree of differentiation of cells and tissues. While THP-1 cells are Stx-sensitive in initial stages of differentiation, further stimulation in vitro by phorbol esters, interferon gamma (IFN-γ) or granulocyte-macrophage stimulating factor (GM-CSF) results in increasing resilience for Stx, accompanied by a reduced receptor expression [115]. The balance between synthesis of lactosylceramide to Gb_3/CD77 by the Gb_3-synthetase and degradation by the α-galactosidase regulates Gb_3/CD77 expression on HeLa cells [104,114], but not on Daudi cells, implying the existence of different regulatory mechanisms [116].

Lipopolysaccharide (LPS) increases Stx receptor expression on human umbilical vein endothelial cells (HUVEC) by 10-fold and renders the cells more susceptible to Stx [117,118]. Similarly, tumor necrosis factor alpha (TNF-α), released from macrophages upon exposure to LPS or Stx, facilitates the effect of Stx on endothelial cells in an additive or synergistic manner. Pre-incubation of endothelial cells with TNF-α increases the number of Stx binding sites by up to 100-fold [118]. This increase in receptor expression results from an increased de novo synthesis following a protein kinase C-

(PKC-)induced increased activity of the Gb_3-synthetase [119] as well as an increased activity of the enzymes catalyzing the synthesis of precursor molecules [120]. Following LPS or TNF-α exposure, increases in receptor number become detectable after 6–8 hand remain for 48 h [119]. Interleukin 1 beta (IL-1β), also released from macrophages after LPS and Stx exposure, sensitizes endothelial cells to Stx with the same kinetics and to the same degree as TNF-α [121]. Via transcription factor NF-κB, IL-1β also induces the production of enzymes which degrade sphingomyelin molecules to ceramides, which in turn serve as substrate for Gb_3/CD77 synthesis [121].

As opposed to HUVEC, human renal microvascular (HRMEC) and glomerular capillary endothelial cells (GCEC) become affected in vitro by Stx concentrations not sufficient to harm HUVEC [103,122]. As early as 5–6 h after addition of Stx1 to GCEC cultures, protein synthesis declines, resulting in cytopathic effects after 10 h [122]. Accordingly, renal endothelial cells possess a 50-fold higher Gb_3/CD77 content as compared to HUVEC and at the same level as Vero cells [103]. The heterogeneity of endothelial cell responses to Stxs [103] also becomes apparent when considering the meaning of cytokines. While these immune system mediators neither influence receptor expression nor the cytotoxic effect of Stxs in renal endothelial cells in vitro [103,122], TNF-α and IL-1β drastically trigger receptor expression by microvascular endothelial cells from the human brain [123,124].

Under experimental conditions, Gb_3/CD77 synthesis can be stimulated with butyric acid which induces cellular differentiation [109,125]. Butyric acid, a metabolic product of the anaerobic intestinal flora, may exhibit a similar effect in vivo on the intestinal epithelium.

3.2. Cellular and Tissue Distribution

Gb_3/CD77 and Gb_4 were detected in several cell lines, primary cultured cells and tissues of different host species with significant variations in tissue distribution between hosts (Table 2). Detection of Gb_3/CD77 and Gb_4, respectively, vastly correlates with the sensitivity of cells and tissues for the cytotoxic effect of Stxs, i.e., differences in clinical symptoms following infections with Stx2e and Stx1/2-producing *E. coli* correlate with receptor specificities of Stx2e versus other Stxs and the presence of Gb_4 and Gb_3/CD77, respectively, on cells and in tissues [22,69,83,126,127].

Table 2. Overview of cellular distribution of Gb_3/CD77-like Stx receptors [1,2] in different species.

Cell Type	Man	Mice	Rabbit	Pig	Cattle	Sheep	Goat
Intestinal epithelial cells	(+) only for Stx2 [21] + only cell lines [21] + intestinal organoids [20]	+ only distal colon [128]	+ [129,130]	? [131]	+ [132,133]		
Paneth cells	+ [134]						
Endothelial cells							
in large blood vessels	+ [118,135–138]				+ [139]; – [137]		
in the microvasculature	+ [137,140–142]						
intestinal	+ [143]		+ [144]		– [131]		
in renal glomeruli	+ [122,145,146]			+ [147]	– [131]		
in the CNS	+ [120,123,124,148]	– [43]	+ [144]	+ [147]			
in the lung		+ [149]					
Nerve cells				? [22]			
retinal pigment epithelial	+ [150]						
Renal tubular epithelial cells	+ [107,145,151–153]	? [154]	– [155]	+ [147]	+ [131,132]		
Renal glomerular epithelial cells	+ [156]		– [155]				
Fibroblasts							
intestinal myofibroblasts	+ [21]				+ [133]		
Monocytes/macrophages	(+) [157] + [158]	+ [159]		+ [147]	+ [160]		
Mesangium cells	(+) [161] + [161,162]		– [155]		– [132]		
Tissue macrophages				+ [147,163]	+ [133]		
Lymphocytes				– [147]	+ [164,165]		
B cells	+ [42,166,167]	+ [168]			+ [164,165]		
αβT cells	– [42,166]	– [154,169]			+ [164,165]		
γδT cells					+ [164,165]		
Granulocytes	(+) [32]			+ [147]	– [170]	+ [170]	+ [171]
Erythrocytes	+ [31,172]			– [22]			
Hematopoetic stem cells	+ [173]						
Platelets	+ [174,175]						

[1] Stx2e binding sites / Gb_4 not considered; for an excellent overview of Stx2e receptor distribution in the tissues of weaned piglets, the reader is referred to Steil et al. [176]; [2] Gb_3 and Gb_4 are also reportedly synthetized by various human and murine immune cells (reviewed by [177]); however, these findings were not considered if no evidence was found that the molecules function as Stx binding sites in these cells; + = Gb_3/CD77 and/or Stx binding sites detected; – = Gb_3/CD77 and/or Stx binding sites not detectable; (+) = evidence for Stx binding sites different from Gb_3/CD77; ? = indication for the presence of Stx binding sites not yet further biochemically characterized.

Stxs were initially recognized as cytolethal toxins but it became apparent later that the toxins cause a broad spectrum of cellular effects that vary with cell type. These merely modulating effects are now considered more important for the pathogenesis of STEC-mediated diseases than the cytolethal effect [11]. The kind of effect on a given cell type is determined by the localization of Gb_3/CD77 in the cellular membrane [178]. In HeLa cells, highly susceptible to cytolethal effects of Stxs, Gb_3/CD77 is embedded in detergent-insoluble, glycosphingolipid-rich microdomains within the cellular membrane, referred to as lipid rafts [178]. Gb_3/CD77 located herein may trigger endocytosis and retrograde transport of Stxs to the biosynthetic/secretory vesicular transport path [178] as well as the activation of signaling cascades starting from the cell surface [179]. Composition of the lipid rafts may vary, as Gb_3/CD77 is strictly colocalized with ganglioside GM_1, a marker for lipid rafts, in polarized Caco-2 [180] and HeLa cells [178], but lipid rafts containing either GM_1 or Gb_3/CD77 are formed in different cell cycle phases in Vero cells [112].

Gb_3/CD77 is located outside lipid rafts in human monocytes and macrophages [178], which are fairly resistant to the protein biosynthesis inhibition by Stx1 but respond with an altered cytokine transcription profile [157]. After disintegration of lipid rafts, Caco cells fail to internalize Stxs [180], whereas human monocytes still do so but primarily transport Stxs to late endosomes, where they become degraded before transferred to the cytosol [178].

3.3. Interactions with Shiga Toxins

3.3.1. Binding Affinity and Kinetics

Binding of Stx holotoxin to Gb_3/CD77 embedded in cellular membranes is characterized by a high association constant of 1×10^9 to 1×10^{10} M^{-1} [108,130,181,182]. The binding constant for soluble trisaccharide to the soluble pentameric B subunit is weak, with a K(a) of 1×10^3 M^{-1} for the B subunit monomer [183]. The holotoxins' high avidity results from the multivalent property of Stxs for receptor binding by deploying up to 15 receptor binding sites. HeLa cells possess additional low affinity binding sites with high binding capacity, which does not correlate to the sensitivity of the cells for Stxs, though [102,181,184]. Because the affinity of Gb_3/CD77 molecules is determined by the lipid part, the presence of Gb_3/CD77 with different lipid moieties is considered causative for biphasic binding kinetics [101]. Other membrane lipids, referred to as auxiliary lipids, influence receptor affinity [185]. Stx1 and Stx2 seem to differ in the receptor binding mechanisms, which may contribute to different toxicities observed [126,186]. Stx binding is temperature-dependent with a maximum binding at 37 °C [102,187]. However, binding also rapidly occurs at 0 °C when internalization is prohibited. Fifty percent of maximum binding is reached after 5 min at 4 °C, 100% after 15 min [184]. The binding constant has been calculated as 1.5×10^6 $M^{-1}s^{-1}$ [181]. Only 20% of cell-bound Stx1 is released again after 20 h at 0 °C [181]. Toxin binding also depends on pH with a broad plateau between pH 5–8 [184]; affinity for Gb_3/CD77 only significantly decreases at pH-values below 3.5 [79].

3.3.2. The Carbohydrate Moiety

Except for Stx2e, all Stxs specifically bind the terminal galabiose (Galα1-4Gal) of Gb_3/CD77 in the membrane of eukaryotic cells [102,127,188,189]. Under artificial conditions, toxins also bind to isolated di- and trisaccharides [127], which are able to block cytolethal effects of Stx at equimolar concentrations [102,114,189]. Treatment of cells and tissues with α-galactosidase impairs toxin binding [69,188,189]. Under certain conditions, Gb_2 (galabiosylceramide, Galα1-4Galβ1Cer) may serve as functional receptor [127,190]. Stx can bind to the P1 blood group antigen also harboring a terminal galabiose [102].

The Stx2e variant preferentially binds Gb_4, with a galabiose located subterminal to N-acetyl-galactosamine [69]. Deacetylation of the carbohydrate does not influence Stx2e binding, indicating that the terminal β1-3 galactose structure is sufficient for binding [69]. The particular

structure is also present in galactosyl-globotetrasylceramide (Gb_5) and in the Forssman blood group antigen which also bind Stx2e [69,127].

3.3.3. The Lipid Moiety

Stxs preferentially bind carbohydrate structures when the oligosaccharide is coupled to a lipid or protein [102]. In mammals, galabiose structures at the terminal, non-reduced end of saccharides have only been detected in glycolipids [114]. The lipid structure impacts on the presentation of the galabiose on the cell surface, i.e., Stx fails to bind to digalactosyldiglycerides [101,188]. The ceramide component of Stx receptors are composed of a sphingosine or dihydrosphingosine molecule to which a long-chained fatty acid is coupled via an amide bond [101]. Varying with the cellular source, Gb_3/CD77 molecules may either harbor hydroxylated plus non-hydroxylated fatty acids [129,191] or non-hydroxylated fatty acids only [101].

The fatty acid length particularly influences the spatial orientation of the carbohydrate. Stxs preferentially recognize receptors harboring C12 to C24 fatty acids [101]. In thin layer chromatograms of glycolipids from human kidneys, Gb_3/CD77 molecules present as two bands, consisting of a mixture of glycolipids with fatty acids of different lengths. One band is dominated by Gb_3/CD77 molecules having incorporated a C24:1 fatty acid and binding Stx1 with low affinity but high capacity, the second band mainly consists of Gb_3/CD77 molecules with a C16:1 fatty acid which bind Stx1 with high affinity and low capacity. Affinity and capacity of Stx1 binding to each of the bands is higher than binding to the respective semisynthetic receptor analog, indicating that a mixture of different receptor molecules with variable fatty acid content promotes Stx binding to physiological membranes. A combination of receptor variation and additional presence of auxiliary lipids may create an uneven surface, fostering binding of the StxB pentamer [101].

The affinity to Gb_3/CD77 molecules with fatty acids of a given length seems to vary between different Stxs. Stx1 prefers Gb_3/CD77 molecules with C20:0 or C22:1, whilst Stx2c prefers receptors with a C18:0 or C18:1 fatty acid. Because both toxins poorly compete for binding to their preferred receptors, the toxins presumably bind to different but overlapping carbohydrate epitopes, being presented differentially in the membrane environment because of the differences in the membrane anchor of the respective Gb_3/CD77 molecules [185]. Relative abundance of Gb_3/CD77 molecules harboring C16 and C22-C24 fatty acids may vary between cells of similar provenience and specialization, as exemplified by the human colon epithelial cell lines Caco-2 and HCT-8 [192], as well as between cells at different stages of differentiation [164].

3.3.4. Receptor-Binding Domains of the Toxins

Stxs bind to receptors via the B subunit pentamer [126,193,194]. Upon receptor binding, the A subunit is located on the membrane-far side [77] and, at least for Stx1, is not involved in the binding process [195]. Binding principally depends on amino acids Asp16, Asp17, Arg33, Trp34, Ala43, Lys53, Gly60 of the matured Stx1 B subunit [81,86,87,89,126] as well as on the disulfide bridge between amino acids 4 and 57 [81]. Binding becomes stabilized by the C-terminal end of the B subunit. Deletion of the last two amino acids (Phe68 and Arg69) reduces Stx1 binding, whereas binding is abolished after deletion of the last four amino acids [89]. The tertiary Stx structure was initially believed to be highly conserved with homologous amino acids also mediating binding of Stx2 group toxins [89,95]. However, up to three independent receptor binding sites exist per B monomer, which differ between toxin types (Figure 4).

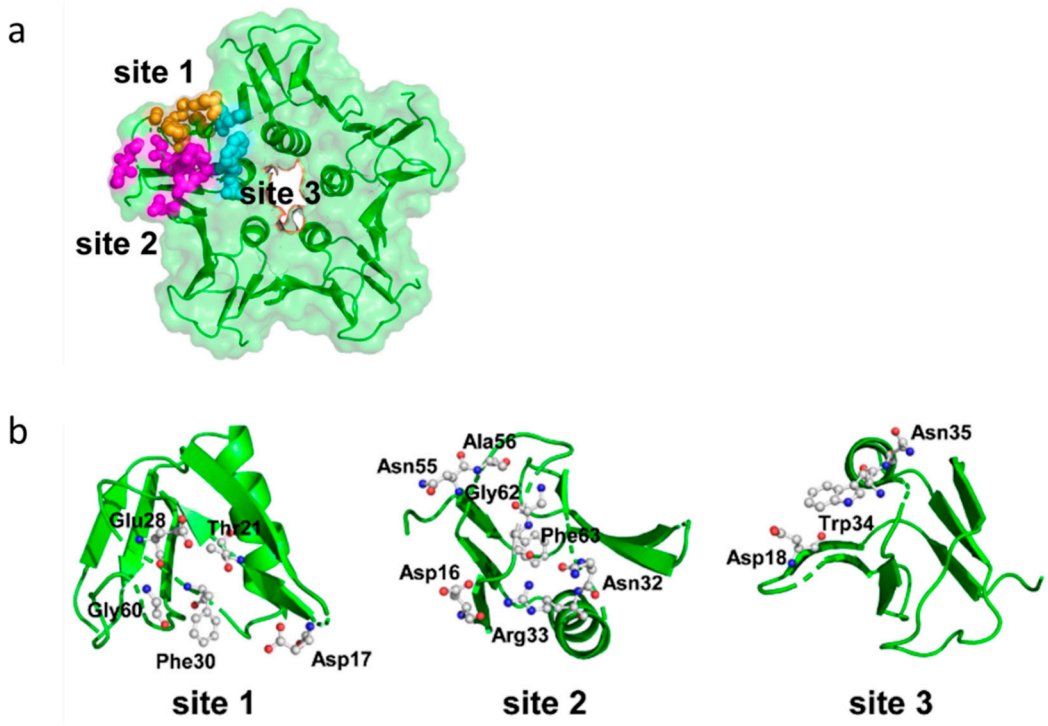

Figure 4. Structural model of Shiga toxin 2 B subunit pentamer holotoxin and Gb_3/CD77 bindings sites. (**a**) Ribbon diagram of Stx2, planar view on the surface of the B subunit pentamer. The three binding sites per B subunit are exemplarily shown for a single B subunit in orange (site 1), magenta (site 2), and cyan (site 3). (**b**) The amino acids involved in receptor binding (C, gray; N, blue; O, red) are represented by ball-and-stick models colored in green. Reproduced from reference [92]. Elsevier, 2018.

Receptor binding site I is a pocket formed by two β-sheets belonging to two neighboring subunits in the pentamer. Polar and acidic side chains of Asp16-17 of the β-sheets form hydrogen bonds with polar groups of the carbohydrates in the receptor [84]. Conserved aromatic rings of Phe30 attach to the sugar rings [77,84]. Receptor specificity for Gb_3/CD77 is mainly determined by Asp18 and Asp17 in Stx1 and Stx2, respectively. In Stx2e, an asparagine residue at this position and amino acids Gln64 and Lys66 presumably interacting with N-acetyl-galactosamine stabilize binding to Gb_4 [83,126]. Although this receptor binding site is formed by two adjacent monomers, competitive binding studies with Gb_3/CD77 separated from the membrane environment showed that the Stx1 B subunit and holotoxin had the same affinity for the receptor [75], competing for Gb_3/CD77 binding in equimolar quantities [126]. This apparent discrepancy may result from only one side of the pocket determining the affinity, while the other only supports binding. Comparison of the amino acid sequence of CD19, a Gb_3/CD77 binding host cell molecule on B cells (see Section 3.3.5), revealed an approximately 50% identity to Stx. This particularly concerns those amino acids within the B subunits which form the receptor binding site between two B subunits in the pentamer. Of note, most homologous amino acids can be found in the (n + 1) B subunit, suggesting that this side of the receptor binding site is sufficient to define the glycolipid binding specificity, while the opposite side only promotes access to the receptor [196].

Based on cristallographic studies, Lingwood et al. [82], considered site I the most important receptor binding site of Stx1. However, Kitova et al. showed by resonance mass spectrometry that binding of Gb_3-homologue P^K trisaccharide to site I only occurs after saturation of five different binding sites in the Stx1 B subunit pentamer [197]. This receptor binding site II is located within the Stx1 B subunit on the opposite side of Phe30 and is formed by a glycine loop (Gly60-62) and Asn32 and Arg33 [84]. Binding energy between isolated Gb_3/CD77 and site II is only approximately 50% of the energy of Gb_3/CD77-site I interactions [84]. However, differences in affinity become significantly smaller in case Gb_3/CD77 is embedded in a lipid membrane [198], because the immediate environment

of the receptor significantly impacts on its binding properties (see Section 4.1.1). The disulfide bond between residues Cys3 and Cys56 in the Stx2 B subunit is conformationally different from the bond between Cys4 and Cys57 in the Stx1 B subunit [80]. Binding of Gb_3/CD77 to the receptor binding site II of Stx2 would require a conformational change of this disulfide bond in the same way as Stx1, because the carbohydrate chain of the receptor would collide with Ser54 [80]. Site II is preferentially utilized by Stx2c, because this toxin harbors an asparagine residue at the position homologous to Asp17 in the Stx1 B subunit, which is not able to establish hydrogen bonds with the carbohydrate moiety of Gb_3/CD77 [82,84]. These variations between toxin subtypes are believed to explain the different receptor affinities of Stx1, Stx2, and Stx2c and influence the biological activities of Stxs in tissues [80].

Additionally, a low-affinity receptor binding site III at the N-terminus of the StxB α-helix has been described, at the basis of the B pentamer where the C-terminus of the A_2 fragment protrudes from the central pore [78,80,199]. However, this binding site appears to be of minor importance for conferring the cytolethal activity of Stx1 [200]. Different from Stx1, the five Trp33 of each subunit in the Stx2 B pentamer have a diverse orientation [80]. In order to bind Gb_3/CD77 at this site, all five tryptophan residues have to be flexible to such an extent that they may twist to the adjacent asparagine residues in position 34 to generate a suitable binding conformation [80].

3.3.5. Interactions with Physiological (Host) Ligands

CD19 is a 95 kDa protein and a member of the Ig superfamily that is well conserved across species [201]. Its extracellular region consists of three potential domains interlinked with disulfide bonds. Expression of CD19 is the first indication of an hematopoetic cell differentiating into a B cell and only gets lost upon terminal differentiation into a plasma cell. CD19 forms a complex with CD21, CD81, and Leu-13 at the cell surface. Ligand binding to CD19 initiates signal transduction and activation of integrin-dependent adhesion, resulting in proliferation and B cell maturation [196], but also apoptosis [202]. CD19 expression was also found to regulate TLR-4 signaling through p38 mitogen-activated protein kinase (MAPKp38) activation [203]. Amino acid sequences of human CD19 and the Stx1 B subunit are nearly 50% homologous. This particularly concerns extracellular domains of CD19 and amino acids forming the receptor binding site I in the Stx1 B subunit pentamer. Consequently, CD19 is capable of binding to Gb_3/CD77 on B cell surfaces [196]. Only when complexed with Gb_3/CD77, CD19 is retrograde transported by the ER-nuclear membrane route [202]. Mutants lacking Gb_3/CD77 possess CD19 molecules with reduced affinity for Gb_3/CD77 and are unable to activate integrin-dependent cellular adhesion [196]. It is assumed that Gb_3/CD77 and CD19 interact on the surface of B cells in a multi-stage process. Initially CD19 is expressed on B cells as an immature protein, devoid of disulfide bonds. Binding of CD19 to Gb_3/CD77, present on the surface of the same B cell, brings thiol groups in closer proximity, fostering establishment of a disulfide bond and maturation of CD19. Mature CD19 molecules participate in two forms of cell-to-cell adhesion which play an essential role for homing of B cells and establishment of germinal centers in lymphatic organs in vivo. On the one hand, CD19 and Gb_3/CD77 on neighboring cells interact and allow binding of B cells to each other and to follicular dendritic cells. On the other hand, CD19 binds to Gb_3/CD77 on the same cell and undergoes conformational changes. These changes are the pre-requisite for signaling from the CD19/CD21/CD81 complex and lead to strong cellular adhesion via integrins. Both types of adhesion anchor B cells in germinal centers. If Gb_3/CD77, and probably CD19, is down-regulated at the end of B cell differentiation, this adhesion is lost and B cells leave the germinal center. In fact, human B cells only express Gb_3/CD77 in germinal centers and terminally differentiated plasma cells lack CD19 [196]. If Stx binds to Gb_3/CD77, the molecules are no longer available for CD19 binding. This may significantly affect human B cell maturation and differentiation by inducing apoptosis, but may also prevent apoptosis by hampering CD19 cross-linking on the cell surface [202].

At protein level, subunit 1 of Interferon-α receptor (IFNAR-1) is homologous to the parts of StxB responsible for pentamer binding to Gb_3/CD77. This homology particularly exists in human and bovine IFNAR-1 [204]. Even though sequence homology of IFNAR-1 is lower than that of

CD19 [196], IFNAR-1 is able to bind Gb_3/CD77 on cell surfaces [204]. Interactions with Gb_3/CD77, as well as with Gb_2 and probably with Gb_4, induce conformational changes of the receptor, transforming it from the low-affinity to the high-affinity state [87]. In this way, glycolipids modulate IFNAR-1 without affecting its expression. Only binding of IFN to its high-affinity receptor allows exertion of biological effects [204]. Presumably because of its pentameric structure, Stx has a higher affinity to certain isoforms of Gb_3/CD77 than IFNAR-1 [87]. Incubation of Daudi cells in the presence of Stx1 results in a significantly reduced binding capacity for IFN-α to levels comparable to mutants devoid of Gb_3/CD77 [204]. These mutants exhibit a markedly lower IFN-dependent activation of cytosolic transcription factors [204], and consequently a lower proliferation inhibiting [205] and anti-viral activity of IFN-α [206]. Accordingly, Stx1 can block the anti-invasive effect of IFN-α on bacterial invasion in HEp-2 cells expressing physiological levels of Gb_3/CD77 [207] and Stx-producing *Shigella flexneri* bacteria are resistant to the respective effect of IFN [207]. Isolated B subunits are not sufficient to remove bound IFNAR from Gb_3/CD77 [206]. Binding competition occurs at the cellular surface, not requiring endocytosis of the Stx or its B subunit [206], but inhibition of protein biosynthesis by Stx may synergize with the blockage of IFN [207]. Interestingly, various effects of IFN-α appear to be mediated by IFNAR molecules interacting with different Gb_3/CD77 isoforms. Gb_3/CD77 isoforms with long-chain fatty acids primarily exist in the plasma membrane and participate—after interacting with IFNAR-1—in conferring the antiviral activity of IFN-α. Gb_3/CD77 isoforms with short-chain fatty acids, on the opposite, are preferentially internalized and confer the cytolethal effect of Stx as well as the IFNAR-1-dependent proliferation-inhibiting effects of IFN-α [206].

In silico analyses revealed an amino acid sequence similarity of Stx with the β-chain of human and murine major histocompatibility complex class II (MHC-II) [208]. Different from CD19, the surface expression of MHC-II is unaffected on Gb_3/CD77-deficient Daudi cell mutants even if the cells possess a decreased total MHC-II protein content. It was assumed that binding of Gb_3/CD77 to MHC molecules can modify their peptide-binding properties [208].

Beyond a direct functional impact, the existence of Stx-like Gb_3/CD77 binding sites in CD19, interferon receptor and MHC-II may be of paramount relevance for the course of STEC infections because such homologies may force the immune system to suppress specific responses to Stxs to prevent autoimmunity. In addition to a direct impact of Stxs on human B cells, this may explain why humans usually only develop low antibody titers against the toxins [196,209].

4. Shiga Toxins' Modes of Action

4.1. Internalization and Enzymatic Activity

4.1.1. Receptor-Mediated Endocytosis

Stxs were the first ligands recognized to utilize glycolipid receptors for endocytosis via clathrin-coated vesicles [95]. In colonic carcinoma cell lines and primary HUVEC, Toll-like receptor 4 (TLR-4), a pattern recognition receptor for LPS, facilitates Stx binding to cells expressing Gb_3 [210]. In these experiments, clathrin-dependent Stx1 holotoxin uptake by the epithelial cells was greater than uptake of Stx1 B subunits, suggesting that the A subunit is implicated in TLR-4-aided toxin internalization [211].

Ten to 15 min after binding to Gb_3/CD77 in lipid rafts [178], receptors become enriched in clathrin-coated membrane pits by lateral movement [187]. The underlying mechanism remains to be elucidated [211] but may involve membrane-mediated mechanisms that drive toxin molecules together [49]. Stx molecules would suppress thermally excited membrane fluctuations not only at the sites at which they bind, but also on the membrane patch between two adjacent toxin molecules, as long as these are not further apart than approximately the size of the toxin itself [212]. Unperturbed fluctuation of the membrane outside this toxin-delineated patch would push the toxin molecules together, even if these were not experiencing a direct attractive force [49]. Furthermore, because Gb_3/CD77 molecules lack a transmembrane domain, interactions with membrane proteins, like

CD19 [202], IFNAR-1 [204], and MHC-II [208], may help to hold back the Stx receptor, cross-linked by bound multivalent toxin, in membrane pits [213]. The high density of certain Gb_3/CD77 isoforms is believed to further support clustering of bound Stx molecules in lipid rafts [178]. Importantly, binding of the complete AB_5 Stx holotoxin seems to be specifically required for the ability of high toxin concentrations to induce an increased rate of toxin endocytosis [211]. In A431 and BHK cells, stimulation of Stx endocytosis is not due to an unspecific aggregation of glycosphingolipids in lipid rafts in the plasma membrane, nor is a mere aggregation of Gb_3 by Stx B subunits sufficient to stimulate Stx internalization. It was suggested that the A subunit of Stx is directly involved in important interactions either to other A subunits, which could possibly cluster the toxins, or to other plasma membrane proteins, which might facilitate toxin internalization like TLR-4 [211]. Alternatively, the A subunit might influence toxin internalization indirectly by affecting the exposure of its associated B subunits. This could change the surface location of the toxin or facilitate interactions with other membrane proteins fostering internalization. Since the interaction of human serum amyloid protein with Stx2 is mediated by both, the A subunit and the B pentamer [214], interactions with soluble proteins may further impact on the binding and internalization process of Stxs to target cells in vivo.

Molecular dynamics simulations suggest that the B subunits induce an increment of negative inward-oriented curvature when interacting with a patch of membrane that contains Gb_3 receptor molecules [215]. When 13 out of 15 Gb_3 binding sites per Stx B subunit molecule are occupied, positioning 10 of the Gb_3 binding pockets at the rim of the B subunits in a location slightly above the normal plane of the membrane, the latter must bend up to reach these sites [215]. Pinching off membrane invaginations enriched for receptor-bound Stx from the plasma membrane likely occurs by fusion of the opposing walls of invaginated tubular endocytic pits [49]. This process may involve the conventional pinchase dynamin [216] and actin as one of the formation triggers [217]. Alternatively, the formation of a highly curved membrane domain sends out a mechanical signal [49], recognized by proteins of the Bin, Amphiphysin, and Rvs (BAR) domain family [218]. Endophilin-A2 was functionally localized on Stx-induced membrane invaginations in relation to the scission reaction [219] and may give rise to a dynein-mediated pulling force.

At the time the toxin is enriched in certain areas of the membrane, Stx can readily be detected in tubular and vacuolar endosomes [187]. After fusion of endosomes with acidic vesicles, vesicles containing 5%–10% of internalized toxin are transported along microtubules [220] to the trans-Golgi network at 37 °C within 60 min [187,213]. The underlying sorting mechanism is determined by the length of the fatty acids in the Gb_3/CD77 molecules [221,222] and independent of Rab9 [223] or Rab5 (S34N mutant) [224]. Instead, γ-Adaptin [225], SNARE proteins VAMP2, VAMP3, and VAMP8 [226,227], Syntaxin 5 [228], the phosphoinositol-binding clathrin adaptor EpsinR [229], Rab5a, and TRAPPC6B [230] are involved in this cAMP-dependent process [222]. While the receptor returns to the cell surface presumably within minutes [231], the toxin remains in the cell even if it is not translocated into the cytosol [187].

Stx does not contain a KDEL-motif [232], but, via the Golgi apparatus and by a specific retrograde transport route relying on the small GTPase Rab6a [226,233], reaches the endoplasmic reticulum (ER) and the nuclear membrane [234]. Transport involves Syntaxin-16 and Syntaxin-5, EpsinR, Arl1, OCRL, retromer, the tethering complex GARP and the GARP interactor TSSC1, the ARF1 GAP protein AGAP2, GPP130, the ERM proteins Ezrin and Moesin, annexins A1 and A2, and UNC50 (as reviewed in [49]). The route of transport is determined by specific, yet ill-defined properties of Gb_3/CD77 indicated by the fact that human CD19 becomes retrograde transported to the nuclear membrane only when complexed with Gb_3/CD77 [202]. For exerting cytotoxic effects, transport of Stxs to the ER is essential, as the indispensable translocation into the cytosol only occurs here [187]. Inhibition of endocytosis by ATP deprivation, inhibition of the cytoskeleton, lowering of intracellular pH or temperatures below 20 °C renders cells resistant to Stxs [114,187,235]. For efficient endocytosis to occur, polarization of cells seems to play a minor role as the toxin was found to be internalized from the apical and baso-lateral side of cells with equal efficacy [109,236].

Interestingly, many toxin-resistant cell lines bind Stx with high affinity [181]. It is assumed that reduced levels of cellular sensitivity are a result of slower internalization, inefficient intracellular processing, a low sensitivity of the protein synthesis machinery, or combinations thereof. Indeed, some cells possess an alternative endocytosis pathway for Stxs, mediated by Gb_3/CD77 molecules located outside lipid rafts in the cell membrane [178,224]. This pathway is clathrin-independent [224] and much slower than clathrin-dependent endocytosis, due to the ~1 min half-life of clathrin-coated pits at the cell surface [237]. Clathrin-independent endocytosis transports Stx to late endosomes in which the toxin is degraded [178]. Stx may be transported efficiently at least to the Golgi apparatus [224], but the respective cells are 1000-fold less sensitive than cells realizing transport to the ER and the nuclear membrane [221]. The considerable variation of eukaryotic cells in the sensitivity to Stx is determined by the lipid moiety of the Gb_3/CD77 isoforms and its consequence for the intracellular transport route, as well as by the ratio of clathrin-dependent and -independent endocytic processes [238].

4.1.2. Gb_3/CD77-Independent Endocytosis

In vitro studies showed that human blood cell-derived microvesicles containing Stx undergo endocytosis in human glomerular endothelial cells where microvesicles release their content of Stx within 12 h of entering the cell and the toxin reaches ribosomes within 24 h, leading to cell death by inhibition of protein synthesis [34]. Evidence exists that Stx2-containing microvesicles play a pivotal role in transport and transfer of Stxs in vivo and are even transferred from cell to cell [34], suggesting that Gb_3-independent targeting of host cells is a yet under-appreciated pathogenic mechanism, presumably with significant implications for the course of STEC-associated diseases. However, this apparently Gb_3-independent process of toxin uptake requires the presence of Gb_3 in order for the initial binding of Stx to platelets [33], monocytes [157], and red blood cells [31] to occur.

Human neutrophils are major toxin carrier cells but lack Gb_3-type Stx receptors. Instead, TLR-4 binds Stx to the neutrophil surface without triggering toxin internalization and intracellular routing [239,240]. Different from human monocytes, in which pronounced cytokine response to Stx depends on Gb_3, brief incubation (90 min) of human neutrophils with Stx1 results in the release of only minute amounts of proinflammatory mediators [241].

4.1.3. Intracellular Processing in the Target Cell

The enzymatic function of Stxs is associated with an enzymatic cleavage product of the A subunit [242]. By tryptic cleavage at arginine residues 248 or 251, two fragments of 27 and 6 kDa are generated that at first remain connected by a disulfide bound. Upon its reduction, the enzymatically active 27 kDa A_1 fragment is released [243]. Proteolytic cleavage of Stx A subunit was detected in bacterial lysates as well as within Vero cells [244]. The former finding indicates that Stx, released from STEC by secretion or in outer membrane vesicles [34], may reach the target cells in a pre-activated stage. Furthermore, Stx2d is activated 10- to 1000-fold for Vero cell toxicity by preincubation with intestinal mucus containing elastase, whereas Stx2, Stx2c, Stx2e, and Stx1 are not activatable [64]. The peculiar feature of Stx2d is determined by two amino acids of the A_2 fragment that represent the only amino acid differences to the non-activatable Stx2c and are cleaved off by elastase. This process requires the presence of the homologous Stx2d B pentamer, suggesting that activation involves B pentamer-dependent cleavage by elastase of the C-terminal two amino acids from the Stx2d A_2 fragment [64].

In the course of cellular intoxication, reduction of Stx likely occurs in endosomes or the trans-Golgi network. At a pH of 5–6, the Stx A subunit is cleaved by a soluble form of Furin, a calcium-sensitive serine protease with a specificity for Arg-X-Arg/Lys-Arg motifs [245,246]. Alternatively, Stxs may also be cleaved by the cytosolic protease calpain but with low efficacy only [245]. In cell-free systems, the purified Stx1 A_1 fragment is 3-times more effective than enzymatically pre-treated toxin and 6-times more effective than holotoxin [247]. The reason for this difference in activity is determined by the structure of the A_2 fragment, in which the methionine in position 260 is positioned in the enzymatically

active cleft of the A_1 fragment blocking the enzymatically active sites of Stx1 and Stx2 holotoxins, while the ribosome binding sites remain exposed to the solvent [248]. The A_1 fragment only becomes fully active after removal of the A_2 fragment [88,248]. Inhibition of endosomal fusion with lysosomes and inhibition of proteolytic degradation of endocytosed proteins prevents cells from the cytotoxic effects of Stxs [235]. Further degradation of Stxs does not take place in sensitized MDCK cells even 2 h after the addition of the toxin [109].

4.1.4. Translocation of the A Subunit into the Cytosol

Translocation of the A_1 fragment into the cytosol is essential for intoxication of cells [104,238] and occurs at the ER. Some reports question that endosomal-lysosomal fusion is required for processing and translocation of the toxin [249]. However, at low pH values in vitro, the Stx1 B subunit undergoes conformational changes [79]. At pH 4.5 marked yet reversible changes at Trp34 take place. This residue is located at the orifice to the central pore formed by the α-helices of the five B subunits in the pentamer. Changes are likely originating from protonation of the aspartate side chains of residues 16 or 18 and the resulting interruption of a salt bridge to the adjacent Arg33. This leads to destabilization of the α-helix' N-terminus or interferes with the polarity in the vicinity of the tryptophan. If pH-value further decreases, the α-helix itself becomes subject to conformational changes. In vitro, these alterations might occur even at higher pH-values, if the B subunits are bound to the receptor and associated with the Stx A subunit [79]. Because the amino acids affected by these conformational changes in the B subunit are detrimental for receptor binding and specificity of the holotoxin [86,87,94,126], changes may facilitate release of the holotoxins from the receptor [231].

During transport to the ER, Stx A subunits dissociate from the B subunits, following proteolysis and disulfide bond reduction [8,245,250]. Fragments of the A subunits associate with host ER intraluminal chaperones ERdj3/HEDJ, GRP94 and BiP, followed by translocation across the ER membrane into the cytosol [251,252]. Stxs, like other AB_5 bacterial toxins, utilize the host cell ER-associated protein degradation machinery to facilitate translocation but A subunits re-fold into their active conformation in the cytosol [253]. In the CT molecule, exerting a similar multimeric structure, α-helices of the five B subunits also form a central pore with a diameter resembling that of the Stx1 B pentamer. This pore is believed to act as a transmembrane channel allowing the A_1 fragment, supported by the A_2 fragment, to pass and to reach the cytoplasmic side of the membrane [79]. In the ER membrane, CT is also complexed with Sec61p, which transports newly synthesized proteins into the ER lumen as well as misfolded proteins back into the cytosol for proteasomal degradation during normal cell growth [254].

Compelling evidence also exists that the B subunit itself is translocated into the cytosol: by creating fusion proteins with the B subunit, exogenic antigens can be channeled into the MHC-I antigen presentation pathway [255–257].

4.1.5. Inhibition of Protein Biosynthesis by Ribosomal Inactivation

Stx acts as one of the most potent inhibitors of the protein synthesis machinery in eukaryotic cells [126] by inactivating 60S ribosomal subunits. Notably, the Stx2 A_1 fragment has a higher affinity for binding to mammalian ribosomes than the Stx1 A_1 fragment [96]. The nucleotide sequence of ribosomal 28S RNA, as the functionally most important component of the 60S subunit, is highly conserved at positions 4320-4329 in eukaryotic cells [258]. A homologous structure in *E. coli* 23S rRNA binds elongation factors [259]. This sequence forms a hairpin structure [242], with an adenine residue at position 4324 in the loop (Figure 5).

In toxin-treated cells as well as in cell-free systems, this adenine residue is specifically cleaved off by the A_1 fragment of Stx in a non-phosphorolytic manner [258,260]. This N-glycosidase-activity is independent of several cofactors (NAD, ATP, NADP, NADPH, elongation factors, aminoacyl transferases) [247] and common to all Stxs [95]. The Stx1 A subunit can depurinate ribosomes at physiological pH but depurinate isolated RNA only at an acidic pH [96], indicating that the ribosome creates a microenvironment supportive of enzymatic activity of Stxs. Comparison of amino acid

sequences of Stx1 and the plant toxin Ricin yielded three regions of homology at amino acids 51–55, 167–171, and 202–207 of Stx1 [261]. The latter two stretches are located in the enzymatic active cleft of the molecule, the bottom of which is formed by Glu167 and Arg170. The upper part of the side wall is formed by the phenolic rings of tyrosine residues 77 and 114 on the one side and by the rings of Trp203 on the other [262].

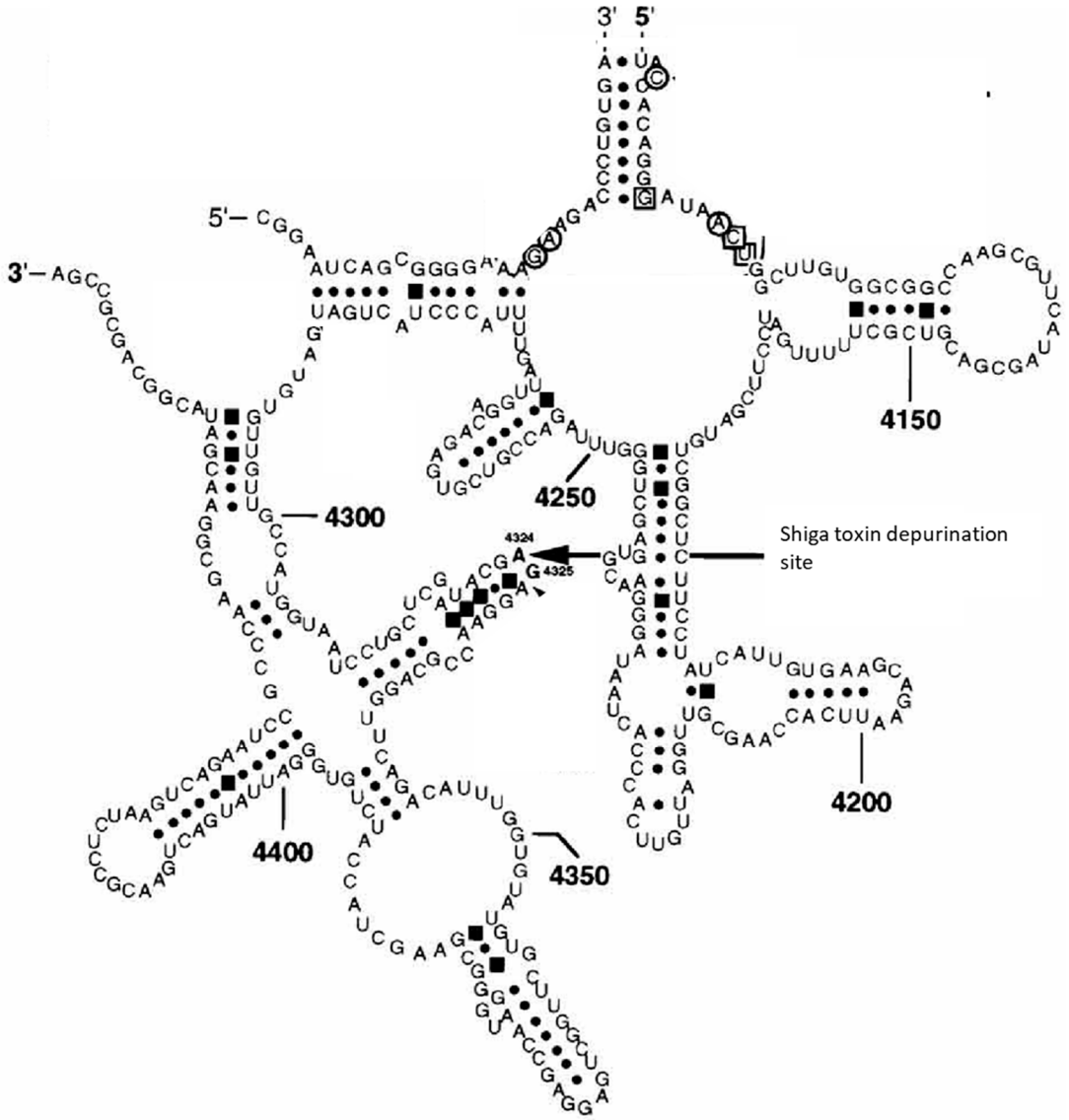

Figure 5. Secondary structure of the 28S rRNA target structure recognized by Shiga toxins. Watson Crick pairs are indicated by dots, non-Watson Crick pairs by quadrants. Reproduced from reference [263]. American Society for Microbiology, 1997.

The following course of events is believed to take place during the biochemical reaction catalyzed by Stxs (Figure 6) [262]:

1. Arg170 binds the ribose-phosphate backbone of 28S rRNA by forming ionic bonds. Tyrosine 77 and 114 and Trp203 stabilize this binding with their aromatic rings and adjust adenine residue 4324 of the rRNA.
2. Tyr77 transfers a proton to a nitrogen atom in the adenine ring and weakens the bond between C1 of the ribose and N9 of the adenine residue.

3. The protonated adenine dissociates, leaving behind a positively charged oxocarbonium ion in the ribose ring, stabilized by Glu167.
4. Finally, a water molecule attacks the oxocarbonium ion, hydroxylating the ribose and restoring the proton donor Tyr77.

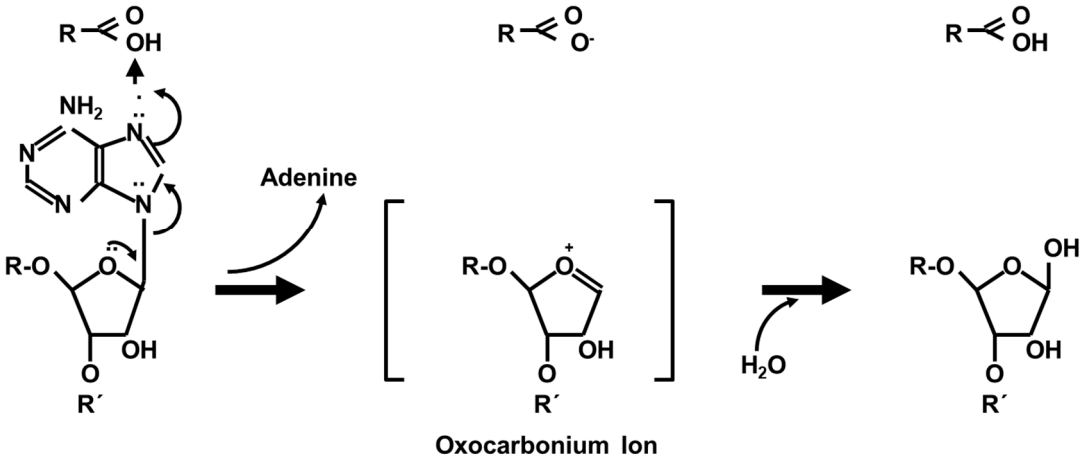

Figure 6. Proposed mechanism of the N-glycosidase activity of Shiga toxins. Reproduced from reference [262]. American Chemical Society, 1992.

Removal of the adenine residue results in a conformational change in the 28S rRNA and decreases the ribosomal affinity for eukaryotic elongation factor 1 (eEF1), detectable by a significant decrease in eEF1-dependent GTPase activity [264]. As a consequence, eEF1-dependent binding of aminoacyl-tRNA to ribosomes is dramatically impaired [264]. Subsequent steps of the protein biosynthesis (aminoacetylation of tRNA, initiation, peptidyl transferase reaction, translocation) are not directly affected by Stx [264]. Nevertheless, ribosomes become effectively and irreversibly inactivated [247]. This particularly holds for those ribosomes which are bound to mRNA and are biochemically active at the time Stx exerts its effect, because Stxs only target 60S ribosomal subunits if part of a complete ribosome [247]. As a consequence, protein biosynthesis is stopped at the step of elongation, resulting in fixation of the polysomal structure [247], withdrawing the concerned mRNA from interactions with remaining yet intact ribosomes. The reaction rate of the inactivation has been calculated as 40 ribosomes per minute per A_1 fragment of Stx1 in cell-free systems [247]. For HeLa cells, a ratio of 1000 ribosomes per toxin molecule was deduced [265], a single Ricin molecule reportedly inactivates 1500 ribosomes per minute [266]. The Stx2 A_1 fragment even exerts a higher affinity for ribosomes, depurinates ribosomes at a higher catalytic rate, and inhibits translation at a significantly higher level than the Stx1 A_1 fragment in human cells [96].

4.1.6. Nuclear Transport and Intra-Nuclear Effect

Although translocation of the A_1 fragment into the cytosol occurs at the ER level, the cytolethal effect of Stxs requires retrograde transport of the toxin to the nuclear membrane in some cell systems [221]. In some cells, even accumulation of Stx B subunits within the nucleus has been observed [221]. This transportation pathway is so efficient that DNA fragments can be targeted to the nucleus by means of chimeric proteins made of Stx1 B subunit and DNA-binding proteins [267].

Interestingly, transport of the Stx1 B subunit to the nucleoli even occurs in cells resistant to the protein biosynthesis-inhibiting effect of Stxs [252]. The underlying pathway, described for human macrophages, does not follow the biosynthetic/secretory pathway via the ER [252]. Transport may occur within the cytosol, because elevation of the endosomal pH, essential for translocation of Stx into the cytosol, blocks this transport [252]. This mechanism, however, would require translocation of the B subunit as postulated by Nakagawa et al. [268]. Indeed, the Stx1 B subunit interacts with BiP, an

ER-located chaperone, associated with the retrograde transport of proteins to the cytosol [252]. Stx B subunit passively diffuses into the nucleus in permeabilized cells but the transport is ATP-dependent in native cells [252]. After reaching the nucleus, the Stx1 B subunit binds to the nuclear protein B23 (Nucleoplasmin) at equimolar ratios, with both isoforms (B23.1 and B23.2) being recognized equally well [252]. B23 is a multi-functional protein also involved in correct formation of ribosomes. Due to the interaction of the Stx1 B subunit and B23, the Stx holotoxin may be particularly guided to the nucleoli, the generation site of its molecular target [252].

Inactivation of ribosomes is the mechanism the cytolethal activity of Stxs is principally based upon but Stx1 also exerts an adenine-specific N-glycosidase-activity for single-stranded DNA [269]. In vitro, the A_1 fragment binds to DNA and slides along it until reaching a suitable target structure [269]. Stx1 does not exert a DNAse-activity itself but removal of several adenine residues weakens the sugar-phosphate backbone of the DNA and gives rise to strand breaks [269]. Such was observed in endothelial cells after inhibition of the protein biosynthesis by the ribosomal effects of Stx1 but several hours before induction of DNAses of the apoptosis program [270].

4.2. Induction of Eukaryotic Cell Death

4.2.1. Consequences of Protein Biosynthesis Inhibition

Irreversible inhibition of protein biosynthesis by Stxs does not immediately result in the ultimate destruction of the affected cell [271]. In highly sensitive cells, protein biosynthesis starts to decline as early as after 30 min and totally ceases at 45 min. However, cells remain capable of uridine uptake for RNA synthesis for several hours [247,265]. The polysome profile of intoxicated cells remains intact [247]. Cells conduct endocytosis for up to 90 min time with the impact of the toxin and keep their intracellular calcium level constant for up to 120 min. Until then, Stx neither impairs membrane integrity nor oxidative phosphorylation [265]. Only after 4 h, DNA of HeLa cells starts to show signs of fragmentation [272].

Manifestation of functional and subsequent morphological alterations takes several hours in which mechanisms inherited by the targeted cells become activated. Electron microscopy shows circumscribed chromatin masses in the nucleus of Vero cells after 6 h only [271]. The cytosol in the vicinity of the nucleus possesses numerous vacuoles, in part lipid vesicles from blebbing of the nucleus, in part autophagic vacuoles containing membranous material [271]. Inhibition of autophagy prevents cells from lysis, even when deployed at a time the impact of Stx has already terminated cellular protein biosynthesis [271].

Such morphological alterations and degradation of DNA are hallmarks of apoptosis [271]. Although apoptosis represents an active form of cellular death and relies on intact protein biosynthesis in many cells [273], several translation inhibitors may induce apoptosis probably due to an accumulating shortage of proteinaceous apoptosis inhibitors and initiation of the genetic program and cell death [274]. In fact, Stx1- and Stx2-induced apoptosis in human endothelial cells is preceded by a significantly lowered expression of Mcl-1, a member of the anti-apoptotic Bcl-2 family [275]. DNA fragmentation following impact of Stxs cannot be observed in every cell system and apoptosis inhibitors may not always prevent cells from lysis [271]. Nevertheless, inhibition of protein biosynthesis by Stxs is an important co-factor for the induction of apoptosis, if cells have become sensitized by another stimulus before [276]. This stimulus may be Stx itself, implying that the toxins may induce apoptosis, independent of their protein biosynthesis-inhibitory action. In addition, Stx1 sensitizes human endothelial cells to LPS-induced apoptosis by inhibition of the expression of the anti-apoptotic protein FLIP, a caspase-8 inhibitor [140]. Caspase-8-mediated cleavage of Bid and relocalization of its cleavage fragment tBid to the mitochondria is necessary for Stx1-mediated apoptosis in Burkitt's lymphoma cells [277].

Cells do not exhibit morphological alterations visible by light microscopy for the first 12 h [247] but then begin to loose membrane integrity [247,271]. Stx1 irreversibly arrests HCT116 cells in the

S phase within 24 h and only prolonged incubation triggers DNA fragmentation. Concomitant to the activation of the S phase checkpoint, levels increase of mRNA and proteins of growth arrest and DNA damage-inducible gene family, i.e., GADD34, GADD45a, and GADD45b but not of key cell cycle related proteins such as CDK2, CDK4, p21, p27, and p53 [113]. Less sensitive cells, e.g., confluent endothelial cells without cytokine stimulation, only exhibit a 40% decline in protein synthesis and cells remain fully viable for up to 48 h [110]. These endothelial cells represent the main target for Stxs in humans and piglets in vitro, suggesting that sublethal damage of cells rather than total destruction may be of utmost importance in the pathogenesis of Stx-mediated diseases [110].

4.2.2. Direct Activation of the Apoptosis Program

Beyond inhibition of protein synthesis, Stxs have also been found to directly induce apoptosis by activating either of two signaling pathways [278]. One pathway originates from cross-linking of Gb_3/CD77 on cellular surfaces (see Section 4.2.3.), whereas the second requires internalization of the enzymatically active A subunit into the cytosol (Figure 7).

Depurination of 28S rRNA at translationally active ribosomes by the Stx A subunit leads to structural alterations in critical regions of the rRNA and functional impairment during translation [263]. These deviations result in the activation of stress-activated protein kinases (SAPK/JNK) and induce a ribotoxic stress response (see Section 4.3) [263], induction of the expression of various chemokine genes (see Section 4.5), and caspase activation [279]. Accordingly, inhibitors of the MAPKp38 protect cells from Stx-induced cell death [279,280], despite the fact that inhibition of certain MAPK like ERK may enhance caspase-3 activation [281]. Even though the absence of inflammatory signs is one hallmark of apoptosis, the Stx-induced signaling pathways leading to the expression of proinflammatory genes and to apoptosis are closely interconnected [279].

Activation of caspase-8 is of pivotal importance for induction of apoptosis in Burkitt's lymphoma cells [278], Hep2 [282], and HeLa cells [272]. Activated caspase-8 cleaves and activates the central effector caspase-3 [272,278,283]. Caspase-3, in turn, cleaves the nuclear factor acinus [284] and caspase-6 [272,285], which cleaves and activates lamin A [286]. In addition, a positive feedback loop exists with caspase-6 directly activating caspase-8 [287]. Activation of acinus and lamin A results in chromatin condensation [284] and disruption of the internal nuclear structure [286]. Caspase-3 inactivates an inhibitor of caspase-dependent DNases (CAD) [272] as well as poly(ADP-Ribose)-polymerase PARP [282], a DNA repair enzyme. Activation of CAD in conjunction with inhibition of DNA repair enzymes results in DNA fragmentation by inter-nucleosomal cleavage. Furthermore, single-stranded DNA becomes more prone to undergo strand breaks following depurination catalyzed by StxA in the nucleus [269]. Treatment with curcumin, inducing expression of heat shock protein Hsp-70, prevents DNA fragmentation and protects cells from the cytolethal effect of Stxs [288].

Stxs also induce activation of caspase-2 and -10 in THP-1 cells [285] and caspase-7 in Burkitt's lymphoma cells [283].

Activation of caspase-8-dependent signaling pathways is of prime importance for the induction of apoptosis by Stx holotoxins in Burkitt's lymphoma cells [278]. Nevertheless, in Stx-treated HeLa and Hep2 cells, caspase-8 also cleaves BID, a pro-apoptotic member of the Bcl-2 family located in the outer mitochondrial membrane [272,282]. Activated BID (truncated BID, tBID) promotes oligomerization of the pro-apoptotic proteins Bax and Bak. The subsequent increase in the permeability of the mitochondrial membrane leads to the collapse of the membrane potential and release of cytochrome C into the cytosol [272]. Cytosolic cytochrome C forms complexes with Apaf-1 (apoptotic protease activating factor) and activates caspase-9 [272,282,285,289]. Activation of caspase-9 promotes cleavage and activation of caspase-3 induced by caspase-8 [272,285].

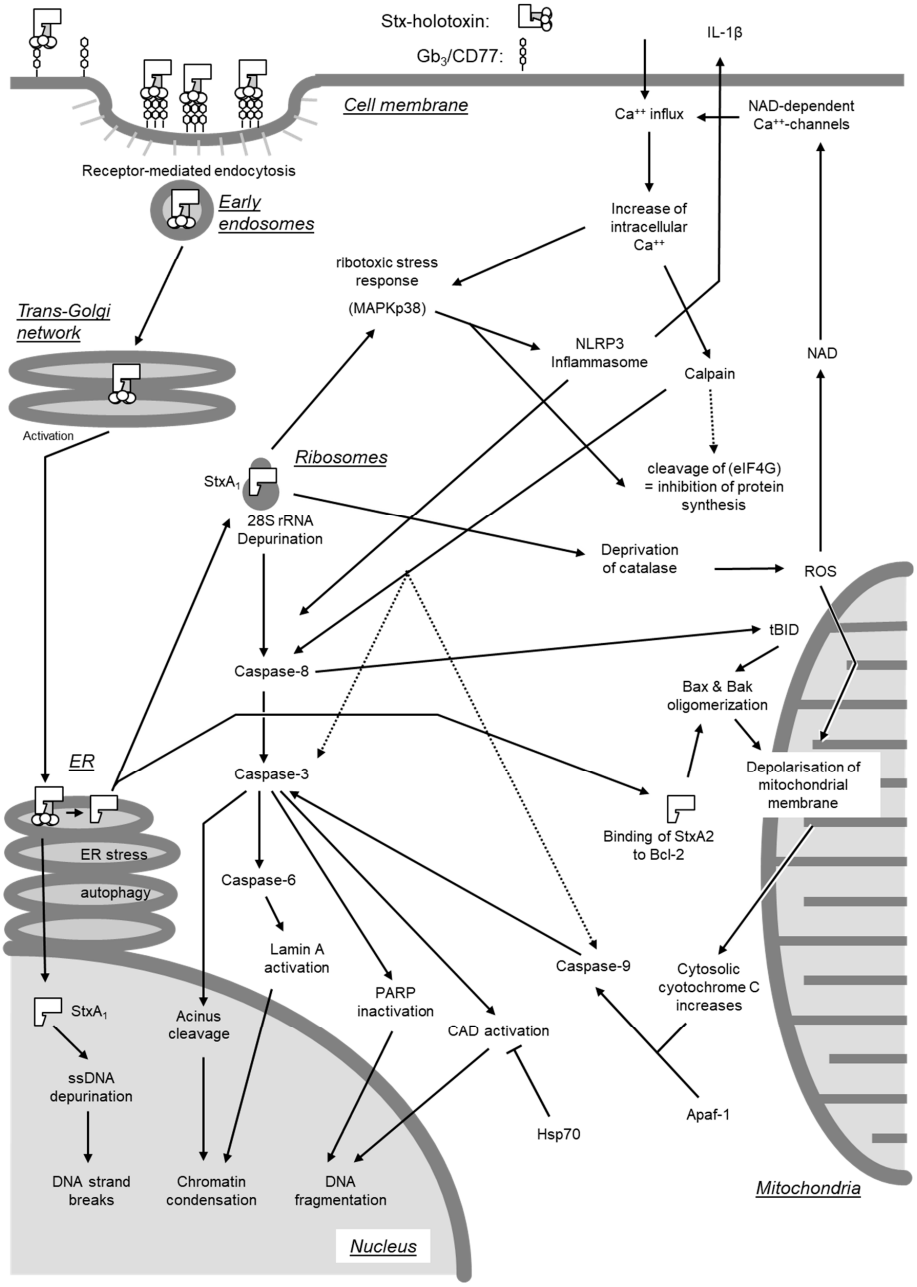

Figure 7. Graphical representation of selected intracellular effects and induction of apoptosis in mammalian cells following internalization of Shiga toxin holotoxins (Stx). Upon binding to the Gb_3/CD77 receptor, Stxs undergo receptor-mediated endocytosis and incorporation into the early endosomal pathway. Along the microtubule, the toxin reaches the trans-Golgi network and, by further retrograde transport, the endoplasmic reticulum (ER) and eventually the nucleus. In the ER, the A subunit of the holotoxin is cleaved and the A_1 fragment is translocated into the cytosol. At the ribosomes, A_1 fragments lead to depurination of 28S rRNA subsequently causing decreased ribosomal binding affinity to e(EF1), irreversible inactivation of ribosomes, and inhibition of protein synthesis (ribotoxic stress response). In the ER, A_1 fragments induce the unfolded protein response (UPR) indicated by activation of ER stress markers (IRE-1, PERK, not shown). C/EBP homologous protein is induced, which acts pro-apoptotic as Bcl-2 is inhibited (not shown). The ribotoxic stress response is linked to NLRP3 inflammasome generation and IL-1β formation. Via nicotinamide dinucleotide (NAD), reactive oxygen species (ROS) initiate an increased Ca^{++} influx into the cytosol by opening

NAD-dependent Ca^{++} channels. Intracellular, the calcium-dependent cysteine protease calpain is activated. Calpain can activate caspase-8 directly, yet many other targets of calpains are known like actin, caspases-3 and -9 (activation), and cleavage of the eukaryotic initiation factor 4G (eIF4G), resulting in inhibition of protein translation. Starting from caspase-8, a cascade of events is initiated encompassing activation of caspase-3 and caspase-6. The subsequent activation of signaling molecules/caspases is also subject to positive feedback loops (e.g., caspase-6 activating caspase-8, not depicted) and linked to the mitochondrial apoptotic pathway (caspase-9). The integrity of DNA is targeted via activation (lamin A, acinus, CAD) or inactivation of factors (PARP), or depurination by Stx A_1 fragment. ROS and tBid cleavage are linked to depolarization of the mitochondrial membrane and Apaf-1/cytosolic cytochrome C-mediated caspase-9 activation. Stress-induced proteins like HSP70 inhibit activation of CAD. Dotted lines indicate fundamental cellular biology mechanisms not yet specifically linked to Stxs; for details and references see text.

Of note, the polypeptide chain of the A subunit of Stx2 contains a sequence motif (NWGRI, amino acid residues 223–227) homologous to the BH1-Domain of the anti-apoptotic Bcl-2 [290]. This domain is indispensable for the anti-apoptotic effect of Bcl-2 and normally is involved in the interaction with other Bcl-2 molecules and with Bax and Bak. By utilizing the BH1-homologous domain, StxA2, after translocation to the mitochondria, may form complexes with Bcl-2, removes Bax and Bak and also induces their oligomerization [290]. Although Stx1 also possesses a sequence (NWGRL, amino acid residues 234–238) with high similarity to the Bcl-2 BH1-domain, only Stx2 but not Stx1, interacts with Bcl-2 via NWGRI [290]. This may explain why the mitochondrial signaling pathway resulting in caspase-9 activation does not play a role in the effect of Stx1 on Burkitt's lymphoma cells [283]. Ectopic expression of Bcl-2 prevents Gb_3/CD77-mediated apoptosis by the Stx1 B subunit (see Section 4.2.3), but not the effect of the corresponding holotoxin [291]. As recently reviewed by Lee et al. [8], enhanced protein and mRNA expression of Bcl-2 is associated with protection from apoptosis induced by Stx1 in toxin-resistant macrophage-like cells under ER stress, while Bcl-2 expression is decreased in toxin-sensitive monocytic cells, leading to rapid apoptosis in the presence of the toxin [292]. Furthermore, amino acid Ser70 of Bcl-2 is phosphorylated, and the protein fails to translocate to mitochondria following Stx1 treatment of macrophage-like cells, whereas phosphorylation of Bcl-2 at Ser70 is significantly reduced in toxin-treated monocytic cells [292]. Although mature macrophage-like THP-1 cells are relatively resistant to the rapid induction of apoptosis by Stxs, downstream signaling through the apoptosis-inducing receptor-ligand pair DR5-TRAIL during ER stress contributes to delayed apoptosis detected in Stx1-treated macrophage-like THP-1 cells [293].

Oxidative stress following an intracellular increase of reactive oxygen species (ROS) causes an increase in permeability of the mitochondrial membrane [289]. Upon intoxication of cells by Stx, this stress may be the consequence of a reduced expression of cellular catalase [280,294]. When acting in concert with LPS, Stx2 activates caspase-4, gasdermin D, and the NLRP3 inflammasome in human THP-1 macrophages in a Gb_3-dependent manner [295]. Resulting Stx2/LPS mediated IL-1β secretion and the inflammatory form of apoptosis ("pyroptosis") are dependent on mitochondrial ROS, downstream of the non-canonical caspase-4 inflammasome and cleaved gasdermin D, which is enriched at the mitochondria [295]. In addition to their mitochondrial effect, ROS induce an increase in cytosolic NAD, thereby triggering an opening of NAD-activated Ca^{++} channels at the cellular membrane [296]. Uncontrolled influx of Ca^{++} ions in Stx-treated cells results in phosphorylation of MAPKp38 [280], creating a positive feedback loop to the ribotoxic stress response. At least in some cell systems, the Ca^{++}-influx appears to play a major role as Ca^{++} channel blocking agents like verapamil protect Vero and HeLa cells from the cytolethal effect of Stxs [249].

4.2.3. Activation of Gb_3/CD77-Dependent Signaling Pathways

Several tumor cell lines resist apoptosis induction by isolated B subunit of Stxs [272,285,297]. By contrast, cross-linking of Gb_3/CD77 at the cell surface by anti-CD77 antibodies or binding of StxB stimulates intracellular signals and apoptosis in Burkitts' lymphoma cells [278,298–300], as well as in

the human renal tubular cell line ACHN [179,298]. In the absence of the A subunit, the B subunits of both Stx1 and Stx2 bind to the glycolipids, but the more stable B pentamer formed by Stx1 binds better than the less stable pentamer of Stx2 [186], implying that both toxins are unequally able to initiate this signaling pathway (Figure 8).

In sensitive cells, Gb_3/CD77 is located in lipid rafts in spatial proximity to Src kinases Yes and Lyn as well as Syk [179,298,301]. Ten minutes after binding of Stx, tyrosine residues of raft proteins become hyper-phosphorylated. Binding of Stx to Gb_3/CD77 initially induces an enrichment of Yes and Lyn in the lipid rafts. Following activation, Yes and Lyn are removed from the lipid rafts but remain associated with the cellular membrane and do not follow the internalization of the Stx-Gb_3/CD77 complexes [179,298]. In B cells like Burkitt's lymphoma cells, the apoptosis-inducing signaling cascade originating from Gb_3/CD77 is closely linked to the signaling pathway originating from the B cell receptor [301]. Activation of the signaling cascade by surface binding of Stxs synergizes with the apoptosis induction, resulting from the cytosolic effects of Stx holotoxins [298].

As early as after 30 s after cross-linking of Gb_3/CD77, a massive influx of extracellular Ca^{++} ions can be observed, reaching its maximum after 120 s and followed by an increase of intracellular cAMP concentrations and activation of protein kinase A (PKA) within minutes [300]. Interestingly the Stx B subunits induce acute von Willebrandt factor secretion from human umbilical vein endothelial cells within 30 s via PKA (Stx2 B subunit) or PKCα (Stx1 B subunit), thereby eliciting rapid cellular effects themselves [302].

After 30 min, the cellular content of cytosolic ceramide increases [300]. Agonists like TNF-α or IL-1β can cause the release of ceramide from sphingomyelin by activating an endogenous sphingomyelinase, whereas uropathogenic *E. coli*, capable of Gb_3/CD77 binding via their P-fimbriae, only induce a minor increase in sphingomyelinase activity in epithelial cells (A498) and no detectable hydrolysis of sphingomyelin [303]. An increase of cytosolic ceramide in Stx-treated Burkitt's lymphoma cells also is not accompanied by a decrease in sphingomyelins [300]. The cellular content of Gb_3 remains constant under these conditions, arguing against a degradation of the Stx receptor after ligand binding as source [300]. The increase in ceramide content may be the result of ceramide synthase activation as observed after stimulation of bovine $\gamma\delta$T cells via the WC1 antigen [304].

Cytosolic ceramide is part of a signaling pathway particularly inducing apoptosis but also modulating cellular growth and differentiation and stimulating cytokine secretion [303]. Elevated intracellular ceramide levels, as inducible by bacterial sphingomyelinase treatment of human endothelial cells, induces increased expression of enzymes of the Gb_3/CD77 synthesis pathway and increased synthesis and surface expression of Gb_3/CD77 [141]. Because of the resulting sensitization of cells to Stx [141], it is tempting to speculate that in cells exhibiting at least some degree of Stx responsiveness, binding of a low number of Stx molecules to Gb_3/CD77 is sufficient to initiate a positive feedback loop comprising of increased receptor expression and subsequent increased toxin uptake. An increased synthesis rate of Gb_3/CD77 also gives rise to elevated cellular concentrations of the Gb_3/CD77 precursor lactosylceramide [141].

Intracellular ceramide was also identified as a TLR-4 agonist and putative signaling intermediate between glycosphingolipid receptors and TLR-4 [305]. Binding of microbial ligands to such receptors like P fimbriae or the B subunit of Stxs increases the levels of ceramide and triggers a TLR-4-dependent response in epithelial cells. This presumptive crossing of signaling pathways is of particular importance as TLR-4 facilitates binding of Stxs to epithelial and endothelial cells co-expressing Gb_3/CD77 [210]. Furthermore, CD19, a Gb_3/CD77 binding molecule, was found to regulate TLR-4 signaling through MAPKp38 activation [203] pointing to a complex network of signaling pathways Stxs can interfere with.

Ceramide and lactosylceramide both induce the generation of ROS in mitochondria [289,306] and thereby activate the mitochondrial signaling pathway of apoptosis induction, which also plays a central role in the Gb_3/CD77-dependent signaling pathway [278,291]. Cross-linking of Gb_3/CD77 on Burkitt's lymphoma cells leads to activation of caspase-8 [283], indicating that Gb_3/CD77 binding also can activate the extrinsic, caspase-dependent apoptosis pathway. Interestingly, even the Stx1 B subunit,

not inheriting any proteolytic activity, can trigger caspase-1 and -3 activation and initiate apoptosis when artificially expressed inside eukaryotic cells [268].

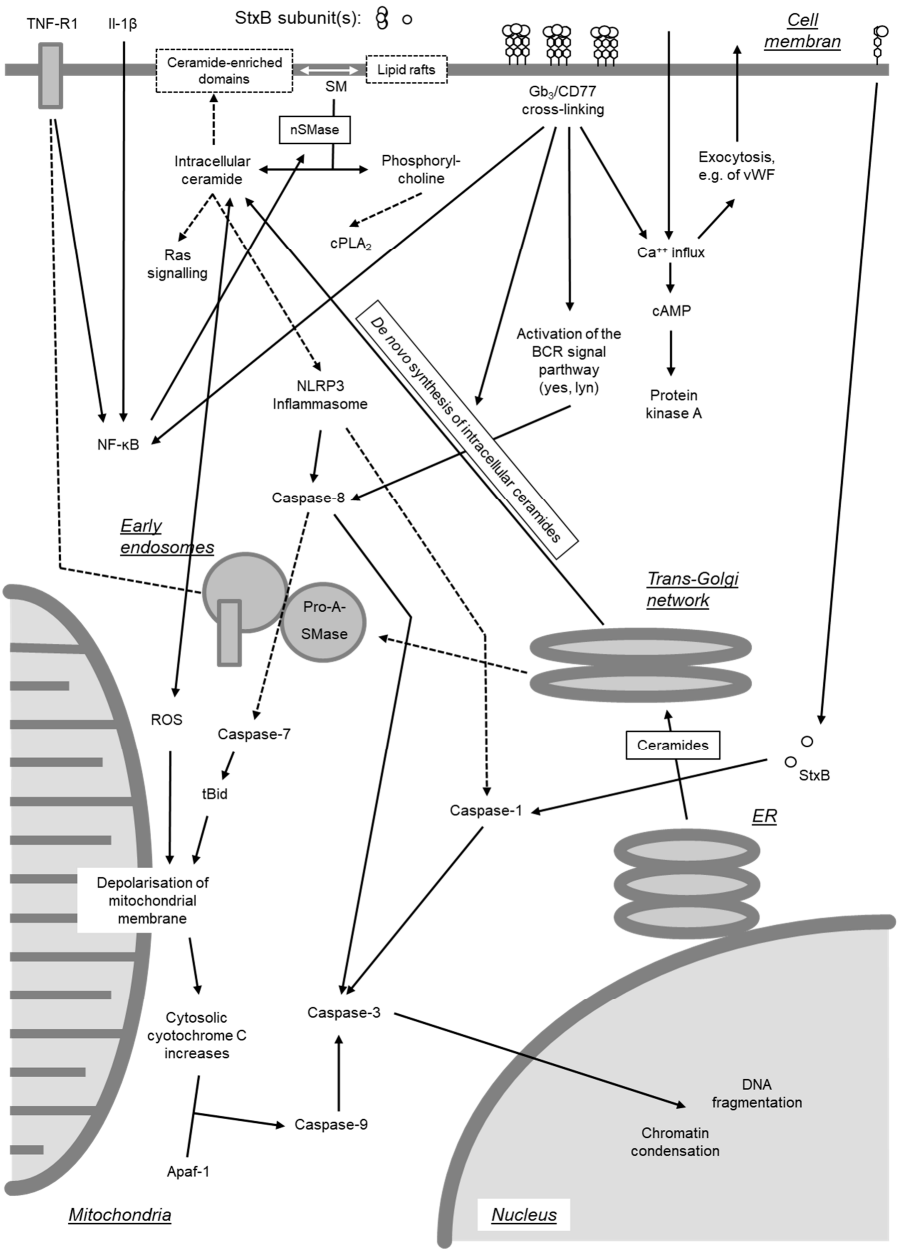

Figure 8. Graphical representation of effects in mammalian cells following binding of Shiga toxin (Stx) B subunits to cell surface receptors. Binding to Gb_3/CD77 cross-links several receptor molecules and thereby activates signaling cascades as well as internalization of the complex. In human B cells, binding of Stx to Gb_3/CD77 in lipid rafts induces an enrichment of Src kinases and initiation of the apoptosis-inducing signaling cascade associated with the B cell receptor. Activation of this cascade synergizes with apoptosis induction resulting from the cytosolic effects of Stx holotoxins. Cross-linking of Gb_3/CD77 also causes a massive influx of extracellular Ca^{++} ions followed by an increase of intracellular cAMP concentrations, activation of protein kinase A (PKA) and, e.g., acute von Willebrandt factor secretion from human endothelial cells. Stxs also likely impact on the sphingomyelinase-ceramide pathway. Sphingomyelinase (SMase) catalyzes sphingomyelin (SM) hydrolysis. Phosphorylcholine and intracellular ceramide activate cytosolic phospholipase A_2 ($cPLA_2$). Intracellular ceramide generates ceramide-enriched regions in the membrane, serves as second messenger (signaling) and activates inflammasomes. Different pathways are affected by ceramide like the Ras and PLA_2 signaling pathway.

Stx binds to the Gb_3/CD77 receptor, activates the first two enzymes of the Gb_3 synthesis pathway and induces their transcription. The de novo synthesis is complex and occurs at the trans-Golgi network and the ER. Intermediates (ceramides, lactosylceramide) induce reactive oxygen species (ROS) at the mitochondria, which are linked to the depolarization of mitochondrial membranes and the release of cytochrome C. Furthermore, ROS can activate SMases. IL-1β and receptors, which undergo crosstalk with Gb_3/CD77-mediated signaling pathways, activate NF-κB. Vesicles containing lysosomal SMases fuse with early endosomes containing TNF receptor (TNF-R1). Subsequently, caspase-7 is activated by caspase-8, leading to activation of SMase and tBid cleavage [307]. The mechanism has not yet confirmed to be implicated in Stx-mediated effects but it is reasonable to assume a possible link between SMase function and crosstalk of TNF-α, Gb_3/CD77 receptor, and apoptosis, which are proven to be associated with Stx. Gb_3/CD77-bound B subunit can also be translocated into the cytosol, trigger caspase-1 and -3 activation and directly initiate apoptosis. Pathways depicted in this figure are interconnected at several levels (inflammasome formation and IL-1β secretion; caspase activation; tBid; ROS) with pathways presented in Figure 7. Dotted lines indicate fundamental cellular biology mechanisms not yet specifically linked to Stxs; for details and further references see text.

4.3. Ribotoxic Stress Response

The ribotoxic stress response resulting from depurination of 28S rRNA [263] is not specific for StxA but can also be induced by other toxins like Ricin or α-Sarcin which modify the rRNA hairpin structure at positions 4320–4329 [263]. In case ribosomes are biochemically active at the time of impact of the toxins, resulting structural alterations in the peptidyltransferase center of the ribosomes activate small GTP-binding proteins, which in turn activate the protein kinase cascade, which, via MEKK1 and SEK1/MKK4, ends in the activation of stress-activated protein kinases SAPK/JNK1 [263]. The mitogen-activated protein kinase kinase kinase (MAP3K) that transduces the signal from intoxicated ribosomes to activate SAP kinases was identified as a zipper sterile-alpha-motif kinase (ZAK) [308]. Depurination of rRNA at position A4324 is detectable as early as 15 min after addition of Ricin to cell cultures [263]. This is followed after 30 min by sustained phosphorylation of SEK1/MKK4 and activation of SAPK/JNK1 which lasts for hours [263]. Activation of this cascade is independent of protein biosynthesis inhibition and also occurs under conditions in which protein translation is only marginally affected [263]. This may explain why cells, even after intoxication by Ricin or Stxs, still are capable of responding with an increased transcription of the immediate early genes *c-fos* and *c-jun*, which becomes apparent after 60 min [263,279,309]. In some cells, the increased transcription of *c-fos* and *c-jun* appears to be the consequence of MAPKp38 activation [279,309,310]. Stx-induced *c-jun* transcription increases concentrations of the c-Jun protein which is particularly present in its phosphorylated form [311]. Remarkably, the increase in phosphorylated c-Jun is accompanied by an increased expression of *mpk-1* (mitogen-activated protein kinase phosphatase 1), even though this phosphatase can inactivate JNK as well as MAPKp38 [311].

In addition to the SAPK/JNK1 and MAPKp38 signaling pathways, Stx also stimulates PKC activity [312]. Stx-treated human monocytes exhibit an increased activity of kinases, which are located in the signaling pathway downstream of atypical isoforms of PKC and are regulated by extracellular signals (extracellular signal-regulated kinases; ERK) [313]. This implies that Stx-induced PKC activity is realized by atypical PKC isoforms activation of which neither requires calcium nor lipids and which, e.g., are involved in LPS signaling [312].

Stxs activate an autoregulatory signaling loop since inactivation of ERK, JNK, or MAPKp38 in the presence of Stx1 results in differential regulation of TNF-α, IL-1β, IL-8, GRO-β, MIP-1α, and MIP-1β. THP-1 cells exposed to Stx1 upregulate the expression of selected dual-specificity phosphatases (DUSPs), enzymes that dephosphorylate and inactivate MAPKs in mammalian cells [314]. DUSP1 inhibition by triptolide showed that ERK and MAPKp38 phosphorylation is regulated by DUSP1, while JNK phosphorylation is not. In turn, inhibition of MAPKp38 signaling blocked the ability of Stx1 to

induce DUSP1 mRNA expression [314]. In addition, signaling through the PI3K/Akt/mTOR pathway was shown to initially activate proinflammatory cytokine expression via the phosphorylation of the eukaryotic translation initiation factor 4E-BP, which is later on down-regulated through the inactivation of the positive regulator glycogen synthase kinase (GSK)-3 [315], suggesting that the activation of cytokine signaling by Stxs ultimately downregulates the proinflammatory cytokine expression.

4.4. Endoplasmic Reticulum Stress and Autophagy

It was assumed that bacterial toxins of the AB_5 type highjack the ER-associated protein degradation pathway to enter target cells by presenting themselves as misfolded proteins [253]. As recently reviewed by Lee et al. [8], Stx1 is capable of inducing ER stress and activating three proximal unfolded protein response (UPR) effectors, PERK, IRE1, and ATF6, involved in the immediate detection of unfolded proteins [316]. Stx1 and Stx2 differentially activate non-overlapping sensors of ER stress rendering the intoxicated cells susceptible to the cytotoxic action of Stxs with significant cleavage of PARP, an enzyme primarily involved in DNA repair and induction of programmed cell death [317]. In Caco-2 cells exposed to Stx2, ER stress promotes autophagic cell death preceding apoptosis [318]. However, induction of autophagy by Stxs has different outcomes depending on the toxin-sensitive or toxin-resistant phenotype of the cells [8]. In toxin-resistant primary human macrophages, Stxs are translocated to lysosomes, and autophagy is induced in the absence of calpain and caspase activation, as well as Atg5 and Beclin-1 cleavage [319]. In toxin-sensitive cells, Stxs are translocated to the ER, the ER stress response is activated and autophagy is induced in association with the activation of calpains and caspase-8 and -3, as well as the cleavage of Atg5 and Beclin-1. Treatment of intestinal epithelial cells with Stx2 initiates autophagic cell death via the ER stress pathway and by triggering pseudokinase TRIB3-mediated DDIT3 expression and AKT1 dephosphorylation [318].

4.5. Induction of Proteinaceous (Inflammatory) Mediators

Involvement of signaling pathways as well as the fact that Stx-dependent activation of SAPK/JNK1 and MAPKp38 can be observed in human monocytes [310], indicate that Stxs may induce the expression of proteinaceous mediators even independent of the toxins' ribotoxic activity. In favor of this notion, the increase in intracellular ceramide concentration—as e.g., observed after Stx1 binding to Gb_3/CD77 in the absence of the toxins' enzymatic activity [300]—has already been associated with an increased cytokine gene expression [303]. Induction of caspase-1 by intracytoplasmic expression of Stx1 B subunit reportedly results in increased synthesis of IL-1β and TNF-α [268]. On the contrary, several studies failed to detect induction of genes following exogenous addition of isolated Stx B subunits or enzymatically inactive holotoxins to cell cultures [279,311,320–324]. Relative to Stx1, Stx2 significantly causes increased expression of GRO, G-CSF, IL-1β, IL-8, and TNF-α in macrophage-like THP-1 cells, which is not due to a difference in cytotoxicity [324].

Activation of inflammatory mediator gene expression by Stxs may also be a consequence of translocation of the transcription activator NF-κB. NF-κB binding sites are present in the promotor regions of many proinflammatory genes. Sakiri et al. [321] showed for THP-1 cells that the Stx1-induced elevation of TNF-α specific mRNA is preceded by the nuclear translocation of NF-κB and AP-1 (activator protein-1) and by the degradation of the NF-κB inhibitor IκBα. In ACHN cells, Stx2 induces increased *TNF-α* transcription via activation of cAMP-dependent PKA, MAPKp38, and NF-κB [325]. In Vero and T84 cells, these effects cannot be induced by purified toxin, but only in combination with a non-identified factor [310] or after infection of the cells with a STEC strain [326]. It is assumed that translocation of NF-κB in the course of the STEC infection is mainly induced by flagellin via TLR-5, as *stx*- and *eae*-negative *E. coli*-strains but not purified flagellin, fail to induce this effect [327].

As a consequence of Stx acting on ribosomes, the intracellular content of mRNA specific for primary response genes is increased in several cell systems. Induction of the genes is refractory to translational blockade. Stxs particularly promote mRNA induction by other agonists, a phenomenon known as super-induction [320,328]. Although other protein biosynthesis inhibitors like cycloheximide increase the cellular content of certain mRNA species by induction of transcriptional activators, as well as by stabilizing mRNA, the latter mechanism seems to be of prime importance for the effects of Stxs [328].

In the human renal proximal tubular cell line HK-2, Stx1 treatment elicits a modest and delayed increase in TNF-α mRNA expression, peaking at 6-fold increase 4 h after toxin exposure [317]. In contrast, Stx2 treatment induces a rapid increase in TNF-α mRNA (200-fold) detected 15 min after toxin exposure. TNF-α mRNA levels then decline by 30 min and begin to increase to levels 100-fold higher than those in control cells by 120 min [317].

In spite of the onset of protein synthesis inhibition after a few hours in less sensitive cells, the elevated total amounts of specific mRNAs give rise to increased neosynthesis of the encoded proteins, which can be detected after 12 h and lasts up to 24 h [328]. The degree of general inhibition of protein synthesis in the cells is negatively correlated with the translational activity for certain proteins [309]. Nevertheless, a massive increase in mRNA is often associated with an only minor increase in the respective protein [309,322,329], and interpreted as a consequence of partial translational blockage [309,322]. It heavily depends on the type and source of cell, which of the aforementioned effects prevail, and consequently what mediators are increasingly expressed and released by cells upon contact to Stxs (Table 3).

Different from other mediators like IL-8 and GRO-β, processing and release of biologically active IL-1β requires the formation of the NLRP3 inflammasome. Indeed, caspase-1 activation, reaching maximal levels at 4 h after treatment of cells with Stx1, correlates with the processing of inactive pro-IL-1β into mature IL-1β [330]. This Stx-mediated inflammasome activation is dependent on the toxin receptor Gb_3 and enzymatically functional Stxs [330].

Table 3. Overview of cytokines and chemokines induced by Shiga toxins or their subunits in cells of varying type and origin.

Cell Type/Line	Species	Toxin	Induction of		Reference
			mRNA [1]	Protein [1]	
Intestinal epithelial cells					
HCT-8	Human	Stx1	IL-8, GRO-α, GRO-β, GRO-γ, ENA-78	IL-8, GRO-α	[328]
		Stx1 + 2	IL-8	IL-8	[309]
Caco-2	Human	Stx1 + 2	IL-8, MCP-1, MIP-1α, MIP-1β, TNF-α	IL-8	[322]
Renal epithelial cells					
Glomerulum, primary	Human	Stx1	IL-1, IL-6, TNF-α	IL-1, IL-6, TNF-α	[331]
Tubulus, primary	Human	Stx1	IL-1, IL-6, TNF-α	IL-1, TNF-α	[332]
HK-2 (proximal tubulus)	Human	Stx1	IL-1β, TNF-α		[317]
		Stx2	IL-1β, IL-8, TNF-α, MIP-1α, MIP-1β	MIP-1α, MIP-1β	[317]
Endothelial cells					
Brain, primary	Human	Stx1	IL-1β, IL-6, TNF-α	IL-6, IL-8	[333]
Aortic, primary	Bovine	Stx1 (+2)	Preproendothelin-1	Endothelin	[139]
Umbilical vein, primary	Human	Stx1	IL-8, GRO-α, GRO-β, GRO-γ, TNF-α	IL-6, IL-8, GRO-α, MCP-1	[334]
		Stx2	IL-8, GRO-α, GRO-β, GRO-γ, IL-6, IL-16, MCP-1, TNF-α	IL-6, IL-8, GM-CSF, GRO-α, MCP-1	[334]
Fibrocytes/-blasts					
NIH3T3	Mouse	StxB1 [2]	IL-1β, TNF-α	IL-1β, TNF-α	[268]
Monocyte/Macrophage-like					
THP-1, differentiated	Human	Stx1 + 2	TNF-α	TNF-α	[312]
THP-1, differentiated	Human	Stx1	IL-1β, TNF-α	IL-1β	[320]
THP-1, differentiated	Human	Stx1	IL-8, MIP-1α, MIP-1α, GRO-α, IL-1α, TNF-α	IL-8, MIP-1α, MIP-1β, GRO-α	[329]
THP-1, differentiated	Human	Stx1 + 2		GRO, G-CSF, IL-1β, IL-8, TNF-α	[324]
THP-1, differentiated	Human	Stx1		TNF-α	[200]
THP-1, un-differentiated	Human	Stx1		IL-1β, TNF-α	[115]
THP-1	Human	Stx1	TNF-α	TNF-α	[321]
Peripheral blood, primary	Human	Stx1 + 2		GM-CSF, TNF-α	[313]
Peripheral blood, primary	Human	Stx1 + 2	IL-8, IL-1β, TNF-α	IL-8, IL-1β, TNF-α	[335,336]
Peripheral blood, primary	Human	Stx1		IL-1β, TNF-α	[115]
Peripheral blood, primary	Human	Stx1		IL-1β, TNF-α, IL-6, G-CSF, IL-8, CCL2, CCL4	[241]

Table 3. *Cont.*

Cell Type/Line	Species	Toxin	Induction of		Reference
			mRNA [1]	Protein [1]	
Peripheral blood, primary	Bovine	Stx1	IL-4, IL-6, IL-10, IFN-γ, TNF-α, IL-8 and GRO-α		[160]
Peripheral blood, primary, non-adherent	Human	Stx1	IL-6	IL-8, IL-1β, IL-6, TNF-α	[157]
Colonic mucosal macrophages, primary	Bovine	Stx1	IL-8, GRO-α, MCP-1, RANTES, IL-10		[133]
Peritoneal exudate	Mouse	Stx2		TNF-α	[337]
Peritoneal exudate	Mouse	Stx1 + 2	TNF-α	IL-1β, IL-6, TNF-α	[159]
Mesangial cells, primary	Human	Stx1	MCP-1		[338]
Neutrophils					
Peripheral blood, primary	Human	Stx1		IL-8, CCL4, G-CSF, TNF-α, IL-1β	[241]
Lymphocytes					
Ileal intraepithelial	Bovine	Stx1	IL-4		[339]

[1] Discrepancies in the lists of mediators at mRNA and at protein level principally result from the fact that not all cited studies have quantified the respective mediators at mRNA and at protein level; [2] Stx1 B subunit.

4.6. Induction of Arachidonic Metabolite Synthesis

The discovery of Zhang et al. [336], that Stx-induced TNF-α expression in human monocytes can be counteracted by treatment of the cells with a synthetic antagonist of platelet-activating factor PAF, points to the existence of yet another Stx-inducible signaling pathway. Indeed, PAF treatment of monocytes together with LPS results in an activation of ceramide synthetase and an increase in intracellular ceramide levels [340]. The latter can also be observed after Stx treatment of Burkitt's lymphoma cells [300]. The B subunit of CT accelerates cellular synthesis of arachidonic acid metabolites [341], implying that a signal originating from glycolipid receptors in lipid rafts is responsible for the ceramide increase. Elevated ceramide contents stimulate secretory phospholipase A_2 ($sPLA_2$) [340], transcription and translation of which is induced by Stx1 in primary human glomerular epithelial cells together with the cytosolic PLA_2 ($cPLA_2$) [342]. The resulting production of arachidonic acid, in concert with higher cyclooxygenase activity, leads to an increased synthesis of prostacyclin (PGI_2) and thromboxan A_2 (TXA_2) [342]. Free arachidonic acid metabolites activate, e.g., PKC and MAPK and, by modifying gene transcription, cause inflammatory responses. Since PGI_2 and TXA_2 partially cause opposite effects, the meaning of these findings for the pathogenesis of Stx-mediated diseases remains unclear [342]. In fact, Stx1-induced TNF-α expression in human monocytes is paralleled by increased prostaglandin E_2 (PGE_2) synthesis, but super-induction of PGE_2 by anisodamin inhibits Stx1-induced TNF-α expression [335].

4.7. Interaction of Shiga Toxins with Soluble Factors

In addition to binding to cellular surface receptors, Stxs were also found to directly interact with soluble extracellular protein, i.e., blood constituents. Stx2 activates human complement via the alternative pathway by direct interaction with complement components, considered to be relevant in HUS pathogenesis. Stx2 binds factor H (FH) at short consensus repeats (SCRs) 6–8 and 18–20 and delays and reduces FH cofactor activity on the cell surface [343]. Complement factor H-related protein 1 (FHR-1) and factor H-like protein 1 (FHL-1), similar proteins with regulatory functions, also bind to Stx2. The FHR-1 binding site for Stx2 is located at SCRs 3–5 and the binding capacity of FHR-1*A allotype is higher than that of FHR-1*B. FHR-1 competes with FH for Stx2 binding and thereby reduces FH cofactor activity [344]. Binding to FH depends on the proteolytic cleavage of Stx2A into the A_1 and A_2 fragments linked by a disulfide bridge. While binding of FH is exclusively exerted by cleaved Stx2, uncleaved Stx2 binds to human neutrophils and triggers leukocyte/platelet aggregate formation [345]. Furthermore, Stx2 downregulates complement inhibitor CD59 mRNA and protein levels on tubular epithelial and glomerular endothelial cells, and this downregulation is believed to further contribute to complement activation and kidney destruction in EHEC-associated HUS [346]. Even low concentrations of human amyloid P component (HuSAP) inhibit the toxic activity of Stx2 for target cells in vitro and protect mice from lethal effects induced by this toxin [347,348]. The interaction of HuSAP with Stx2 is mediated both by the A subunit and the B pentamer [214]. The soluble extracellular domain of TLR-4 inhibits the binding of Stx2 to neutrophils and the complex Stx2/soluble TLR-4 escapes from capture by HuSAP, allowing the toxin to target and damage human cells [349]. Bovine lactoferrin mitigates the bioactivity of Stx2, but not of Stx1, and this effect at least partly results from degradation of the Stx2 receptor-binding B-subunit [350]. Interactions with these soluble factors, which may occur in the course of STEC-mediated diseases at several stages of the pathogenesis, are likely to interfere with many aspects of Stx–host cell interactions in vitro, although the relevance of this awaits to be fully understood.

4.8. Transcellular Transport

The full spectrum of Stx cellular uptake mechanisms also remains to be characterized [8]. Macropinocytosis is an alternative pathway for the uptake of Stxs into cells that do not express Gb_3 [351]. This pathway in human intestinal epithelial cells, mediated through Src activation, stimulates toxin transcellular transcytosis [352]. Transcytosis across T84 monolayers is facilitated by changes in the actin

cytoskeleton induced by latrunculin B, but not cytochalasin D or jasplakinolide. An actin turnover may thus play an important role in Stx1 transcellular transcytosis across intestinal epithelium in vivo since EHEC attachment to epithelial cells causes an actin rearrangement [353]. Neither cell viability nor epithelial barrier function are compromised by this process [28,29]. Differences in translocation rates and directionality, effects of cellular drugs, and competition experiments indicate that Stx1 and Stx2 are transcytosed following different pathways [27,29]. Intracellular toxin is found in association with endosomes, Golgi, ER, and the nuclear membrane, indicative of retrograde transport [30], but the fact that transcytosis is not affected by disruption of the Golgi apparatus [29] implies that transcytosis is independent of retrograde transport [354]. Recent studies indicate that Stx2 can cross enteroid-derived monolayers without loss of epithelial barrier function and still induce stromal cells death [20].

Apparently, toxin uptake by Gb_3-negative intestinal epithelial cells does not only involve such cells as an inert transport route, but also affects intestinal epithelial cell functions in vitro and in vitro. Stx1 uptake causes galectin-3 depletion from enterocytes by increasing the apical galectin-3 secretion and impairing trafficking of several brush border structural proteins and transporters, including villin, dipeptidyl peptidase IV, and the sodium-proton exchanger 2, a major colonic sodium absorptive protein [352]. The mistargeting of proteins responsible for the absorptive function might be a key event in Stx1-induced diarrhea [352].

5. Conclusive Summary

Although primarily recognized as ribotoxic protein synthesis inhibitors, Stxs deploy a plethora of interactions with cells of the STEC-infected host. At first, after released by strictly luminal enteropathogens, the toxins are transcytosed through intestinal epithelial cells partially through Gb_3-independent epithelial cell damage. Having crossed the intestinal barrier, interaction with Gb_3/CD77-positive cells results in the generation of host cell-derived microvesicles. Seconded by proteins like soluble TLR-4, serumamyloid P, and complement factor H, binding of Stx to Gb_3/CD77 on sensitive cells in different organs occurs. Signaling from the cell surface results in internalization and translocation to the cytosol, initiation of endoplasmic and ribotoxic stress responses, and eventually protein synthesis inhibition and intranuclear DNA damage. These effects culminate in cellular death events, mainly involving apoptosis. Furthermore, Stxs can cause alteration of multiple intracellular signaling pathways and thereby disturb intercellular communication implicated in innate immune responses, namely inflammation. Such effects may even extend to alterations of adaptive immune responses. Significant variations in the effects of Stxs on host cells have been observed for different types of cells, tissues, and hosts. Our contemporary understanding of the interactions of Stxs with host cells at the molecular level, reviewed in here, mainly comes from cell cultures studies deploying primary cells and cell lines from human and mice. Despite numerous efforts to establish suitable animal models, none of them completely replicate the EHEC infection and HUS observed in humans patients [12]. However, the pathogenesis of ED, a disease with significant economic impact in pork production and caused by particular STEC variants producing Stx2e, may follow very similar paths as a human EHEC-mediated disease. Intervention measures deduced from an in-depth understanding of this molecular interplay may foster our basic understanding of cellular biology and microbial pathogenesis and pave the way to the creation of host-directed active compounds to mitigate the pathological conditions of STEC infections in the mammalian body.

Funding: The author received funding by the Deutsche Forschungsgemeinschaft (DFG; SFB 535 and project GE2509/1-1) and in the framework of ANTIGONE (Anticipating the Global Onset of Novel Epidemics) by the European Commission FP7 (project no. 278976) in support of the literature review presented in this manuscript.

Acknowledgments: I greatly acknowledge the long-standing support and mentorship by Georg Baljer, Lothar H. Wieler and Rolf Bauerfeind (Institute for Hygiene and Infectious Diseases of Animals, Justus-Liebig-University, Giessen, Germany), Helge Karch (Institute for Hygiene, University of Münster, Münster, Germany) and Evelyn A. Dean-Nystrom (National Animal Disease Center, Ames, USA). I am grateful to Jan-Dirk Häger for critical reading of the manuscript and help with preparation of Figures 7 and 8.

Conflicts of Interest: The authors declare no conflict of interest. The funders had no role in the design of the study; in the collection, analyses, or interpretation of data; in the writing of the manuscript, or in the decision to publish the results.

References

1. Karmali, M.A. Infection by verocytotoxin-producing Escherichia coli. *Clin. Microbiol. Rev.* **1989**, *2*, 15–38. [CrossRef] [PubMed]
2. Wieler, L.H.; Franke, S.; Menge, C.; Rose, M.; Bauerfeind, R.; Karch, H.; Baljer, G. The immune response in edema disease of weaned piglets measured with a recombinant B subunit of shiga-like toxin II. *Dtsch. Tierarztl. Wochenschr.* **1995**, *102*, 40–43. [PubMed]
3. Bielaszewska, M.; Mellmann, A.; Zhang, W.; Kock, R.; Fruth, A.; Bauwens, A.; Peters, G.; Karch, H. Characterisation of the Escherichia coli strain associated with an outbreak of haemolytic uraemic syndrome in Germany, 2011: A microbiological study. *Lancet Infect. Dis.* **2011**, *11*, 671–676. [CrossRef]
4. Hamm, K.; Barth, S.A.; Stalb, S.; Geue, L.; Liebler-Tenorio, E.; Teifke, J.P.; Lange, E.; Tauscher, K.; Kotterba, G.; Bielaszewska, M.; et al. Experimental Infection of Calves with Escherichia coli O104:H4 outbreak strain. *Sci. Rep.* **2016**, *6*, 32812. [CrossRef]
5. Stalb, S.; Barth, S.A.; Sobotta, K.; Liebler-Tenorio, E.; Geue, L.; Menge, C. Pro-inflammatory capacity of Escherichia coli O104:H4 outbreak strain during colonization of intestinal epithelial cells from human and cattle. *Int. J. Med. Microbiol.* **2018**, *308*, 899–911. [CrossRef]
6. Cray, W.C., Jr.; Moon, H.W. Experimental infection of calves and adult cattle with Escherichia coli O157:H7. *Appl. Environ. Microbiol.* **1995**, *61*, 1586–1590. [CrossRef]
7. Matthias, D. [Localization of beta-hemolytic E. coli in various organs of swine with edema disease]. *Zentralbl. Bakteriol. [Orig]* **1969**, *212*, 103–108.
8. Lee, M.S.; Koo, S.; Jeong, D.G.; Tesh, V.L. Shiga Toxins as Multi-Functional Proteins: Induction of Host Cellular Stress Responses, Role in Pathogenesis and Therapeutic Applications. *Toxins (Basel)* **2016**, *8*, 77. [CrossRef]
9. Lee, M.S.; Tesh, V.L. Roles of Shiga Toxins in Immunopathology. *Toxins (Basel)* **2019**, *11*, 212. [CrossRef]
10. Harel, Y.; Silva, M.; Giroir, B.; Weinberg, A.; Cleary, T.B.; Beutler, B. A reporter transgene indicates renal-specific induction of tumor necrosis factor (TNF) by shiga-like toxin. Possible involvement of TNF in hemolytic uremic syndrome. *J. Clin. Investig.* **1993**, *92*, 2110–2116. [CrossRef]
11. Proulx, F.; Seidman, E.G.; Karpman, D. Pathogenesis of Shiga toxin-associated hemolytic uremic syndrome. *Pediatr. Res.* **2001**, *50*, 163–171. [CrossRef] [PubMed]
12. Mayer, C.L.; Leibowitz, C.S.; Kurosawa, S.; Stearns-Kurosawa, D.J. Shiga toxins and the pathophysiology of hemolytic uremic syndrome in humans and animals. *Toxins (Basel)* **2012**, *4*, 1261–1287. [CrossRef] [PubMed]
13. Law, D. Adhesion and its role in the virulence of enteropathogenic Escherichia coli. *Clin. Microbiol. Rev.* **1994**, *7*, 152–173. [CrossRef] [PubMed]
14. Barth, S.A.; Menge, C.; Eichhorn, I.; Semmler, T.; Wieler, L.H.; Pickard, D.; Belka, A.; Berens, C.; Geue, L. The Accessory Genome of Shiga Toxin-Producing Escherichia coli Defines a Persistent Colonization Type in Cattle. *Appl. Environ. Microbiol.* **2016**, *82*, 5455–5464. [CrossRef] [PubMed]
15. Kaper, J.B. The locus of enterocyte effacement pathogenicity island of Shiga toxin-producing Escherichia coli O157:H7 and other attaching and effacing E. coli. *Jpn. J. Med. Sci. Biol.* **1998**, *51*, S101–S107. [CrossRef] [PubMed]
16. Monteiro, R.; Ageorges, V.; Rojas-Lopez, M.; Schmidt, H.; Weiss, A.; Bertin, Y.; Forano, E.; Jubelin, G.; Henderson, I.R.; Livrelli, V.; et al. A secretome view of colonisation factors in Shiga toxin-encoding Escherichia coli (STEC): from enterohaemorrhagic E. coli (EHEC) to related enteropathotypes. *FEMS Microbiol. Lett.* **2016**, *363*. [CrossRef]
17. Ritchie, M.; Partington, S.; Jessop, J.; Kelly, M.T. Comparison of a direct fecal Shiga-like toxin assay and sorbitol-MacConkey agar culture for laboratory diagnosis of enterohemorrhagic Escherichia coli infection. *J. Clin. Microbiol.* **1992**, *30*, 461–464. [CrossRef]
18. Donohue-Rolfe, A.; Keusch, G.T. Shigella dysenteriae 1 cytotoxin: periplasmic protein releasable by polymyxin B and osmotic shock. *Infect. Immun.* **1983**, *39*, 270–274. [CrossRef]

19. Bauwens, A.; Kunsmann, L.; Marejkova, M.; Zhang, W.; Karch, H.; Bielaszewska, M.; Mellmann, A. Intrahost milieu modulates production of outer membrane vesicles, vesicle-associated Shiga toxin 2a and cytotoxicity in Escherichia coli O157:H7 and O104:H4. *Environ. Microbiol. Rep.* **2017**, *9*, 626–634. [CrossRef]
20. Pradhan, S.; Karve, S.S.; Weiss, A.A.; Hawkins, J.; Poling, H.M.; Helmrath, M.A.; Wells, J.M.; McCauley, H.A. Tissue Responses to Shiga Toxin in Human Intestinal Organoids. *Cell Mol. Gastroenterol. Hepatol.* **2020**. [CrossRef]
21. Schuller, S.; Frankel, G.; Phillips, A.D. Interaction of Shiga toxin from Escherichia coli with human intestinal epithelial cell lines and explants: Stx2 induces epithelial damage in organ culture. *Cell Microbiol.* **2004**, *6*, 289–301. [CrossRef] [PubMed]
22. Boyd, B.; Tyrrell, G.; Maloney, M.; Gyles, C.; Brunton, J.; Lingwood, C. Alteration of the glycolipid binding specificity of the pig edema toxin from globotetraosyl to globotriaosyl ceramide alters in vivo tissue targetting and results in a verotoxin 1-like disease in pigs. *J. Exp. Med.* **1993**, *177*, 1745–1753. [CrossRef]
23. Hall, G.A.; Chanter, N.; Bland, A.P. Comparison in gnotobiotic pigs of lesions caused by verotoxigenic and non-verotoxigenic Escherichia coli. *Vet. Pathol.* **1988**, *25*, 205–210. [CrossRef] [PubMed]
24. Kelly, J.; Oryshak, A.; Wenetsek, M.; Grabiec, J.; Handy, S. The colonic pathology of Escherichia coli O157:H7 infection. *Am. J. Surg. Pathol.* **1990**, *14*, 87–92. [CrossRef]
25. Richardson, S.E.; Karmali, M.A.; Becker, L.E.; Smith, C.R. The histopathology of the hemolytic uremic syndrome associated with verocytotoxin-producing Escherichia coli infections. *Hum. Pathol.* **1988**, *19*, 1102–1108. [CrossRef]
26. Philpott, D.J.; McKay, D.M.; Sherman, P.M.; Perdue, M.H. Infection of T84 cells with enteropathogenic Escherichia coli alters barrier and transport functions. *Am. J. Physiol.* **1996**, *270*, G634–G645. [CrossRef] [PubMed]
27. Hurley, B.P.; Thorpe, C.M.; Acheson, D.W. Shiga toxin translocation across intestinal epithelial cells is enhanced by neutrophil transmigration. *Infect. Immun.* **2001**, *69*, 6148–6155. [CrossRef]
28. Acheson, D.W.; Moore, R.; De Breucker, S.; Lincicome, L.; Jacewicz, M.; Skutelsky, E.; Keusch, G.T. Translocation of Shiga toxin across polarized intestinal cells in tissue culture. *Infect. Immun.* **1996**, *64*, 3294–3300. [CrossRef]
29. Hurley, B.P.; Jacewicz, M.; Thorpe, C.M.; Lincicome, L.L.; King, A.J.; Keusch, G.T.; Acheson, D.W. Shiga toxins 1 and 2 translocate differently across polarized intestinal epithelial cells. *Infect. Immun.* **1999**, *67*, 6670–6677. [CrossRef]
30. Philpott, D.J.; Ackerley, C.A.; Kiliaan, A.J.; Karmali, M.A.; Perdue, M.H.; Sherman, P.M. Translocation of verotoxin-1 across T84 monolayers: mechanism of bacterial toxin penetration of epithelium. *Am. J. Physiol.* **1997**, *273*, G1349–G1358. [CrossRef]
31. Bitzan, M.; Richardson, S.; Huang, C.; Boyd, B.; Petric, M.; Karmali, M.A. Evidence that verotoxins (Shiga-like toxins) from Escherichia coli bind to P blood group antigens of human erythrocytes in vitro. *Infect. Immun.* **1994**, *62*, 3337–3347. [CrossRef] [PubMed]
32. te Loo, D.M.; Monnens, L.A.; van Der Velden, T.J.; Vermeer, M.A.; Preyers, F.; Demacker, P.N.; van Den Heuvel, L.P.; van Hinsbergh, V.W. Binding and transfer of verocytotoxin by polymorphonuclear leukocytes in hemolytic uremic syndrome. *Blood* **2000**, *95*, 3396–3402. [CrossRef] [PubMed]
33. Stahl, A.L.; Sartz, L.; Nelsson, A.; Bekassy, Z.D.; Karpman, D. Shiga toxin and lipopolysaccharide induce platelet-leukocyte aggregates and tissue factor release, a thrombotic mechanism in hemolytic uremic syndrome. *PLoS ONE* **2009**, *4*, e6990. [CrossRef] [PubMed]
34. Stahl, A.L.; Arvidsson, I.; Johansson, K.E.; Chromek, M.; Rebetz, J.; Loos, S.; Kristoffersson, A.C.; Bekassy, Z.D.; Morgelin, M.; Karpman, D. A novel mechanism of bacterial toxin transfer within host blood cell-derived microvesicles. *PLoS Pathog.* **2015**, *11*, e1004619. [CrossRef] [PubMed]
35. Koster, F.; Levin, J.; Walker, L.; Tung, K.S.; Gilman, R.H.; Rahaman, M.M.; Majid, M.A.; Islam, S.; Williams, R.C., Jr. Hemolytic-uremic syndrome after shigellosis. Relation to endotoxemia and circulating immune complexes. *N. Engl. J. Med.* **1978**, *298*, 927–933. [CrossRef] [PubMed]
36. Boyd, B.; Lingwood, C. Verotoxin receptor glycolipid in human renal tissue. *Nephron* **1989**, *51*, 207–210. [CrossRef]
37. Koster, F.T.; Boonpucknavig, V.; Sujaho, S.; Gilman, R.H.; Rahaman, M.M. Renal histopathology in the hemolytic-uremic syndrome following shigellosis. *Clin. Nephrol.* **1984**, *21*, 126–133.

38. Bauwens, A.; Betz, J.; Meisen, I.; Kemper, B.; Karch, H.; Muthing, J. Facing glycosphingolipid-Shiga toxin interaction: dire straits for endothelial cells of the human vasculature. *Cell Mol. Life Sci.* **2013**, *70*, 425–457. [CrossRef]
39. Wiley, R.G.; Donohue-Rolfe, A.; Keusch, G.T. Axonally transported Shigella cytotoxin is neuronotoxic. *J. Neuropathol. Exp. Neurol.* **1985**, *44*, 496–506. [CrossRef]
40. Liu, J.; Akahoshi, T.; Sasahana, T.; Kitasato, H.; Namai, R.; Sasaki, T.; Inoue, M.; Kondo, H. Inhibition of neutrophil apoptosis by verotoxin 2 derived from Escherichia coli O157:H7. *Infect. Immun.* **1999**, *67*, 6203–6205. [CrossRef]
41. King, A.J.; Sundaram, S.; Cendoroglo, M.; Acheson, D.W.; Keusch, G.T. Shiga toxin induces superoxide production in polymorphonuclear cells with subsequent impairment of phagocytosis and responsiveness to phorbol esters. *J. Infect. Dis.* **1999**, *179*, 503–507. [CrossRef] [PubMed]
42. Cohen, A.; Madrid-Marina, V.; Estrov, Z.; Freedman, M.H.; Lingwood, C.A.; Dosch, H.M. Expression of glycolipid receptors to Shiga-like toxin on human B lymphocytes: a mechanism for the failure of long-lived antibody response to dysenteric disease. *Int. Immunol.* **1990**, *2*, 1–8. [CrossRef] [PubMed]
43. Pradhan, S.; Pellino, C.; MacMaster, K.; Coyle, D.; Weiss, A.A. Shiga Toxin Mediated Neurologic Changes in Murine Model of Disease. *Front. Cell. Infect. Microbiol.* **2016**, *6*, 114. [CrossRef] [PubMed]
44. Karmali, M.A.; Petric, M.; Lim, C.; Fleming, P.C.; Arbus, G.S.; Lior, H. The association between idiopathic hemolytic uremic syndrome and infection by verotoxin-producing Escherichia coli. *J. Infect. Dis.* **1985**, *151*, 775–782. [CrossRef]
45. Wurzner, R.; Riedl, M.; Rosales, A.; Orth-Holler, D. Treatment of enterohemorrhagic Escherichia coli-induced hemolytic uremic syndrome (eHUS). *Semin. Thromb. Hemost.* **2014**, *40*, 508–516. [CrossRef]
46. Thomas, D.E.; Elliott, E.J. Interventions for preventing diarrhea-associated hemolytic uremic syndrome: systematic review. *BMC Public Health* **2013**, *13*, 799. [CrossRef]
47. Fricke, R.; Bastert, O.; Gotter, V.; Brons, N.; Kamp, J.; Selbitz, H.J. Implementation of a vaccine against Shigatoxin 2e in a piglet producing farm with problems of Oedema disease: case study. *Porcine Health Manag.* **2015**, *1*, 6. [CrossRef]
48. Vande Walle, K.; Vanrompay, D.; Cox, E. Bovine innate and adaptive immune responses against Escherichia coli O157:H7 and vaccination strategies to reduce faecal shedding in ruminants. *Vet. Immunol. Immunopathol.* **2013**, *152*, 109–120. [CrossRef]
49. Johannes, L. Shiga Toxin-A Model for Glycolipid-Dependent and Lectin-Driven Endocytosis. *Toxins (Basel)* **2017**, *9*, 340. [CrossRef]
50. Geyer, P.E.; Maak, M.; Nitsche, U.; Perl, M.; Novotny, A.; Slotta-Huspenina, J.; Dransart, E.; Holtorf, A.; Johannes, L.; Janssen, K.P. Gastric Adenocarcinomas Express the Glycosphingolipid Gb3/CD77: Targeting of Gastric Cancer Cells with Shiga Toxin B-Subunit. *Mol. Cancer Ther.* **2016**, *15*, 1008–1017. [CrossRef]
51. Maak, M.; Nitsche, U.; Keller, L.; Wolf, P.; Sarr, M.; Thiebaud, M.; Rosenberg, R.; Langer, R.; Kleeff, J.; Friess, H.; et al. Tumor-specific targeting of pancreatic cancer with Shiga toxin B-subunit. *Mol. Cancer Ther.* **2011**, *10*, 1918–1928. [CrossRef] [PubMed]
52. Kavaliauskiene, S.; Dyve Lingelem, A.B.; Skotland, T.; Sandvig, K. Protection against Shiga Toxins. *Toxins (Basel)* **2017**, *9*, 44. [CrossRef] [PubMed]
53. Pohlentz, G.; Steil, D.; Rubin, D.; Mellmann, A.; Karch, H.; Muthing, J. Pectin-derived neoglycolipids: Tools for differentiation of Shiga toxin subtypes and inhibitors of Shiga toxin-mediated cellular injury. *Carbohydr. Polym.* **2019**, *212*, 323–333. [CrossRef] [PubMed]
54. Schmidt, N.; Barth, S.A.; Frahm, J.; Meyer, U.; Danicke, S.; Geue, L.; Menge, C. Decreased STEC shedding by cattle following passive and active vaccination based on recombinant Escherichia coli Shiga toxoids. *Vet. Res.* **2018**, *49*, 28. [CrossRef] [PubMed]
55. Allen, K.J.; Rogan, D.; Finlay, B.B.; Potter, A.A.; Asper, D.J. Vaccination with type III secreted proteins leads to decreased shedding in calves after experimental infection with Escherichia coli O157. *Can. J. Vet. Res.* **2011**, *75*, 98–105.
56. Wileman, B.W.; Thomson, D.U.; Olson, K.C.; Jaeger, J.R.; Pacheco, L.A.; Bolte, J.; Burkhardt, D.T.; Emery, D.A.; Straub, D. Escherichia coli O157:H7 shedding in vaccinated beef calves born to cows vaccinated prepartum with Escherichia coli O157:H7 SRP vaccine. *J. Food Prot.* **2011**, *74*, 1599–1604. [CrossRef]
57. Konowalchuk, J.; Speirs, J.I.; Stavric, S. Vero response to a cytotoxin of Escherichia coli. *Infect. Immun.* **1977**, *18*, 775–779. [CrossRef]

58. O'Brien, A.D.; LaVeck, G.D. Purification and characterization of a Shigella dysenteriae 1-like toxin produced by Escherichia coli. *Infect. Immun.* **1983**, *40*, 675–683. [CrossRef]
59. Scheutz, F.; Teel, L.D.; Beutin, L.; Pierard, D.; Buvens, G.; Karch, H.; Mellmann, A.; Caprioli, A.; Tozzoli, R.; Morabito, S.; et al. Multicenter evaluation of a sequence-based protocol for subtyping Shiga toxins and standardizing Stx nomenclature. *J. Clin. Microbiol.* **2012**, *50*, 2951–2963. [CrossRef]
60. Strockbine, N.A.; Jackson, M.P.; Sung, L.M.; Holmes, R.K.; O'Brien, A.D. Cloning and sequencing of the genes for Shiga toxin from Shigella dysenteriae type 1. *J. Bacteriol.* **1988**, *170*, 1116–1122. [CrossRef]
61. Zhang, W.; Bielaszewska, M.; Kuczius, T.; Karch, H. Identification, characterization, and distribution of a Shiga toxin 1 gene variant (stx(1c)) in Escherichia coli strains isolated from humans. *J. Clin. Microbiol.* **2002**, *40*, 1441–1446. [CrossRef] [PubMed]
62. Burk, C.; Dietrich, R.; Acar, G.; Moravek, M.; Bulte, M.; Martlbauer, E. Identification and characterization of a new variant of Shiga toxin 1 in Escherichia coli ONT:H19 of bovine origin. *J. Clin. Microbiol.* **2003**, *41*, 2106–2112. [CrossRef] [PubMed]
63. Schmitt, C.K.; McKee, M.L.; O'Brien, A.D. Two copies of Shiga-like toxin II-related genes common in enterohemorrhagic Escherichia coli strains are responsible for the antigenic heterogeneity of the O157:H- strain E32511. *Infect. Immun.* **1991**, *59*, 1065–1073. [CrossRef]
64. Melton-Celsa, A.R.; Kokai-Kun, J.F.; O'Brien, A.D. Activation of Shiga toxin type 2d (Stx2d) by elastase involves cleavage of the C-terminal two amino acids of the A2 peptide in the context of the appropriate B pentamer. *Mol. Microbiol.* **2002**, *43*, 207–215. [CrossRef] [PubMed]
65. Weinstein, D.L.; Jackson, M.P.; Samuel, J.E.; Holmes, R.K.; O'Brien, A.D. Cloning and sequencing of a Shiga-like toxin type II variant from Escherichia coli strain responsible for edema disease of swine. *J. Bacteriol.* **1988**, *170*, 4223–4230. [CrossRef] [PubMed]
66. Schmidt, H.; Scheef, J.; Morabito, S.; Caprioli, A.; Wieler, L.H.; Karch, H. A new Shiga toxin 2 variant (Stx2f) from Escherichia coli isolated from pigeons. *Appl. Environ. Microbiol.* **2000**, *66*, 1205–1208. [CrossRef] [PubMed]
67. Leung, P.H.; Peiris, J.S.; Ng, W.W.; Robins-Browne, R.M.; Bettelheim, K.A.; Yam, W.C. A newly discovered verotoxin variant, VT2g, produced by bovine verocytotoxigenic Escherichia coli. *Appl. Environ. Microbiol.* **2003**, *69*, 7549–7553. [CrossRef] [PubMed]
68. Gannon, V.P.; Gyles, C.L. Characteristics of the Shiga-like toxin produced by Escherichia coli associated with porcine edema disease. *Vet. Microbiol.* **1990**, *24*, 89–100. [CrossRef]
69. DeGrandis, S.; Law, H.; Brunton, J.; Gyles, C.; Lingwood, C.A. Globotetraosylceramide is recognized by the pig edema disease toxin. *J. Biol. Chem.* **1989**, *264*, 12520–12525.
70. Gannon, V.P.; Gyles, C.L.; Wilcock, B.P. Effects of Escherichia coli Shiga-like toxins (verotoxins) in pigs. *Can J. Vet. Res.* **1989**, *53*, 306–312.
71. Schmidt, H. Shiga-toxin-converting bacteriophages. *Res. Microbiol.* **2001**, *152*, 687–695. [CrossRef]
72. Herold, S.; Karch, H.; Schmidt, H. Shiga toxin-encoding bacteriophages–genomes in motion. *Int. J. Med. Microbiol.* **2004**, *294*, 115–121. [CrossRef]
73. DeGrandis, S.; Ginsberg, J.; Toone, M.; Climie, S.; Friesen, J.; Brunton, J. Nucleotide sequence and promoter mapping of the Escherichia coli Shiga-like toxin operon of bacteriophage H-19B. *J. Bacteriol.* **1987**, *169*, 4313–4319. [CrossRef]
74. Jackson, M.P.; Newland, J.W.; Holmes, R.K.; O'Brien, A.D. Nucleotide sequence analysis of the structural genes for Shiga-like toxin I encoded by bacteriophage 933J from Escherichia coli. *Microb. Pathog.* **1987**, *2*, 147–153. [CrossRef]
75. Ramotar, K.; Boyd, B.; Tyrrell, G.; Gariepy, J.; Lingwood, C.; Brunton, J. Characterization of Shiga-like toxin I B subunit purified from overproducing clones of the SLT-I B cistron. *Biochem. J.* **1990**, *272*, 805–811. [CrossRef]
76. Seidah, N.G.; Donohue-Rolfe, A.; Lazure, C.; Auclair, F.; Keusch, G.T.; Chretien, M. Complete amino acid sequence of Shigella toxin B-chain. A novel polypeptide containing 69 amino acids and one disulfide bridge. *J. Biol. Chem.* **1986**, *261*, 13928–13931.
77. Stein, P.E.; Boodhoo, A.; Tyrrell, G.J.; Brunton, J.L.; Read, R.J. Crystal structure of the cell-binding B oligomer of verotoxin-1 from E. coli. *Nature* **1992**, *355*, 748–750. [CrossRef] [PubMed]
78. Bast, D.J.; Banerjee, L.; Clark, C.; Read, R.J.; Brunton, J.L. The identification of three biologically relevant globotriaosyl ceramide receptor binding sites on the Verotoxin 1 B subunit. *Mol. Microbiol.* **1999**, *32*, 953–960. [CrossRef] [PubMed]

79. Saleh, M.T.; Gariepy, J. Local conformational change in the B-subunit of Shiga-like toxin 1 at endosomal pH. *Biochemistry* **1993**, *32*, 918–922. [CrossRef]
80. Fraser, M.E.; Fujinaga, M.; Cherney, M.M.; Melton-Celsa, A.R.; Twiddy, E.M.; O'Brien, A.D.; James, M.N. Structure of shiga toxin type 2 (Stx2) from Escherichia coli O157:H7. *J. Biol. Chem.* **2004**, *279*, 27511–27517. [CrossRef]
81. Jackson, M.P.; Wadolkowski, E.A.; Weinstein, D.L.; Holmes, R.K.; O'Brien, A.D. Functional analysis of the Shiga toxin and Shiga-like toxin type II variant binding subunits by using site-directed mutagenesis. *J. Bacteriol.* **1990**, *172*, 653–658. [CrossRef]
82. Lingwood, C.A.; Mylvaganam, M.; Arab, S.; Khine, A.A.; Magnusson, G.; Grinstein, S.; Nyholm, P.G. Shiga toxin (verotoxin) binding to its receptor glycolipid. In *Escherichia coli O157:H7 and Other Shiga Toxin-Producing E. coli Strains*; Kaper, J.B., O'Brien, A.D., Eds.; ASM Press: Washington, DC, USA, 1998; pp. 129–139.
83. Tyrrell, G.J.; Ramotar, K.; Toye, B.; Boyd, B.; Lingwood, C.A.; Brunton, J.L. Alteration of the carbohydrate binding specificity of verotoxins from Gal alpha 1-4Gal to GalNAc beta 1-3Gal alpha 1-4Gal and vice versa by site-directed mutagenesis of the binding subunit. *Proc. Natl. Acad. Sci. USA* **1992**, *89*, 524–528. [CrossRef] [PubMed]
84. Nyholm, P.G.; Magnusson, G.; Zheng, Z.; Norel, R.; Binnington-Boyd, B.; Lingwood, C.A. Two distinct binding sites for globotriaosyl ceramide on verotoxins: identification by molecular modelling and confirmation using deoxy analogues and a new glycolipid receptor for all verotoxins. *Chem. Biol.* **1996**, *3*, 263–275. [CrossRef]
85. Clark, C.; Bast, D.; Sharp, A.M.; St Hilaire, P.M.; Agha, R.; Stein, P.E.; Toone, E.J.; Read, R.J.; Brunton, J.L. Phenylalanine 30 plays an important role in receptor binding of verotoxin-1. *Mol. Microbiol.* **1996**, *19*, 891–899. [CrossRef] [PubMed]
86. Perera, L.P.; Samuel, J.E.; Holmes, R.K.; O'Brien, A.D. Identification of three amino acid residues in the B subunit of Shiga toxin and Shiga-like toxin type II that are essential for holotoxin activity. *J. Bacteriol.* **1991**, *173*, 1151–1160. [CrossRef] [PubMed]
87. Lingwood, C.A.; Yiu, S.K. Glycolipid modification of alpha 2 interferon binding. Sequence similarity between the alpha 2 interferon receptor and verotoxin (Shiga-like toxin) B-subunit. *Biochem. J.* **1992**, *283 Pt 1*, 25–26. [CrossRef]
88. Fraser, M.E.; Chernaia, M.M.; Kozlov, Y.V.; James, M.N. Crystal structure of the holotoxin from Shigella dysenteriae at 2.5 A resolution. *Nat. Struct. Biol.* **1994**, *1*, 59–64. [CrossRef]
89. Perera, L.P.; Samuel, J.E.; Holmes, R.K.; O'Brien, A.D. Mapping the minimal contiguous gene segment that encodes functionally active Shiga-like toxin II. *Infect. Immun.* **1991**, *59*, 829–835. [CrossRef]
90. Austin, P.R.; Jablonski, P.E.; Bohach, G.A.; Dunker, A.K.; Hovde, C.J. Evidence that the A2 fragment of Shiga-like toxin type I is required for holotoxin integrity. *Infect. Immun.* **1994**, *62*, 1768–1775. [CrossRef]
91. Haddad, J.E.; Jackson, M.P. Identification of the Shiga toxin A-subunit residues required for holotoxin assembly. *J. Bacteriol.* **1993**, *175*, 7652–7657. [CrossRef]
92. Legros, N.; Pohlentz, G.; Steil, D.; Muthing, J. Shiga toxin-glycosphingolipid interaction: Status quo of research with focus on primary human brain and kidney endothelial cells. *Int. J. Med. Microbiol.* **2018**, *308*, 1073–1084. [CrossRef] [PubMed]
93. Gyles, C.L.; De Grandis, S.A.; MacKenzie, C.; Brunton, J.L. Cloning and nucleotide sequence analysis of the genes determining verocytotoxin production in a porcine edema disease isolate of Escherichia coli. *Microb. Pathog.* **1988**, *5*, 419–426. [CrossRef]
94. Takeda, Y.; Kurazono, H.; Yamasaki, S. Vero toxins (Shiga-like toxins) produced by enterohemorrhagic Escherichia coli (verocytotoxin-producing E. coli). *Microbiol. Immunol.* **1993**, *37*, 591–599. [CrossRef]
95. Jackson, M.P. Structure-function analyses of Shiga toxin and the Shiga-like toxins. *Microb. Pathog.* **1990**, *8*, 235–242. [CrossRef]
96. Basu, D.; Li, X.P.; Kahn, J.N.; May, K.L.; Kahn, P.C.; Tumer, N.E. The A1 Subunit of Shiga Toxin 2 Has Higher Affinity for Ribosomes and Higher Catalytic Activity than the A1 Subunit of Shiga Toxin 1. *Infect. Immun.* **2016**, *84*, 149–161. [CrossRef]
97. Fuller, C.A.; Pellino, C.A.; Flagler, M.J.; Strasser, J.E.; Weiss, A.A. Shiga toxin subtypes display dramatic differences in potency. *Infect. Immun.* **2011**, *79*, 1329–1337. [CrossRef]
98. Kim, S.H.; Ryu, S.H.; Lee, S.H.; Lee, Y.H.; Lee, S.R.; Huh, J.W.; Kim, S.U.; Kim, E.; Kim, S.; Jon, S.; et al. Instability of toxin A subunit of AB(5) toxins in the bacterial periplasm caused by deficiency of their cognate B subunits. *Biochim. Biophys. Acta* **2011**, *1808*, 2359–2365. [CrossRef]

99. Pellino, C.A.; Karve, S.S.; Pradhan, S.; Weiss, A.A. AB5 Preassembly Is Not Required for Shiga Toxin Activity. *J. Bacteriol.* **2016**, *198*, 1621–1630. [CrossRef] [PubMed]
100. Le Nours, J.; Paton, A.W.; Byres, E.; Troy, S.; Herdman, B.P.; Johnson, M.D.; Paton, J.C.; Rossjohn, J.; Beddoe, T. Structural basis of subtilase cytotoxin SubAB assembly. *J. Biol. Chem.* **2013**, *288*, 27505–27516. [CrossRef]
101. Pellizzari, A.; Pang, H.; Lingwood, C.A. Binding of verocytotoxin 1 to its receptor is influenced by differences in receptor fatty acid content. *Biochemistry* **1992**, *31*, 1363–1370. [CrossRef]
102. Lindberg, A.A.; Brown, J.E.; Stromberg, N.; Westling-Ryd, M.; Schultz, J.E.; Karlsson, K.A. Identification of the carbohydrate receptor for Shiga toxin produced by Shigella dysenteriae type 1. *J. Biol. Chem.* **1987**, *262*, 1779–1785. [PubMed]
103. Obrig, T.G.; Louise, C.B.; Lingwood, C.A.; Boyd, B.; Barley-Maloney, L.; Daniel, T.O. Endothelial heterogeneity in Shiga toxin receptors and responses. *J. Biol. Chem.* **1993**, *268*, 15484–15488.
104. Jacewicz, M.S.; Mobassaleh, M.; Gross, S.K.; Balasubramanian, K.A.; Daniel, P.F.; Raghavan, S.; McCluer, R.H.; Keusch, G.T. Pathogenesis of Shigella diarrhea: XVII. A mammalian cell membrane glycolipid, Gb3, is required but not sufficient to confer sensitivity to Shiga toxin. *J. Infect. Dis.* **1994**, *169*, 538–546. [CrossRef] [PubMed]
105. Mobassaleh, M.; Mishra, K.; Keusch, G.T. A quantitative immunostaining method for the measurement of UDP-galactose:lactosylceramide galactosyltransferase for the synthesis of globotriaosylceramide in rabbit small intestine and HeLa cells. *Anal. Biochem.* **1993**, *214*, 295–300. [CrossRef] [PubMed]
106. Taga, S.; Tetaud, C.; Mangeney, M.; Tursz, T.; Wiels, J. Sequential changes in glycolipid expression during human B cell differentiation: enzymatic bases. *Biochim. Biophys. Acta* **1995**, *1254*, 56–65. [CrossRef]
107. Lingwood, C.A. Verotoxin-binding in human renal sections. *Nephron* **1994**, *66*, 21–28. [CrossRef]
108. Olsnes, S.; Reisbig, R.; Eiklid, K. Subunit structure of Shigella cytotoxin. *J. Biol. Chem.* **1981**, *256*, 8732–8738.
109. Sandvig, K.; Prydz, K.; Ryd, M.; van Deurs, B. Endocytosis and intracellular transport of the glycolipid-binding ligand Shiga toxin in polarized MDCK cells. *J. Cell Biol.* **1991**, *113*, 553–562. [CrossRef]
110. Obrig, T.G.; Del Vecchio, P.J.; Brown, J.E.; Moran, T.P.; Rowland, B.M.; Judge, T.K.; Rothman, S.W. Direct cytotoxic action of Shiga toxin on human vascular endothelial cells. *Infect. Immun.* **1988**, *56*, 2373–2378. [CrossRef]
111. Pudymaitis, A.; Lingwood, C.A. Susceptibility to verotoxin as a function of the cell cycle. *J. Cell Physiol.* **1992**, *150*, 632–639. [CrossRef]
112. Majoul, I.; Schmidt, T.; Pomasanova, M.; Boutkevich, E.; Kozlov, Y.; Soling, H.D. Differential expression of receptors for Shiga and Cholera toxin is regulated by the cell cycle. *J. Cell Sci.* **2002**, *115*, 817–826.
113. Bhattacharjee, R.N.; Park, K.S.; Uematsu, S.; Okada, K.; Hoshino, K.; Takeda, K.; Takeuchi, O.; Akira, S.; Iida, T.; Honda, T. Escherichia coli verotoxin 1 mediates apoptosis in human HCT116 colon cancer cells by inducing overexpression of the GADD family of genes and S phase arrest. *FEBS Lett.* **2005**, *579*, 6604–6610. [CrossRef] [PubMed]
114. Brown, J.E.; Echeverria, P.; Lindberg, A.A. Digalactosyl-containing glycolipids as cell surface receptors for shiga toxin of Shigella dysenteriae 1 and related cytotoxins of Escherichia coli. *Rev. Infect. Dis.* **1991**, *13 Suppl 4*, S298–303. [CrossRef]
115. Ramegowda, B.; Tesh, V.L. Differentiation-associated toxin receptor modulation, cytokine production, and sensitivity to Shiga-like toxins in human monocytes and monocytic cell lines. *Infect. Immun.* **1996**, *64*, 1173–1180. [CrossRef] [PubMed]
116. Pudymaitis, A.; Armstrong, G.; Lingwood, C.A. Verotoxin-resistant cell clones are deficient in the glycolipid globotriosylceramide: differential basis of phenotype. *Arch. Biochem. Biophys.* **1991**, *286*, 448–452. [CrossRef]
117. Louise, C.B.; Obrig, T.G. Shiga toxin-associated hemolytic uremic syndrome: combined cytotoxic effects of shiga toxin and lipopolysaccharide (endotoxin) on human vascular endothelial cells in vitro. *Infect. Immun.* **1992**, *60*, 1536–1543. [CrossRef]
118. van de Kar, N.C.; Monnens, L.A.; Karmali, M.A.; van Hinsbergh, V.W. Tumor necrosis factor and interleukin-1 induce expression of the verocytotoxin receptor globotriaosylceramide on human endothelial cells: implications for the pathogenesis of the hemolytic uremic syndrome. *Blood* **1992**, *80*, 2755–2764. [CrossRef]
119. van de Kar, N.C.; Kooistra, T.; Vermeer, M.; Lesslauer, W.; Monnens, L.A.; van Hinsbergh, V.W. Tumor necrosis factor alpha induces endothelial galactosyl transferase activity and verocytotoxin receptors. Role of specific tumor necrosis factor receptors and protein kinase C. *Blood* **1995**, *85*, 734–743. [CrossRef]

120. Stricklett, P.K.; Hughes, A.K.; Ergonul, Z.; Kohan, D.E. Molecular basis for up-regulation by inflammatory cytokines of Shiga toxin 1 cytotoxicity and globotriaosylceramide expression. *J. Infect. Dis.* **2002**, *186*, 976–982. [CrossRef]
121. Kaye, S.A.; Louise, C.B.; Boyd, B.; Lingwood, C.A.; Obrig, T.G. Shiga toxin-associated hemolytic uremic syndrome: interleukin-1 beta enhancement of Shiga toxin cytotoxicity toward human vascular endothelial cells in vitro. *Infect. Immun.* **1993**, *61*, 3886–3891. [CrossRef]
122. van Setten, P.A.; van Hinsbergh, V.W.; van der Velden, T.J.; van de Kar, N.C.; Vermeer, M.; Mahan, J.D.; Assmann, K.J.; van den Heuvel, L.P.; Monnens, L.A. Effects of TNF alpha on verocytotoxin cytotoxicity in purified human glomerular microvascular endothelial cells. *Kidney Int.* **1997**, *51*, 1245–1256. [CrossRef] [PubMed]
123. Eisenhauer, P.B.; Chaturvedi, P.; Fine, R.E.; Ritchie, A.J.; Pober, J.S.; Cleary, T.G.; Newburg, D.S. Tumor necrosis factor alpha increases human cerebral endothelial cell Gb3 and sensitivity to Shiga toxin. *Infect. Immun.* **2001**, *69*, 1889–1894. [CrossRef] [PubMed]
124. Ramegowda, B.; Samuel, J.E.; Tesh, V.L. Interaction of Shiga toxins with human brain microvascular endothelial cells: cytokines as sensitizing agents. *J. Infect. Dis.* **1999**, *180*, 1205–1213. [CrossRef]
125. Keusch, G.T.; Acheson, D.W.; Aaldering, L.; Erban, J.; Jacewicz, M.S. Comparison of the effects of Shiga-like toxin 1 on cytokine- and butyrate-treated human umbilical and saphenous vein endothelial cells. *J. Infect. Dis.* **1996**, *173*, 1164–1170. [CrossRef] [PubMed]
126. Head, S.C.; Karmali, M.A.; Lingwood, C.A. Preparation of VT1 and VT2 hybrid toxins from their purified dissociated subunits. Evidence for B subunit modulation of a subunit function. *J. Biol. Chem.* **1991**, *266*, 3617–3621. [PubMed]
127. Samuel, J.E.; Perera, L.P.; Ward, S.; O'Brien, A.D.; Ginsburg, V.; Krivan, H.C. Comparison of the glycolipid receptor specificities of Shiga-like toxin type II and Shiga-like toxin type II variants. *Infect. Immun.* **1990**, *58*, 611–618. [CrossRef]
128. Imai, Y.; Fukui, T.; Kurohane, K.; Miyamoto, D.; Suzuki, Y.; Ishikawa, T.; Ono, Y.; Miyake, M. Restricted expression of shiga toxin binding sites on mucosal epithelium of mouse distal colon. *Infect. Immun.* **2003**, *71*, 985–990. [CrossRef]
129. Keusch, G.T.; Jacewicz, M.; Mobassaleh, M.; Donohue-Rolfe, A. Shiga toxin: intestinal cell receptors and pathophysiology of enterotoxic effects. *Rev. Infect. Dis.* **1991**, *13*, S304–S310. [CrossRef]
130. Mobassaleh, M.; Donohue-Rolfe, A.; Jacewicz, M.; Grand, R.J.; Keusch, G.T. Pathogenesis of shigella diarrhea: evidence for a developmentally regulated glycolipid receptor for shigella toxin involved in the fluid secretory response of rabbit small intestine. *J. Infect. Dis.* **1988**, *157*, 1023–1031. [CrossRef]
131. Pruimboom-Brees, I.M.; Morgan, T.W.; Ackermann, M.R.; Nystrom, E.D.; Samuel, J.E.; Cornick, N.A.; Moon, H.W. Cattle lack vascular receptors for Escherichia coli O157:H7 Shiga toxins. *Proc. Natl. Acad. Sci. USA* **2000**, *97*, 10325–10329. [CrossRef]
132. Hoey, D.E.; Currie, C.; Else, R.W.; Nutikka, A.; Lingwood, C.A.; Gally, D.L.; Smith, D.G. Expression of receptors for verotoxin 1 from Escherichia coli O157 on bovine intestinal epithelium. *J. Med. Microbiol.* **2002**, *51*, 143–149. [CrossRef] [PubMed]
133. Stamm, I.; Mohr, M.; Bridger, P.S.; Schropfer, E.; Konig, M.; Stoffregen, W.C.; Dean-Nystrom, E.A.; Baljer, G.; Menge, C. Epithelial and mesenchymal cells in the bovine colonic mucosa *Differ.* in their responsiveness to Escherichia coli Shiga toxin 1. *Infect. Immun.* **2008**, *76*, 5381–5391. [CrossRef]
134. Schuller, S.; Heuschkel, R.; Torrente, F.; Kaper, J.B.; Phillips, A.D. Shiga toxin binding in normal and inflamed human intestinal mucosa. *Microbes Infect.* **2007**, *9*, 35–39. [CrossRef] [PubMed]
135. Louise, C.B.; Obrig, T.G. Shiga toxin-associated hemolytic-uremic syndrome: Combined cytotoxic effects of Shiga toxin, interleukin-1 beta, and tumor necrosis factor alpha on human vascular endothelial cells in vitro. *Infect. Immun.* **1991**, *59*, 4173–4179. [CrossRef] [PubMed]
136. Molostvov, G.; Morris, A.; Rose, P.; Basu, S. Interaction of cytokines and growth factor in the regulation of verotoxin-induced apoptosis in cultured human endothelial cells. *Br. J. Haematol.* **2001**, *113*, 891–897. [CrossRef]
137. Ohmi, K.; Kiyokawa, N.; Takeda, T.; Fujimoto, J. Human microvascular endothelial cells are strongly sensitive to Shiga toxins. *Biochem. Biophys. Res. Commun.* **1998**, *251*, 137–141. [CrossRef]

138. Yoshida, T.; Fukada, M.; Koide, N.; Ikeda, H.; Sugiyama, T.; Kato, Y.; Ishikawa, N.; Yokochi, T. Primary cultures of human endothelial cells are susceptible to low doses of Shiga toxins and undergo apoptosis. *J. Infect. Dis.* **1999**, *180*, 2048–2052. [CrossRef]
139. Bitzan, M.M.; Wang, Y.; Lin, J.; Marsden, P.A. Verotoxin and ricin have novel effects on preproendothelin-1 expression but fail to modify nitric oxide synthase (ecNOS) expression and NO production in vascular endothelium. *J. Clin. Investig.* **1998**, *101*, 372–382. [CrossRef]
140. Erwert, R.D.; Winn, R.K.; Harlan, J.M.; Bannerman, D.D. Shiga-like toxin inhibition of FLICE-like inhibitory protein expression sensitizes endothelial cells to bacterial lipopolysaccharide-induced apoptosis. *J. Biol. Chem.* **2002**, *277*, 40567–40574. [CrossRef]
141. Obrig, T.G.; Seaner, R.M.; Bentz, M.; Lingwood, C.A.; Boyd, B.; Smith, A.; Narrow, W. Induction by sphingomyelinase of shiga toxin receptor and shiga toxin 2 sensitivity in human microvascular endothelial cells. *Infect. Immun.* **2003**, *71*, 845–849. [CrossRef]
142. Pijpers, A.H.; van Setten, P.A.; van den Heuvel, L.P.; Assmann, K.J.; Dijkman, H.B.; Pennings, A.H.; Monnens, L.A.; van Hinsbergh, V.W. Verocytotoxin-induced apoptosis of human microvascular endothelial cells. *J. Am. Soc. Nephrol.* **2001**, *12*, 767–778. [PubMed]
143. Jacewicz, M.S.; Acheson, D.W.; Binion, D.G.; West, G.A.; Lincicome, L.L.; Fiocchi, C.; Keusch, G.T. Responses of human intestinal microvascular endothelial cells to Shiga toxins 1 and 2 and pathogenesis of hemorrhagic colitis. *Infect. Immun.* **1999**, *67*, 1439–1444. [CrossRef] [PubMed]
144. Richardson, S.E.; Rotman, T.A.; Jay, V.; Smith, C.R.; Becker, L.E.; Petric, M.; Olivieri, N.F.; Karmali, M.A. Experimental verocytotoxemia in rabbits. *Infect. Immun.* **1992**, *60*, 4154–4167. [CrossRef] [PubMed]
145. Chaisri, U.; Nagata, M.; Kurazono, H.; Horie, H.; Tongtawe, P.; Hayashi, H.; Watanabe, T.; Tapchaisri, P.; Chongsa-nguan, M.; Chaicumpa, W. Localization of Shiga toxins of enterohaemorrhagic Escherichia coli in kidneys of paediatric and geriatric patients with fatal haemolytic uraemic syndrome. *Microb. Pathog.* **2001**, *31*, 59–67. [CrossRef]
146. Louise, C.B.; Obrig, T.G. Human renal microvascular endothelial cells as a potential target in the development of the hemolytic uremic syndrome as related to fibrinolysis factor expression, in vitro. *Microvasc. Res.* **1994**, *47*, 377–387. [CrossRef]
147. Winter, K.R.; Stoffregen, W.C.; Dean-Nystrom, E.A. Shiga toxin binding to isolated porcine tissues and peripheral blood leukocytes. *Infect. Immun.* **2004**, *72*, 6680–6684. [CrossRef]
148. Legros, N.; Dusny, S.; Humpf, H.U.; Pohlentz, G.; Karch, H.; Muthing, J. Shiga toxin glycosphingolipid receptors and their lipid membrane ensemble in primary human blood-brain barrier endothelial cells. *Glycobiology* **2017**, *27*, 99–109. [CrossRef]
149. Rutjes, N.W.; Binnington, B.A.; Smith, C.R.; Maloney, M.D.; Lingwood, C.A. Differential tissue targeting and pathogenesis of verotoxins 1 and 2 in the mouse animal model. *Kidney Int.* **2002**, *62*, 832–845. [CrossRef]
150. Park, J.Y.; Jeong, Y.J.; Park, S.K.; Yoon, S.J.; Choi, S.; Jeong, D.G.; Chung, S.W.; Lee, B.J.; Kim, J.H.; Tesh, V.L.; et al. Shiga Toxins Induce Apoptosis and ER Stress in Human Retinal Pigment Epithelial Cells. *Toxins (Basel)* **2017**, *9*, 319. [CrossRef]
151. Chark, D.; Nutikka, A.; Trusevych, N.; Kuzmina, J.; Lingwood, C. Differential carbohydrate epitope recognition of globotriaosyl ceramide by verotoxins and a monoclonal antibody. *Eur. J. Biochem.* **2004**, *271*, 405–417. [CrossRef]
152. Hughes, A.K.; Stricklett, P.K.; Kohan, D.E. Cytotoxic effect of Shiga toxin-1 on human proximal tubule cells. *Kidney Int.* **1998**, *54*, 426–437. [CrossRef] [PubMed]
153. Kiyokawa, N.; Taguchi, T.; Mori, T.; Uchida, H.; Sato, N.; Takeda, T.; Fujimoto, J. Induction of apoptosis in normal human renal tubular epithelial cells by Escherichia coli Shiga toxins 1 and 2. *J. Infect. Dis.* **1998**, *178*, 178–184. [CrossRef]
154. Imai, Y.; Fukui, T.; Ikegaya, A.; Ishikawa, T.; Ono, Y.; Kurohane, K. Lack of Shiga-like toxin binding sites in germinal centres of mouse lymphoid tissues. *Immunology* **2002**, *105*, 509–514. [CrossRef]
155. Zoja, C.; Corna, D.; Farina, C.; Sacchi, G.; Lingwood, C.; Doyle, M.P.; Padhye, V.V.; Abbate, M.; Remuzzi, G. Verotoxin glycolipid receptors determine the localization of microangiopathic process in rabbits given verotoxin-1. *J. Lab. Clin. Med.* **1992**, *120*, 229–238. [PubMed]
156. Hughes, A.K.; Stricklett, P.K.; Schmid, D.; Kohan, D.E. Cytotoxic effect of Shiga toxin-1 on human glomerular epithelial cells. *Kidney Int.* **2000**, *57*, 2350–2359. [CrossRef] [PubMed]

157. van Setten, P.A.; Monnens, L.A.; Verstraten, R.G.; van den Heuvel, L.P.; van Hinsbergh, V.W. Effects of verocytotoxin-1 on nonadherent human monocytes: binding characteristics, protein synthesis, and induction of cytokine release. *Blood* **1996**, *88*, 174–183. [CrossRef]
158. Kniep, B.; Monner, D.A.; Schwulera, U.; Muhlradt, P.F. Glycosphingolipids of the globo-series are associated with the monocytic lineage of human myeloid cells. *Eur. J. Biochem.* **1985**, *149*, 187–191. [CrossRef]
159. Tesh, V.L.; Ramegowda, B.; Samuel, J.E. Purified Shiga-like toxins induce expression of proinflammatory cytokines from murine peritoneal macrophages. *Infect. Immun.* **1994**, *62*, 5085–5094. [CrossRef]
160. Menge, C.; Loos, D.; Bridger, P.S.; Barth, S.; Werling, D.; Baljer, G. Bovine macrophages sense Escherichia coli Shiga toxin 1. *Innate Immun.* **2015**, *21*, 655–664. [CrossRef]
161. Van Setten, P.A.; van Hinsbergh, V.W.; Van den Heuvel, L.P.; van der Velden, T.J.; van de Kar, N.C.; Krebbers, R.J.; Karmali, M.A.; Monnens, L.A. Verocytotoxin inhibits mitogenesis and protein synthesis in purified human glomerular mesangial cells without affecting cell viability: evidence for two distinct mechanisms. *J. Am. Soc. Nephrol.* **1997**, *8*, 1877–1888.
162. Robinson, L.A.; Hurley, R.M.; Lingwood, C.; Matsell, D.G. Escherichia coli verotoxin binding to human paediatric glomerular mesangial cells. *Pediatr. Nephrol.* **1995**, *9*, 700–704. [CrossRef]
163. Mengeling, W.L.; Vorwald, A.C.; Cornick, N.A.; Lager, K.M.; Moon, H.W. In vitro detection of Shiga toxin using porcine alveolar macrophages. *J. Vet. Diagn. Investig.* **2001**, *13*, 421–424. [CrossRef] [PubMed]
164. Menge, C.; Stamm, I.; Wuhrer, M.; Geyer, R.; Wieler, L.H.; Baljer, G. Globotriaosylceramide (Gb(3)/CD77) is synthesized and surface expressed by bovine lymphocytes upon activation in vitro. *Vet. Immunol. Immunopathol.* **2001**, *83*, 19–36. [CrossRef]
165. Menge, C.; Blessenohl, M.; Eisenberg, T.; Stamm, I.; Baljer, G. Bovine ileal intraepithelial lymphocytes represent target cells for Shiga toxin 1 from Escherichia coli. *Infect. Immun.* **2004**, *72*, 1896–1905. [CrossRef]
166. Mangeney, M.; Richard, Y.; Coulaud, D.; Tursz, T.; Wiels, J. CD77: an antigen of germinal center B cells entering apoptosis. *Eur. J. Immunol.* **1991**, *21*, 1131–1140. [CrossRef] [PubMed]
167. Mangeney, M.; Rousselet, G.; Taga, S.; Tursz, T.; Wiels, J. The fate of human CD77+ germinal center B lymphocytes after rescue from apoptosis. *Mol. Immunol.* **1995**, *32*, 333–339. [CrossRef]
168. Gruner, K.R.; van Eijk, R.V.; Muhlradt, P.F. Structure elucidation of marker glycolipids of alloantigen-activated murine T lymphocytes. *Biochemistry* **1981**, *20*, 4518–4522. [CrossRef]
169. Kniep, B.; Hunig, T.R.; Fitch, F.W.; Heuer, J.; Kolsch, E.; Muhlradt, P.F. Neutral glycosphingolipids of murine myeloma cells and helper, cytolytic, and suppressor T lymphocytes. *Biochemistry* **1983**, *22*, 251–255. [CrossRef]
170. Menge, C.; Eisenberg, T.; Stamm, I.; Baljer, G. Comparison of binding and effects of Escherichia coli Shiga toxin 1 on bovine and ovine granulocytes. *Vet. Immunol. Immunopathol.* **2006**, *113*, 392–403. [CrossRef]
171. Eisenberg, T. *Untersuchungen zur Wirkung von Shigatoxin 1 von Escherichia coli auf Zellen der unspezifischen Immunabwehr bei Rind, Schaf und Ziege*, Dissertation ed.; Fachbereich Veterinärmedizin, Justus-Liebig-Universität Giessen: Hesse, Germany, 2003.
172. Newburg, D.S.; Chaturvedi, P.; Lopez, E.L.; Devoto, S.; Fayad, A.; Cleary, T.G. Susceptibility to hemolytic-uremic syndrome relates to erythrocyte glycosphingolipid patterns. *J. Infect. Dis.* **1993**, *168*, 476–479. [CrossRef]
173. Betz, J.; Dorn, I.; Kouzel, I.U.; Bauwens, A.; Meisen, I.; Kemper, B.; Bielaszewska, M.; Mormann, M.; Weymann, L.; Sibrowski, W.; et al. Shiga toxin of enterohaemorrhagic Escherichia coli directly injures developing human erythrocytes. *Cell Microbiol.* **2016**, *18*, 1339–1348. [CrossRef]
174. Cooling, L.L.; Walker, K.E.; Gille, T.; Koerner, T.A. Shiga toxin binds human platelets via globotriaosylceramide (Pk antigen) and a novel platelet glycosphingolipid. *Infect. Immun.* **1998**, *66*, 4355–4366. [CrossRef]
175. Karpman, D.; Papadopoulou, D.; Nilsson, K.; Sjogren, A.C.; Mikaelsson, C.; Lethagen, S. Platelet activation by Shiga toxin and circulatory factors as a pathogenetic mechanism in the hemolytic uremic syndrome. *Blood* **2001**, *97*, 3100–3108. [CrossRef]
176. Steil, D.; Bonse, R.; Meisen, I.; Pohlentz, G.; Vallejo, G.; Karch, H.; Muthing, J. A Topographical Atlas of Shiga Toxin 2e Receptor Distribution in the Tissues of Weaned Piglets. *Toxins (Basel)* **2016**, *8*, 357. [CrossRef]
177. Zhang, T.; de Waard, A.A.; Wuhrer, M.; Spaapen, R.M. The Role of Glycosphingolipids in Immune Cell Functions. *Front. Immunol.* **2019**, *10*, 90. [CrossRef]

178. Falguieres, T.; Mallard, F.; Baron, C.; Hanau, D.; Lingwood, C.; Goud, B.; Salamero, J.; Johannes, L. Targeting of Shiga toxin B-subunit to retrograde transport route in association with detergent-resistant membranes. *Mol. Biol. Cell* **2001**, *12*, 2453–2468. [CrossRef] [PubMed]
179. Katagiri, Y.U.; Mori, T.; Nakajima, H.; Katagiri, C.; Taguchi, T.; Takeda, T.; Kiyokawa, N.; Fujimoto, J. Activation of Src family kinase yes induced by Shiga toxin binding to globotriaosyl ceramide (Gb3/CD77) in low density, detergent-insoluble microdomains. *J. Biol. Chem.* **1999**, *274*, 35278–35282. [CrossRef]
180. Kovbasnjuk, O.; Edidin, M.; Donowitz, M. Role of lipid rafts in Shiga toxin 1 interaction with the apical surface of Caco-2 cells. *J. Cell Sci.* **2001**, *114*, 4025–4031. [PubMed]
181. Eiklid, K.; Olsnes, S. Interaction of Shigella shigae cytotoxin with receptors on sensitive and insensitive cells. *J. Recept Res.* **1980**, *1*, 199–213. [CrossRef] [PubMed]
182. Fuchs, G.; Mobassaleh, M.; Donohue-Rolfe, A.; Montgomery, R.K.; Grand, R.J.; Keusch, G.T. Pathogenesis of Shigella diarrhea: rabbit intestinal cell microvillus membrane binding site for Shigella toxin. *Infect. Immun.* **1986**, *53*, 372–377. [CrossRef] [PubMed]
183. St Hilaire, P.M.; Boyd, M.K.; Toone, E.J. Interaction of the Shiga-like toxin type 1 B-subunit with its carbohydrate receptor. *Biochemistry* **1994**, *33*, 14452–14463. [CrossRef] [PubMed]
184. Jacewicz, M.; Feldman, H.A.; Donohue-Rolfe, A.; Balasubramanian, K.A.; Keusch, G.T. Pathogenesis of Shigella diarrhea. XIV. Analysis of Shiga toxin receptors on cloned HeLa cells. *J. Infect. Dis.* **1989**, *159*, 881–889. [CrossRef] [PubMed]
185. Kiarash, A.; Boyd, B.; Lingwood, C.A. Glycosphingolipid receptor function is modified by fatty acid content. Verotoxin 1 and verotoxin 2c preferentially recognize different globotriaosyl ceramide fatty acid homologues. *J. Biol. Chem.* **1994**, *269*, 11138–11146.
186. Karve, S.S.; Weiss, A.A. Glycolipid binding preferences of Shiga toxin variants. *PLoS ONE* **2014**, *9*, e101173. [CrossRef]
187. Sandvig, K.; Olsnes, S.; Brown, J.E.; Petersen, O.W.; van Deurs, B. Endocytosis from coated pits of Shiga toxin: a glycolipid-binding protein from Shigella dysenteriae 1. *J. Cell Biol.* **1989**, *108*, 1331–1343. [CrossRef]
188. Lingwood, C.A.; Law, H.; Richardson, S.; Petric, M.; Brunton, J.L.; De Grandis, S.; Karmali, M. Glycolipid binding of purified and recombinant Escherichia coli produced verotoxin in vitro. *J. Biol. Chem.* **1987**, *262*, 8834–8839.
189. Waddell, T.; Head, S.; Petric, M.; Cohen, A.; Lingwood, C. Globotriosyl ceramide is specifically recognized by the Escherichia coli verocytotoxin 2. *Biochem. Biophys. Res. Commun.* **1988**, *152*, 674–679. [CrossRef]
190. Cohen, A.; Hannigan, G.E.; Williams, B.R.; Lingwood, C.A. Roles of globotriosyl- and galabiosylceramide in verotoxin binding and high affinity interferon receptor. *J. Biol. Chem.* **1987**, *262*, 17088–17091.
191. Newburg, D.S.; Ashkenazi, S.; Cleary, T.G. Human milk contains the Shiga toxin and Shiga-like toxin receptor glycolipid Gb3. *J. Infect. Dis.* **1992**, *166*, 832–836. [CrossRef]
192. Kouzel, I.U.; Pohlentz, G.; Schmitz, J.S.; Steil, D.; Humpf, H.U.; Karch, H.; Muthing, J. Shiga Toxin Glycosphingolipid Receptors in Human Caco-2 and HCT-8 Colon Epithelial Cell Lines. *Toxins (Basel)* **2017**, *9*, 338. [CrossRef]
193. Ito, H.; Yutsudo, T.; Hirayama, T.; Takeda, Y. Isolation and some properties of A and B subunits of Vero toxin 2 and in vitro formation of hybrid toxins between subunits of Vero toxin 1 and Vero toxin 2 from Escherichia coli O157:H7. *Microb. Pathog.* **1988**, *5*, 189–195. [CrossRef]
194. Weinstein, D.L.; Jackson, M.P.; Perera, L.P.; Holmes, R.K.; O'Brien, A.D. In vivo formation of hybrid toxins comprising Shiga toxin and the Shiga-like toxins and role of the B subunit in localization and cytotoxic activity. *Infect. Immun.* **1989**, *57*, 3743–3750. [CrossRef] [PubMed]
195. Jacewicz, M.; Clausen, H.; Nudelman, E.; Donohue-Rolfe, A.; Keusch, G.T. Pathogenesis of shigella diarrhea. XI. Isolation of a shigella toxin-binding glycolipid from rabbit jejunum and HeLa cells and its identification as globotriaosylceramide. *J. Exp. Med.* **1986**, *163*, 1391–1404. [CrossRef] [PubMed]
196. Maloney, M.D.; Lingwood, C.A. CD19 has a potential CD77 (globotriaosyl ceramide)-binding site with sequence similarity to verotoxin B-subunits: implications of molecular mimicry for B cell adhesion and enterohemorrhagic Escherichia coli pathogenesis. *J. Exp. Med.* **1994**, *180*, 191–201. [CrossRef] [PubMed]
197. Kitova, E.N.; Kitov, P.I.; Bundle, D.R.; Klassen, J.S. The observation of multivalent complexes of Shiga-like toxin with globotriaoside and the determination of their stoichiometry by nanoelectrospray Fourier-transform ion cyclotron resonance mass spectrometry. *Glycobiology* **2001**, *11*, 605–611. [CrossRef]

198. Soltyk, A.M.; MacKenzie, C.R.; Wolski, V.M.; Hirama, T.; Kitov, P.I.; Bundle, D.R.; Brunton, J.L. A mutational analysis of the globotriaosylceramide-binding sites of verotoxin VT1. *J. Biol. Chem.* **2002**, *277*, 5351–5359. [CrossRef]
199. Ling, H.; Boodhoo, A.; Hazes, B.; Cummings, M.D.; Armstrong, G.D.; Brunton, J.L.; Read, R.J. Structure of the shiga-like toxin I B-pentamer complexed with an analogue of its receptor Gb3. *Biochemistry* **1998**, *37*, 1777–1788. [CrossRef]
200. Wolski, V.M.; Soltyk, A.M.; Brunton, J.L. Mouse toxicity and cytokine release by verotoxin 1 B subunit mutants. *Infect. Immun.* **2001**, *69*, 579–583. [CrossRef]
201. Tedder, T.F. CD19: A promising B cell target for rheumatoid arthritis. *Nat. Rev. Rheumatol.* **2009**, *5*, 572–577. [CrossRef]
202. Khine, A.A.; Firtel, M.; Lingwood, C.A. CD77-dependent retrograde transport of CD19 to the nuclear membrane: functional relationship between CD77 and CD19 during germinal center B-cell apoptosis. *J. Cell Physiol.* **1998**, *176*, 281–292. [CrossRef]
203. Iwata, Y.; Yoshizaki, A.; Komura, K.; Shimizu, K.; Ogawa, F.; Hara, T.; Muroi, E.; Bae, S.; Takenaka, M.; Yukami, T.; et al. CD19, a response regulator of B lymphocytes, regulates wound healing through hyaluronan-induced TLR4 signaling. *Am. J. Pathol.* **2009**, *175*, 649–660. [CrossRef] [PubMed]
204. Ghislain, J.; Lingwood, C.A.; Fish, E.N. Evidence for glycosphingolipid modification of the type 1 IFN receptor. *J. Immunol.* **1994**, *153*, 3655–3663. [PubMed]
205. Maloney, M.D.; Binnington-Boyd, B.; Lingwood, C.A. Globotriaosyl ceramide modulates interferon-alpha-induced growth inhibition and CD19 expression in Burkitt's lymphoma cells. *Glycoconj. J.* **1999**, *16*, 821–828. [CrossRef]
206. Khine, A.A.; Lingwood, C.A. Functional significance of globotriaosyl ceramide in interferon-alpha(2)/type 1 interferon receptor-mediated antiviral activity. *J. Cell Physiol.* **2000**, *182*, 97–108. [CrossRef]
207. Bukholm, G.; Degre, M. Shiga toxin inhibits the anti-invasive effect of interferons. *J. Infect. Dis.* **1988**, *157*, 849–850. [CrossRef]
208. George, T.; Boyd, B.; Price, M.; Lingwood, C.; Maloney, M. MHC class II proteins contain a potential binding site for the verotoxin receptor glycolipid CD77. *Cell Mol. Biol. (Noisy-le-grand)* **2001**, *47*, 1179–1185.
209. Reymond, D.; Johnson, R.P.; Karmali, M.A.; Petric, M.; Winkler, M.; Johnson, S.; Rahn, K.; Renwick, S.; Wilson, J.; Clarke, R.C.; et al. Neutralizing antibodies to Escherichia coli Vero cytotoxin 1 and antibodies to O157 lipopolysaccharide in healthy farm family members and urban residents. *J. Clin. Microbiol.* **1996**, *34*, 2053–2057. [CrossRef]
210. Torgersen, M.L.; Engedal, N.; Pedersen, A.M.; Husebye, H.; Espevik, T.; Sandvig, K. Toll-like receptor 4 facilitates binding of Shiga toxin to colon carcinoma and primary umbilical vein endothelial cells. *FEMS Immunol. Med. Microbiol.* **2011**, *61*, 63–75. [CrossRef]
211. Torgersen, M.L.; Lauvrak, S.U.; Sandvig, K. The A-subunit of surface-bound Shiga toxin stimulates clathrin-dependent uptake of the toxin. *FEBS J.* **2005**, *272*, 4103–4113. [CrossRef]
212. Pezeshkian, W.; Gao, H.; Arumugam, S.; Becken, U.; Bassereau, P.; Florent, J.C.; Ipsen, J.H.; Johannes, L.; Shillcock, J.C. Mechanism of Shiga Toxin Clustering on Membranes. *ACS Nano* **2017**, *11*, 314–324. [CrossRef]
213. Sandvig, K.; van Deurs, B. Endocytosis and intracellular sorting of ricin and Shiga toxin. *FEBS Lett.* **1994**, *346*, 99–102. [CrossRef]
214. Marcato, P.; Vander Helm, K.; Mulvey, G.L.; Armstrong, G.D. Serum amyloid P component binding to Shiga toxin 2 requires both a subunit and B pentamer. *Infect. Immun.* **2003**, *71*, 6075–6078. [CrossRef] [PubMed]
215. Pezeshkian, W.; Hansen, A.G.; Johannes, L.; Khandelia, H.; Shillcock, J.C.; Kumar, P.B.; Ipsen, J.H. Membrane invagination induced by Shiga toxin B-subunit: from molecular structure to tube formation. *Soft Matter* **2016**, *12*, 5164–5171. [CrossRef]
216. Lauvrak, S.U.; Torgersen, M.L.; Sandvig, K. Efficient endosome-to-Golgi transport of Shiga toxin is dependent on dynamin and clathrin. *J. Cell Sci.* **2004**, *117*, 2321–2331. [CrossRef] [PubMed]
217. Taylor, M.J.; Lampe, M.; Merrifield, C.J. A feedback loop between dynamin and actin recruitment during clathrin-mediated endocytosis. *PLoS Biol.* **2012**, *10*, e1001302. [CrossRef] [PubMed]
218. Rao, Y.; Haucke, V. Membrane shaping by the Bin/amphiphysin/Rvs (BAR) domain protein superfamily. *Cell Mol. Life Sci.* **2011**, *68*, 3983–3993. [CrossRef]

219. Renard, H.F.; Simunovic, M.; Lemiere, J.; Boucrot, E.; Garcia-Castillo, M.D.; Arumugam, S.; Chambon, V.; Lamaze, C.; Wunder, C.; Kenworthy, A.K.; et al. Endophilin-A2 functions in membrane scission in clathrin-independent endocytosis. *Nature* **2015**, *517*, 493–496. [CrossRef]
220. Hehnly, H.; Sheff, D.; Stamnes, M. Shiga toxin facilitates its retrograde transport by modifying microtubule dynamics. *Mol. Biol. Cell* **2006**, *17*, 4379–4389. [CrossRef]
221. Arab, S.; Lingwood, C.A. Intracellular targeting of the endoplasmic reticulum/nuclear envelope by retrograde transport may determine cell hypersensitivity to verotoxin via globotriaosyl ceramide fatty acid isoform traffic. *J. Cell Physiol.* **1998**, *177*, 646–660. [CrossRef]
222. Sandvig, K.; Ryd, M.; Garred, O.; Schweda, E.; Holm, P.K.; van Deurs, B. Retrograde transport from the Golgi complex to the ER of both Shiga toxin and the nontoxic Shiga B-fragment is regulated by butyric acid and cAMP. *J. Cell Biol.* **1994**, *126*, 53–64. [CrossRef]
223. Johannes, L.; Goud, B. Facing inward from compartment shores: how many pathways were we looking for? *Traffic* **2000**, *1*, 119–123. [CrossRef]
224. Nichols, B.J.; Kenworthy, A.K.; Polishchuk, R.S.; Lodge, R.; Roberts, T.H.; Hirschberg, K.; Phair, R.D.; Lippincott-Schwartz, J. Rapid cycling of lipid raft markers between the cell surface and Golgi complex. *J. Cell Biol.* **2001**, *153*, 529–541. [CrossRef] [PubMed]
225. Mallard, F.; Antony, C.; Tenza, D.; Salamero, J.; Goud, B.; Johannes, L. Direct pathway from early/recycling endosomes to the Golgi apparatus revealed through the study of shiga toxin B-fragment transport. *J. Cell Biol.* **1998**, *143*, 973–990. [CrossRef] [PubMed]
226. Mallard, F.; Tang, B.L.; Galli, T.; Tenza, D.; Saint-Pol, A.; Yue, X.; Antony, C.; Hong, W.; Goud, B.; Johannes, L. Early/recycling endosomes-to-TGN transport involves two SNARE complexes and a Rab6 isoform. *J. Cell Biol.* **2002**, *156*, 653–664. [CrossRef]
227. Renard, H.F.; Garcia-Castillo, M.D.; Chambon, V.; Lamaze, C.; Johannes, L. Shiga toxin stimulates clathrin-independent endocytosis of the VAMP2, VAMP3 and VAMP8 SNARE proteins. *J. Cell Sci.* **2015**, *128*, 2891–2902. [CrossRef] [PubMed]
228. Tai, G.; Lu, L.; Wang, T.L.; Tang, B.L.; Goud, B.; Johannes, L.; Hong, W. Participation of the syntaxin 5/Ykt6/GS28/GS15 SNARE complex in transport from the early/recycling endosome to the trans-Golgi network. *Mol. Biol. Cell* **2004**, *15*, 4011–4022. [CrossRef]
229. Saint-Pol, A.; Yelamos, B.; Amessou, M.; Mills, I.G.; Dugast, M.; Tenza, D.; Schu, P.; Antony, C.; McMahon, H.T.; Lamaze, C.; et al. Clathrin adaptor epsinR is required for retrograde sorting on early endosomal membranes. *Dev. Cell* **2004**, *6*, 525–538. [CrossRef]
230. Kouzel, I.U.; Kehl, A.; Berger, P.; Liashkovich, I.; Steil, D.; Makalowski, W.; Suzuki, Y.; Pohlentz, G.; Karch, H.; Mellmann, A.; et al. RAB5A and TRAPPC6B are novel targets for Shiga toxin 2a inactivation in kidney epithelial cells. *Sci. Rep.* **2020**, *10*, 4945. [CrossRef]
231. Goldstein, J.L.; Anderson, R.G.; Brown, M.S. Coated pits, coated vesicles, and receptor-mediated endocytosis. *Nature* **1979**, *279*, 679–685. [CrossRef]
232. Girod, A.; Storrie, B.; Simpson, J.C.; Johannes, L.; Goud, B.; Roberts, L.M.; Lord, J.M.; Nilsson, T.; Pepperkok, R. Evidence for a COP-I-independent transport route from the Golgi complex to the endoplasmic reticulum. *Nat. Cell Biol.* **1999**, *1*, 423–430. [CrossRef]
233. White, J.; Johannes, L.; Mallard, F.; Girod, A.; Grill, S.; Reinsch, S.; Keller, P.; Tzschaschel, B.; Echard, A.; Goud, B.; et al. Rab6 coordinates a novel Golgi to ER retrograde transport pathway in live cells. *J. Cell Biol.* **1999**, *147*, 743–760. [CrossRef] [PubMed]
234. Sandvig, K.; Garred, O.; Prydz, K.; Kozlov, J.V.; Hansen, S.H.; van Deurs, B. Retrograde transport of endocytosed Shiga toxin to the endoplasmic reticulum. *Nature* **1992**, *358*, 510–512. [CrossRef] [PubMed]
235. Jacewicz, M.; Keusch, G.T. Pathogenesis of Shigella diarrhea. VIII. Evidence for a translocation step in the cytotoxic action of Shiga toxin. *J. Infect. Dis.* **1983**, *148*, 844–854. [CrossRef] [PubMed]
236. Melby, E.L.; Jacobsen, J.; Olsnes, S.; Sandvig, K. Entry of protein toxins in polarized epithelial cells. *Cancer Res.* **1993**, *53*, 1755–1760.
237. Marsh, M.; McMahon, H.T. The structural era of endocytosis. *Science* **1999**, *285*, 215–220. [CrossRef]
238. Sandvig, K.; Grimmer, S.; Lauvrak, S.U.; Torgersen, M.L.; Skretting, G.; van Deurs, B.; Iversen, T.G. Pathways followed by ricin and Shiga toxin into cells. *Histochem. Cell Biol.* **2002**, *117*, 131–141. [CrossRef]

239. Arfilli, V.; Carnicelli, D.; Rocchi, L.; Ricci, F.; Pagliaro, P.; Tazzari, P.L.; Brigotti, M. Shiga toxin 1 and ricin A chain bind to human polymorphonuclear leucocytes through a common receptor. *Biochem. J.* **2010**, *432*, 173–180. [CrossRef]
240. Brigotti, M.; Carnicelli, D.; Arfilli, V.; Tamassia, N.; Borsetti, F.; Fabbri, E.; Tazzari, P.L.; Ricci, F.; Pagliaro, P.; Spisni, E.; et al. Identification of TLR4 as the receptor that recognizes Shiga toxins in human neutrophils. *J. Immunol.* **2013**, *191*, 4748–4758. [CrossRef]
241. Brigotti, M.; Carnicelli, D.; Arfilli, V.; Porcellini, E.; Galassi, E.; Valerii, M.C.; Spisni, E. Human monocytes stimulated by Shiga toxin 1a via globotriaosylceramide release proinflammatory molecules associated with hemolytic uremic syndrome. *Int. J. Med. Microbiol.* **2018**, *308*, 940–946. [CrossRef]
242. O'Brien, A.D.; Tesh, V.L.; Donohue-Rolfe, A.; Jackson, M.P.; Olsnes, S.; Sandvig, K.; Lindberg, A.A.; Keusch, G.T. Shiga toxin: biochemistry, genetics, mode of action, and role in pathogenesis. *Curr. Top. Microbiol. Immunol.* **1992**, *180*, 65–94.
243. O'Brien, A.D.; Holmes, R.K. Shiga and Shiga-like toxins. *Microbiol. Rev.* **1987**, *51*, 206–220. [CrossRef] [PubMed]
244. Samuel, J.E.; Gordon, V.M. Evidence that proteolytic separation of Shiga-like toxin type IIv A subunit into A1 and A2 subunits is not required for toxin activity. *J. Biol. Chem.* **1994**, *269*, 4853–4859. [PubMed]
245. Garred, O.; Dubinina, E.; Holm, P.K.; Olsnes, S.; van Deurs, B.; Kozlov, J.V.; Sandvig, K. Role of processing and intracellular transport for optimal toxicity of Shiga toxin and toxin mutants. *Exp. Cell Res.* **1995**, *218*, 39–49. [CrossRef] [PubMed]
246. Sandvig, K.; Garred, O.; van Deurs, B. Intracellular transport and processing of protein toxins produced by enteric bacteria. *Adv. Exp. Med. Biol.* **1997**, *412*, 225–232. [PubMed]
247. Reisbig, R.; Olsnes, S.; Eiklid, K. The cytotoxic activity of Shigella toxin. Evidence for catalytic inactivation of the 60 S ribosomal subunit. *J. Biol. Chem.* **1981**, *256*, 8739–8744. [PubMed]
248. Li, X.P.; Tumer, N.E. Differences in Ribosome Binding and Sarcin/Ricin Loop Depurination by Shiga and Ricin Holotoxins. *Toxins (Basel)* **2017**, *9*, 133. [CrossRef]
249. Sandvig, K.; Brown, J.E. Ionic requirements for entry of Shiga toxin from Shigella dysenteriae 1 into cells. *Infect. Immun.* **1987**, *55*, 298–303. [CrossRef]
250. Garred, O.; Dubinina, E.; Polesskaya, A.; Olsnes, S.; Kozlov, J.; Sandvig, K. Role of the disulfide bond in Shiga toxin A-chain for toxin entry into cells. *J. Biol. Chem.* **1997**, *272*, 11414–11419. [CrossRef]
251. Yu, M.; Haslam, D.B. Shiga toxin is transported from the endoplasmic reticulum following interaction with the luminal chaperone HEDJ/ERdj3. *Infect. Immun.* **2005**, *73*, 2524–2532. [CrossRef]
252. Falguieres, T.; Johannes, L. Shiga toxin B-subunit binds to the chaperone BiP and the nucleolar protein B23. *Biol. Cell* **2005**, *98*, 125–134. [CrossRef]
253. Hazes, B.; Read, R.J. Accumulating evidence suggests that several AB-toxins subvert the endoplasmic reticulum-associated protein degradation pathway to enter target cells. *Biochemistry* **1997**, *36*, 11051–11054. [CrossRef] [PubMed]
254. Suzuki, T.; Yan, Q.; Lennarz, W.J. Complex, two-way traffic of molecules across the membrane of the endoplasmic reticulum. *J. Biol. Chem.* **1998**, *273*, 10083–10086. [CrossRef] [PubMed]
255. Haicheur, N.; Bismuth, E.; Bosset, S.; Adotevi, O.; Warnier, G.; Lacabanne, V.; Regnault, A.; Desaymard, C.; Amigorena, S.; Ricciardi-Castagnoli, P.; et al. The B subunit of Shiga toxin fused to a tumor antigen elicits CTL and targets dendritic cells to allow MHC class I-restricted presentation of peptides derived from exogenous antigens. *J. Immunol.* **2000**, *165*, 3301–3308. [CrossRef] [PubMed]
256. Haicheur, N.; Benchetrit, F.; Amessou, M.; Leclerc, C.; Falguieres, T.; Fayolle, C.; Bismuth, E.; Fridman, W.H.; Johannes, L.; Tartour, E. The B subunit of Shiga toxin coupled to full-size antigenic protein elicits humoral and cell-mediated immune responses associated with a Th1-dominant polarization. *Int. Immunol.* **2003**, *15*, 1161–1171. [CrossRef]
257. Lee, R.S.; Tartour, E.; van der Bruggen, P.; Vantomme, V.; Joyeux, I.; Goud, B.; Fridman, W.H.; Johannes, L. Major histocompatibility complex class I presentation of exogenous soluble tumor antigen fused to the B-fragment of Shiga toxin. *Eur. J. Immunol.* **1998**, *28*, 2726–2737. [CrossRef]
258. Endo, Y.; Tsurugi, K.; Yutsudo, T.; Takeda, Y.; Ogasawara, T.; Igarashi, K. Site of action of a Vero toxin (VT2) from Escherichia coli O157:H7 and of Shiga toxin on eukaryotic ribosomes. RNA N-glycosidase activity of the toxins. *Eur. J. Biochem.* **1988**, *171*, 45–50. [CrossRef]

259. Moazed, D.; Robertson, J.M.; Noller, H.F. Interaction of elongation factors EF-G and EF-Tu with a conserved loop in 23S RNA. *Nature* **1988**, *334*, 362–364. [CrossRef]
260. Ogasawara, T.; Ito, K.; Igarashi, K.; Yutsudo, T.; Nakabayashi, N.; Takeda, Y. Inhibition of protein synthesis by a Vero toxin (VT2 or Shiga-like toxin II) produced by Escherichia coli O157:H7 at the level of elongation factor 1-dependent aminoacyl-tRNA binding to ribosomes. *Microb. Pathog.* **1988**, *4*, 127–135. [CrossRef]
261. Yamasaki, S.; Furutani, M.; Ito, K.; Igarashi, K.; Nishibuchi, M.; Takeda, Y. Importance of arginine at position 170 of the A subunit of Vero toxin 1 produced by enterohemorrhagic Escherichia coli for toxin activity. *Microb. Pathog.* **1991**, *11*, 1–9. [CrossRef]
262. Deresiewicz, R.L.; Calderwood, S.B.; Robertus, J.D.; Collier, R.J. Mutations affecting the activity of the Shiga-like toxin I A-chain. *Biochemistry* **1992**, *31*, 3272–3280. [CrossRef]
263. Iordanov, M.S.; Pribnow, D.; Magun, J.L.; Dinh, T.H.; Pearson, J.A.; Chen, S.L.; Magun, B.E. Ribotoxic stress response: activation of the stress-activated protein kinase JNK1 by inhibitors of the peptidyl transferase reaction and by sequence-specific RNA damage to the alpha-sarcin/ricin loop in the 28S rRNA. *Mol. Cell Biol.* **1997**, *17*, 3373–3381. [CrossRef] [PubMed]
264. Obrig, T.G.; Moran, T.P.; Brown, J.E. The mode of action of Shiga toxin on peptide elongation of eukaryotic protein synthesis. *Biochem. J.* **1987**, *244*, 287–294. [CrossRef]
265. Brown, J.E.; Rothman, S.W.; Doctor, B.P. Inhibition of protein synthesis in intact HeLa cells by Shigella dysenteriae 1 toxin. *Infect. Immun.* **1980**, *29*, 98–107. [CrossRef] [PubMed]
266. Jimenez, A.; Vazquez, D. Plant and fungal protein and glycoprotein toxins inhibiting eukaryote protein synthesis. *Annu Rev. Microbiol.* **1985**, *39*, 649–672. [CrossRef] [PubMed]
267. Facchini, L.M.; Lingwood, C.A. A verotoxin 1 B subunit-lambda CRO chimeric protein specifically binds both DNA and globotriaosylceramide (Gb(3)) to effect nuclear targeting of exogenous DNA in Gb(3) positive cells. *Exp. Cell Res.* **2001**, *269*, 117–129. [CrossRef] [PubMed]
268. Nakagawa, I.; Nakata, M.; Kawabata, S.; Hamada, S. Regulated expression of the Shiga toxin B gene induces apoptosis in mammalian fibroblastic cells. *Mol. Microbiol.* **1999**, *33*, 1190–1199. [CrossRef] [PubMed]
269. Brigotti, M.; Accorsi, P.; Carnicelli, D.; Rizzi, S.; Gonzalez Vara, A.; Montanaro, L.; Sperti, S. Shiga toxin 1: damage to DNA in vitro. *Toxicon* **2001**, *39*, 341–348. [CrossRef]
270. Brigotti, M.; Alfieri, R.; Sestili, P.; Bonelli, M.; Petronini, P.G.; Guidarelli, A.; Barbieri, L.; Stirpe, F.; Sperti, S. Damage to nuclear DNA induced by Shiga toxin 1 and ricin in human endothelial cells. *FASEB J.* **2002**, *16*, 365–372. [CrossRef]
271. Sandvig, K.; van Deurs, B. Toxin-induced cell lysis: protection by 3-methyladenine and cycloheximide. *Exp. Cell Res.* **1992**, *200*, 253–262. [CrossRef]
272. Fujii, J.; Matsui, T.; Heatherly, D.P.; Schlegel, K.H.; Lobo, P.I.; Yutsudo, T.; Ciraolo, G.M.; Morris, R.E.; Obrig, T. Rapid apoptosis induced by Shiga toxin in HeLa cells. *Infect. Immun.* **2003**, *71*, 2724–2735. [CrossRef]
273. Arends, M.J.; Wyllie, A.H. Apoptosis: mechanisms and roles in pathology. *Int. Rev. Exp. Pathol.* **1991**, *32*, 223–254. [PubMed]
274. Chen, Y.; Zychlinsky, A. Apoptosis induced by bacterial pathogens. *Microb. Pathog.* **1994**, *17*, 203–212. [CrossRef] [PubMed]
275. Erwert, R.D.; Eiting, K.T.; Tupper, J.C.; Winn, R.K.; Harlan, J.M.; Bannerman, D.D. Shiga toxin induces decreased expression of the anti-apoptotic protein Mcl-1 concomitant with the onset of endothelial apoptosis. *Microb. Pathog.* **2003**, *35*, 87–93. [CrossRef]
276. Inward, C.D.; Williams, J.; Chant, I.; Crocker, J.; Milford, D.V.; Rose, P.E.; Taylor, C.M. Verocytotoxin-1 induces apoptosis in vero cells. *J. Infect.* **1995**, *30*, 213–218. [CrossRef]
277. Garibal, J.; Hollville, E.; Renouf, B.; Tetaud, C.; Wiels, J. Caspase-8-mediated cleavage of Bid and protein phosphatase 2A-mediated activation of Bax are necessary for Verotoxin-1-induced apoptosis in Burkitt's lymphoma cells. *Cell Signal* **2010**, *22*, 467–475. [CrossRef]
278. Tetaud, C.; Falguieres, T.; Carlier, K.; Lecluse, Y.; Garibal, J.; Coulaud, D.; Busson, P.; Steffensen, R.; Clausen, H.; Johannes, L.; et al. Two distinct Gb3/CD77 signaling pathways leading to apoptosis are triggered by anti-Gb3/CD77 mAb and verotoxin-1. *J. Biol. Chem.* **2003**, *278*, 45200–45208. [CrossRef]
279. Smith, W.E.; Kane, A.V.; Campbell, S.T.; Acheson, D.W.; Cochran, B.H.; Thorpe, C.M. Shiga toxin 1 triggers a ribotoxic stress response leading to p38 and JNK activation and induction of apoptosis in intestinal epithelial cells. *Infect. Immun.* **2003**, *71*, 1497–1504. [CrossRef]

280. Ikeda, M.; Gunji, Y.; Yamasaki, S.; Takeda, Y. Shiga toxin activates p38 MAP kinase through cellular Ca(2+) increase in Vero cells. *FEBS Lett.* **2000**, *485*, 94–98. [CrossRef]
281. Nelin, L.D.; White, H.A.; Jin, Y.; Trittmann, J.K.; Chen, B.; Liu, Y. The Src family tyrosine kinases src and yes have differential effects on inflammation-induced apoptosis in human pulmonary microvascular endothelial cells. *Am. J. Physiol. Lung Cell Mol. Physiol.* **2016**, *310*, L880–L888. [CrossRef]
282. Ching, J.C.; Jones, N.L.; Ceponis, P.J.; Karmali, M.A.; Sherman, P.M. Escherichia coli shiga-like toxins induce apoptosis and cleavage of poly(ADP-ribose) polymerase via in vitro activation of caspases. *Infect. Immun.* **2002**, *70*, 4669–4677. [CrossRef]
283. Kiyokawa, N.; Mori, T.; Taguchi, T.; Saito, M.; Mimori, K.; Suzuki, T.; Sekino, T.; Sato, N.; Nakajima, H.; Katagiri, Y.U.; et al. Activation of the caspase cascade during Stx1-induced apoptosis in Burkitt's lymphoma cells. *J. Cell Biochem.* **2001**, *81*, 128–142. [CrossRef]
284. Sahara, S.; Aoto, M.; Eguchi, Y.; Imamoto, N.; Yoneda, Y.; Tsujimoto, Y. Acinus is a caspase-3-activated protein required for apoptotic chromatin condensation. *Nature* **1999**, *401*, 168–173. [CrossRef] [PubMed]
285. Kojio, S.; Zhang, H.; Ohmura, M.; Gondaira, F.; Kobayashi, N.; Yamamoto, T. Caspase-3 activation and apoptosis induction coupled with the retrograde transport of shiga toxin: inhibition by brefeldin A. *FEMS Immunol. Med. Microbiol.* **2000**, *29*, 275–281. [CrossRef] [PubMed]
286. Takahashi, A.; Alnemri, E.S.; Lazebnik, Y.A.; Fernandes-Alnemri, T.; Litwack, G.; Moir, R.D.; Goldman, R.D.; Poirier, G.G.; Kaufmann, S.H.; Earnshaw, W.C. Cleavage of lamin A by Mch2 alpha but not CPP32: multiple interleukin 1 beta-converting enzyme-related proteases with distinct substrate recognition properties are active in apoptosis. *Proc. Natl. Acad. Sci. USA* **1996**, *93*, 8395–8400. [CrossRef] [PubMed]
287. Lee, S.Y.; Cherla, R.P.; Caliskan, I.; Tesh, V.L. Shiga Toxin 1 Induces Apoptosis in the Human Myelogenous Leukemia Cell Line THP-1 by a Caspase-8-Dependent, Tumor Necrosis Factor Receptor-Independent Mechanism. *Infect. Immun.* **2005**, *73*, 5115–5126. [CrossRef] [PubMed]
288. Sood, A.; Mathew, R.; Trachtman, H. Cytoprotective effect of curcumin in human proximal tubule epithelial cells exposed to shiga toxin. *Biochem. Biophys. Res. Commun.* **2001**, *283*, 36–41. [CrossRef]
289. Edelmann, B.; Bertsch, U.; Tchikov, V.; Winoto-Morbach, S.; Perrotta, C.; Jakob, M.; Adam-Klages, S.; Kabelitz, D.; Schutze, S. Caspase-8 and caspase-7 sequentially mediate proteolytic activation of acid sphingomyelinase in TNF-R1 receptosomes. *EMBO J.* **2011**, *30*, 379–394. [CrossRef]
290. Suzuki, A.; Doi, H.; Matsuzawa, F.; Aikawa, S.; Takiguchi, K.; Kawano, H.; Hayashida, M.; Ohno, S. Bcl-2 antiapoptotic protein mediates verotoxin II-induced cell death: possible association between bcl-2 and tissue failure by E. coli O157:H7. *Genes Dev.* **2000**, *14*, 1734–1740.
291. Gordon, J.; Challa, A.; Levens, J.M.; Gregory, C.D.; Williams, J.M.; Armitage, R.J.; Cook, J.P.; Roberts, L.M.; Lord, J.M. CD40 ligand, Bcl-2, and Bcl-xL spare group I Burkitt lymphoma cells from CD77-directed killing via Verotoxin-1 B chain but fail to protect against the holotoxin. *Cell Death Differ.* **2000**, *7*, 785–794. [CrossRef]
292. Lee, M.S.; Cherla, R.P.; Leyva-Illades, D.; Tesh, V.L. Bcl-2 regulates the onset of shiga toxin 1-induced apoptosis in THP-1 cells. *Infect. Immun.* **2009**, *77*, 5233–5244. [CrossRef] [PubMed]
293. Lee, M.S.; Cherla, R.P.; Lentz, E.K.; Leyva-Illades, D.; Tesh, V.L. Signaling through C/EBP homologous protein and death receptor 5 and calpain activation differentially regulate THP-1 cell maturation-dependent apoptosis induced by Shiga toxin type 1. *Infect. Immun.* **2010**, *78*, 3378–3391. [CrossRef] [PubMed]
294. Matsunaga, T.; Nakajima, T.; Sonoda, M.; Kawai, S.; Kobayashi, J.; Inoue, I.; Satomi, A.; Katayama, S.; Hara, A.; Hokari, S.; et al. Reactive oxygen species as a risk factor in verotoxin-1-exposed rats. *Biochem. Biophys. Res. Commun.* **1999**, *260*, 813–819. [CrossRef] [PubMed]
295. Platnich, J.M.; Chung, H.; Lau, A.; Sandall, C.F.; Bondzi-Simpson, A.; Chen, H.M.; Komada, T.; Trotman-Grant, A.C.; Brandelli, J.R.; Chun, J.; et al. Shiga Toxin/Lipopolysaccharide Activates Caspase-4 and Gasdermin D to Trigger Mitochondrial Reactive Oxygen Species Upstream of the NLRP3 Inflammasome. *Cell Rep.* **2018**, *25*, 1525–1536.e1527. [CrossRef]
296. Herson, P.S.; Lee, K.; Pinnock, R.D.; Hughes, J.; Ashford, M.L. Hydrogen peroxide induces intracellular calcium overload by activation of a non-selective cation channel in an insulin-secreting cell line. *J. Biol. Chem.* **1999**, *274*, 833–841. [CrossRef]
297. Williams, J.M.; Lea, N.; Lord, J.M.; Roberts, L.M.; Milford, D.V.; Taylor, C.M. Comparison of ribosome-inactivating proteins in the induction of apoptosis. *Toxicol. Lett.* **1997**, *91*, 121–127. [CrossRef]
298. Katagiri, Y.U.; Kiyokawa, N.; Fujimoto, J. The effect of shiga toxin binding to globotriaosylceramidein rafts of human kidney cells and Burkitt´slymphoma cells. *Trends Glycosci. Glycotech.* **2001**, *13*, 281–290. [CrossRef]

299. Mangeney, M.; Lingwood, C.A.; Taga, S.; Caillou, B.; Tursz, T.; Wiels, J. Apoptosis induced in Burkitt's lymphoma cells via Gb3/CD77, a glycolipid antigen. *Cancer Res.* **1993**, *53*, 5314–5319.
300. Taga, S.; Carlier, K.; Mishal, Z.; Capoulade, C.; Mangeney, M.; Lecluse, Y.; Coulaud, D.; Tetaud, C.; Pritchard, L.L.; Tursz, T.; et al. Intracellular signaling events in CD77-mediated apoptosis of Burkitt's lymphoma cells. *Blood* **1997**, *90*, 2757–2767. [CrossRef]
301. Mori, T.; Kiyokawa, N.; Katagiri, Y.U.; Taguchi, T.; Suzuki, T.; Sekino, T.; Sato, N.; Ohmi, K.; Nakajima, H.; Takeda, T.; et al. Globotriaosyl ceramide (CD77/Gb3) in the glycolipid-enriched membrane domain participates in B-cell receptor-mediated apoptosis by regulating lyn kinase activity in human B cells. *Exp. Hematol.* **2000**, *28*, 1260–1268. [CrossRef]
302. Liu, F.; Huang, J.; Sadler, J.E. Shiga toxin (Stx)1B and Stx2B induce von Willebrand factor secretion from human umbilical vein endothelial cells through different signaling pathways. *Blood* **2011**, *118*, 3392–3398. [CrossRef]
303. Hedlund, M.; Duan, R.D.; Nilsson, A.; Svanborg, C. Sphingomyelin, glycosphingolipids and ceramide signalling in cells exposed to P-fimbriated Escherichia coli. *Mol. Microbiol.* **1998**, *29*, 1297–1306. [CrossRef] [PubMed]
304. Kirkham, P.A.; Takamatsu, H.H.; Lam, E.W.; Parkhouse, R.M. Ligation of the WC1 receptor induces gamma delta T cell growth arrest through fumonisin B1-sensitive increases in cellular ceramide. *J. Immunol.* **2000**, *165*, 3564–3570. [CrossRef] [PubMed]
305. Fischer, H.; Ellstrom, P.; Ekstrom, K.; Gustafsson, L.; Gustafsson, M.; Svanborg, C. Ceramide as a TLR4 agonist; a putative signalling intermediate between sphingolipid receptors for microbial ligands and TLR4. *Cell Microbiol.* **2007**, *9*, 1239–1251. [CrossRef]
306. Garcia-Ruiz, C.; Colell, A.; Paris, R.; Fernandez-Checa, J.C. Direct interaction of GD3 ganglioside with mitochondria generates reactive oxygen species followed by mitochondrial permeability transition, cytochrome c release, and caspase activation. *FASEB J.* **2000**, *14*, 847–858. [CrossRef]
307. Andrieu-Abadie, N.; Gouaze, V.; Salvayre, R.; Levade, T. Ceramide in apoptosis signaling: relationship with oxidative stress. *Free Radic. Biol. Med.* **2001**, *31*, 717–728. [CrossRef]
308. Jandhyala, D.M.; Ahluwalia, A.; Obrig, T.; Thorpe, C.M. ZAK: a MAP3Kinase that transduces Shiga toxin- and ricin-induced proinflammatory cytokine expression. *Cell Microbiol.* **2008**, *10*, 1468–1477. [CrossRef]
309. Thorpe, C.M.; Hurley, B.P.; Lincicome, L.L.; Jacewicz, M.S.; Keusch, G.T.; Acheson, D.W. Shiga toxins stimulate secretion of interleukin-8 from intestinal epithelial cells. *Infect. Immun.* **1999**, *67*, 5985–5993. [CrossRef]
310. Cameron, P.; Bingham, D.; Paul, A.; Pavelka, M.; Cameron, S.; Rotondo, D.; Plevin, R. Essential role for verotoxin in sustained stress-activated protein kinase and nuclear factor kappa B signaling, stimulated by Escherichia coli O157:H7 in Vero cells. *Infect. Immun.* **2002**, *70*, 5370–5380. [CrossRef]
311. Kojima, S.; Yanagihara, I.; Kono, G.; Sugahara, T.; Nasu, H.; Kijima, M.; Hattori, A.; Kodama, T.; Nagayama, K.I.; Honda, T. mkp-1 encoding mitogen-activated protein kinase phosphatase 1, a verotoxin 1 responsive gene, detected by differential display reverse transcription-PCR in Caco-2 cells. *Infect. Immun.* **2000**, *68*, 2791–2796. [CrossRef]
312. Foster, G.H.; Armstrong, C.S.; Sakiri, R.; Tesh, V.L. Shiga toxin-induced tumor necrosis factor alpha expression: requirement for toxin enzymatic activity and monocyte protein kinase C and protein tyrosine kinases. *Infect. Immun.* **2000**, *68*, 5183–5189. [CrossRef]
313. Cameron, P.; Smith, S.J.; Giembycz, M.A.; Rotondo, D.; Plevin, R. Verotoxin activates mitogen-activated protein kinase in human peripheral blood monocytes: role in apoptosis and proinflammatory cytokine release. *Br. J. Pharmacol.* **2003**, *140*, 1320–1330. [CrossRef]
314. Leyva-Illades, D.; Cherla, R.P.; Lee, M.S.; Tesh, V.L. Regulation of cytokine and chemokine expression by the ribotoxic stress response elicited by Shiga toxin type 1 in human macrophage-like THP-1 cells. *Infect. Immun.* **2012**, *80*, 2109–2120. [CrossRef]
315. Cherla, R.P.; Lee, S.Y.; Mulder, R.A.; Lee, M.S.; Tesh, V.L. Shiga toxin 1-induced proinflammatory cytokine production is regulated by the phosphatidylinositol 3-kinase/Akt/mammalian target of rapamycin signaling pathway. *Infect. Immun.* **2009**, *77*, 3919–3931. [CrossRef]
316. Lee, S.Y.; Lee, M.S.; Cherla, R.P.; Tesh, V.L. Shiga toxin 1 induces apoptosis through the endoplasmic reticulum stress response in human monocytic cells. *Cell Microbiol.* **2008**, *10*, 770–780. [CrossRef]

317. Lentz, E.K.; Leyva-Illades, D.; Lee, M.S.; Cherla, R.P.; Tesh, V.L. Differential response of the human renal proximal tubular epithelial cell line HK-2 to Shiga toxin types 1 and 2. *Infect. Immun.* **2011**, *79*, 3527–3540. [CrossRef]
318. Tang, B.; Li, Q.; Zhao, X.H.; Wang, H.G.; Li, N.; Fang, Y.; Wang, K.; Jia, Y.P.; Zhu, P.; Gu, J.; et al. Shiga toxins induce autophagic cell death in intestinal epithelial cells via the endoplasmic reticulum stress pathway. *Autophagy* **2015**, *11*, 344–354. [CrossRef]
319. Lee, M.S.; Cherla, R.P.; Jenson, M.H.; Leyva-Illades, D.; Martinez-Moczygemba, M.; Tesh, V.L. Shiga toxins induce autophagy leading to differential signalling pathways in toxin-sensitive and toxin-resistant human cells. *Cell Microbiol.* **2011**, *13*, 1479–1496. [CrossRef]
320. Harrison, L.M.; van Haaften, W.C.; Tesh, V.L. Regulation of proinflammatory cytokine expression by Shiga toxin 1 and/or lipopolysaccharides in the human monocytic cell line THP-1. *Infect. Immun.* **2004**, *72*, 2618–2627. [CrossRef]
321. Sakiri, R.; Ramegowda, B.; Tesh, V.L. Shiga toxin type 1 activates tumor necrosis factor-alpha gene transcription and nuclear translocation of the transcriptional activators nuclear factor-kappaB and activator protein-1. *Blood* **1998**, *92*, 558–566. [CrossRef]
322. Yamasaki, C.; Natori, Y.; Zeng, X.T.; Ohmura, M.; Yamasaki, S.; Takeda, Y. Induction of cytokines in a human colon epithelial cell line by Shiga toxin 1 (Stx1) and Stx2 but not by non-toxic mutant Stx1 which lacks N-glycosidase activity. *FEBS Lett.* **1999**, *442*, 231–234. [CrossRef]
323. Yamasaki, C.; Nishikawa, K.; Zeng, X.T.; Katayama, Y.; Natori, Y.; Komatsu, N.; Oda, T. Induction of cytokines by toxins that have an identical RNA N-glycosidase activity: Shiga toxin, ricin, and modeccin. *Biochim. Biophys. Acta* **2004**, *1671*, 44–50. [CrossRef]
324. Brandelli, J.R.; Griener, T.P.; Laing, A.; Mulvey, G.; Armstrong, G.D. The Effects of Shiga Toxin 1, 2 and Their Subunits on Cytokine and Chemokine Expression by Human Macrophage-Like THP-1 Cells. *Toxins (Basel)* **2015**, *7*, 4054–4066. [CrossRef]
325. Nakamura, A.; Johns, E.J.; Imaizumi, A.; Yanagawa, Y.; Kohsaka, T. Activation of beta(2)-adrenoceptor prevents shiga toxin 2-induced TNF-alpha gene transcription. *J. Am. Soc. Nephrol.* **2001**, *12*, 2288–2299.
326. Dahan, S.; Busuttil, V.; Imbert, V.; Peyron, J.F.; Rampal, P.; Czerucka, D. Enterohemorrhagic Escherichia coli infection induces interleukin-8 production via activation of mitogen-activated protein kinases and the transcription factors NF-kappaB and AP-1 in T84 cells. *Infect. Immun.* **2002**, *70*, 2304–2310. [CrossRef]
327. Berin, M.C.; Darfeuille-Michaud, A.; Egan, L.J.; Miyamoto, Y.; Kagnoff, M.F. Role of EHEC O157:H7 virulence factors in the activation of intestinal epithelial cell NF-kappaB and MAP kinase pathways and the upregulated expression of interleukin 8. *Cell Microbiol.* **2002**, *4*, 635–648. [CrossRef]
328. Thorpe, C.M.; Smith, W.E.; Hurley, B.P.; Acheson, D.W. Shiga toxins induce, superinduce, and stabilize a variety of C-X-C chemokine mRNAs in intestinal epithelial cells, resulting in increased chemokine expression. *Infect. Immun.* **2001**, *69*, 6140–6147. [CrossRef]
329. Harrison, L.M.; van den Hoogen, C.; van Haaften, W.C.; Tesh, V.L. Chemokine expression in the monocytic cell line THP-1 in response to purified shiga toxin 1 and/or lipopolysaccharides. *Infect. Immun.* **2005**, *73*, 403–412. [CrossRef]
330. Lee, M.S.; Kwon, H.; Lee, E.Y.; Kim, D.J.; Park, J.H.; Tesh, V.L.; Oh, T.K.; Kim, M.H. Shiga Toxins Activate the NLRP3 Inflammasome Pathway To Promote Both Production of the Proinflammatory Cytokine Interleukin-1beta and Apoptotic Cell Death. *Infect. Immun.* **2016**, *84*, 172–186. [CrossRef]
331. Hughes, A.K.; Stricklett, P.K.; Kohan, D.E. Shiga toxin-1 regulation of cytokine production by human glomerular epithelial cells. *Nephron* **2001**, *88*, 14–23. [CrossRef]
332. Hughes, A.K.; Stricklett, P.K.; Kohan, D.E. Shiga toxin-1 regulation of cytokine production by human proximal tubule cells. *Kidney Int.* **1998**, *54*, 1093–1106. [CrossRef]
333. Eisenhauer, P.B.; Jacewicz, M.S.; Conn, K.J.; Koul, O.; Wells, J.M.; Fine, R.E.; Newburg, D.S. Escherichia coli Shiga toxin 1 and TNF-alpha induce cytokine release by human cerebral microvascular endothelial cells. *Microb. Pathog.* **2004**, *36*, 189–196. [CrossRef] [PubMed]
334. Matussek, A.; Lauber, J.; Bergau, A.; Hansen, W.; Rohde, M.; Dittmar, K.E.; Gunzer, M.; Mengel, M.; Gatzlaff, P.; Hartmann, M.; et al. Molecular and functional analysis of Shiga toxin-induced response patterns in human vascular endothelial cells. *Blood* **2003**, *102*, 1323–1332. [CrossRef] [PubMed]

335. Zhang, H.M.; Ou, Z.L.; Gondaira, F.; Ohmura, M.; Kojio, S.; Yamamoto, T. Protective effect of anisodamine against Shiga toxin-1: Inhibition of cytokine production and increase in the survival of mice. *J. Lab. Clin. Med.* **2001**, *137*, 93–100. [CrossRef] [PubMed]
336. Zhang, H.M.; Ohmura, M.; Gondaira, F.; Yamamoto, T. Inhibition of Shiga toxin-induced tumor necrosis factor-alpha production and gene expression in human monocytic cells by CV6209. *Life Sci.* **2001**, *68*, 1931–1937. [CrossRef]
337. Barrett, T.J.; Potter, M.E.; Strockbine, N.A. Evidence for participation of the macrophage in Shiga-like toxin II-induced lethality in mice. *Microb. Pathog.* **1990**, *9*, 95–103. [CrossRef]
338. Simon, M.; Cleary, T.G.; Hernandez, J.D.; Abboud, H.E. Shiga toxin 1 elicits diverse biologic responses in mesangial cells. *Kidney Int.* **1998**, *54*, 1117–1127. [CrossRef]
339. Moussay, E.; Stamm, I.; Taubert, A.; Baljer, G.; Menge, C. Escherichia coli Shiga toxin 1 enhances il-4 transcripts in bovine ileal intraepithelial lymphocytes. *Vet. Immunol. Immunopathol.* **2006**, *113*, 367–382. [CrossRef]
340. Balsinde, J.; Balboa, M.A.; Dennis, E.A. Inflammatory activation of arachidonic acid signaling in murine P388D1 macrophages via sphingomyelin synthesis. *J. Biol. Chem.* **1997**, *272*, 20373–20377. [CrossRef] [PubMed]
341. Peterson, J.W.; Finkelstein, R.A.; Cantu, J.; Gessell, D.L.; Chopra, A.K. Cholera toxin B subunit activates arachidonic acid metabolism. *Infect. Immun.* **1999**, *67*, 794–799. [CrossRef]
342. Schmid, D.I.; Kohan, D.E. Effect of shigatoxin-1 on arachidonic acid release by human glomerular epithelial cells. *Kidney Int.* **2001**, *60*, 1026–1036. [CrossRef]
343. Orth, D.; Khan, A.B.; Naim, A.; Grif, K.; Brockmeyer, J.; Karch, H.; Joannidis, M.; Clark, S.J.; Day, A.J.; Fidanzi, S.; et al. Shiga toxin activates complement and binds factor H: evidence for an active role of complement in hemolytic uremic syndrome. *J. Immunol.* **2009**, *182*, 6394–6400. [CrossRef]
344. Poolpol, K.; Orth-Holler, D.; Speth, C.; Zipfel, P.F.; Skerka, C.; de Cordoba, S.R.; Brockmeyer, J.; Bielaszewska, M.; Wurzner, R. Interaction of Shiga toxin 2 with complement regulators of the factor H protein family. *Mol. Immunol.* **2014**, *58*, 77–84. [CrossRef] [PubMed]
345. Brigotti, M.; Orth-Holler, D.; Carnicelli, D.; Porcellini, E.; Galassi, E.; Tazzari, P.L.; Ricci, F.; Manoli, F.; Manet, I.; Talasz, H.; et al. The structure of the Shiga toxin 2a A-subunit dictates the interactions of the toxin with blood components. *Cell Microbiol.* **2019**, *21*, e13000. [CrossRef] [PubMed]
346. Ehrlenbach, S.; Rosales, A.; Posch, W.; Wilflingseder, D.; Hermann, M.; Brockmeyer, J.; Karch, H.; Satchell, S.C.; Wurzner, R.; Orth-Holler, D. Shiga toxin 2 reduces complement inhibitor CD59 expression on human renal tubular epithelial and glomerular endothelial cells. *Infect. Immun.* **2013**, *81*, 2678–2685. [CrossRef]
347. Kimura, T.; Tani, S.; Matsumoto Yi, Y.; Takeda, T. Serum amyloid P component is the Shiga toxin 2-neutralizing factor in human blood. *J. Biol. Chem.* **2001**, *276*, 41576–41579. [CrossRef] [PubMed]
348. Armstrong, G.D.; Mulvey, G.L.; Marcato, P.; Griener, T.P.; Kahan, M.C.; Tennent, G.A.; Sabin, C.A.; Chart, H.; Pepys, M.B. Human serum amyloid P component protects against Escherichia coli O157:H7 Shiga toxin 2 in vivo: therapeutic implications for hemolytic-uremic syndrome. *J. Infect. Dis.* **2006**, *193*, 1120–1124. [CrossRef] [PubMed]
349. Brigotti, M.; Arfilli, V.; Carnicelli, D.; Ricci, F.; Tazzari, P.L.; Ardissino, G.; Scavia, G.; Morabito, S.; He, X. Soluble Toll-Like Receptor 4 Impairs the Interaction of Shiga Toxin 2a with Human Serum Amyloid P Component. *Toxins (Basel)* **2018**, *10*, 379. [CrossRef]
350. Kieckens, E.; Rybarczyk, J.; Barth, S.A.; Menge, C.; Cox, E.; Vanrompay, D. Effect of lactoferrin on release and bioactivity of Shiga toxins from different Escherichia coli O157:H7 strains. *Vet. Microbiol.* **2017**, *202*, 29–37. [CrossRef]
351. Malyukova, I.; Murray, K.F.; Zhu, C.; Boedeker, E.; Kane, A.; Patterson, K.; Peterson, J.R.; Donowitz, M.; Kovbasnjuk, O. Macropinocytosis in Shiga toxin 1 uptake by human intestinal epithelial cells and transcellular transcytosis. *Am. J. Physiol. Gastrointest. Liver Physiol.* **2009**, *296*, G78–G92. [CrossRef]
352. Laiko, M.; Murtazina, R.; Malyukova, I.; Zhu, C.; Boedeker, E.C.; Gutsal, O.; O'Malley, R.; Cole, R.N.; Tarr, P.I.; Murray, K.F.; et al. Shiga toxin 1 interaction with enterocytes causes apical protein mistargeting through the depletion of intracellular galectin-3. *Exp. Cell Res.* **2010**, *316*, 657–666. [CrossRef]

353. Maluykova, I.; Gutsal, O.; Laiko, M.; Kane, A.; Donowitz, M.; Kovbasnjuk, O. Latrunculin B facilitates Shiga toxin 1 transcellular transcytosis across T84 intestinal epithelial cells. *Biochim. Biophys. Acta* **2008**, *1782*, 370–377. [CrossRef] [PubMed]
354. Schuller, S. Shiga toxin interacion with human intestinal epithelium. *Toxins (Basel)* **2011**, *3*, 626–639. [CrossRef] [PubMed]